

THE EFFECT OF OXYGEN TRANSFER CONDITIONS ON RECOMBINANT  
GLUCOSE ISOMERASE PRODUCTION BY PICHIA PASTORIS UNDER  
GLYCERALDEHYDE-3-PHOSPHATE DEHYDROGENASE PROMOTER

A THESIS SUBMITTED TO  
THE GRADUATE SCHOOL OF NATURE AND APPLIED SCIENCES  
OF  
MIDDLE EAST TECHNICAL UNIVERSITY

BY

HANDE GÜNEŞ

IN PARTIAL FULFILLMENT OF THE REQUIREMENTS  
FOR  
THE DEGREE OF MASTER OF SCIENCE  
IN  
CHEMICAL ENGINEERING

AUGUST 2015



Approval of the thesis:

**THE EFFECT OF OXYGEN TRANSFER CONDITIONS ON  
RECOMBINANT GLUCOSE ISOMERASE PRODUCTION BY PICHIA  
PASTORIS UNDER GLYCERALDEHYDE-3-PHOSPHATE  
DEHYDROGENASE PROMOTER**

submitted by **HANDE GÜNEŞ** in partial fulfillment of the requirements for the degree of **Master of Science in Chemical Engineering Department, Middle East Technical University** by,

Prof. Dr. Gülbin Dural Ünver

Director, Graduate School of **Natural and Applied Sciences**

\_\_\_\_\_

Prof. Dr. Halil Kalıpçılar

Head of Department, **Chemical Engineering**

\_\_\_\_\_

Prof. Dr. Pınar Çalık

Supervisor, **Chemical Engineering Dept., METU**

\_\_\_\_\_

Prof. Dr. Tunçer H. Özdamar

Co-supervisor, **Chemical Engineering Dept., Ankara Uni.**

\_\_\_\_\_

**Examining Committee Members:**

Prof. Dr. Halil Kalıpçılar

Chemical Engineering Dept., METU

\_\_\_\_\_

Prof. Dr. Pınar Çalık

Chemical Engineering Dept., METU

\_\_\_\_\_

Prof. Dr. Tunçer H. Özdamar

Chemical Engineering Dept., Ankara University

\_\_\_\_\_

Assoc. Prof. Dr. Tuba Hande Ergüder Bayramoğlu

Environmental Engineering Dept., METU

\_\_\_\_\_

Asst. Prof. Dr. Erhan Bat

Chemical Engineering Dept., METU

\_\_\_\_\_

**Date:** 20.08.2015

**I hereby declare that all information in this document has been obtained and presented in accordance with academic rules and ethical conduct. I also declare that, as required by these rules and conduct, I have fully cited and referenced all material and results that are not original to this work.**

Name, Last name: Hande Güneş

Signature :

## ABSTRACT

### THE EFFECT OF OXYGEN TRANSFER CONDITIONS ON RECOMBINANT GLUCOSE ISOMERASE PRODUCTION BY *Pichia pastoris* UNDER GLYCERALDEHYDE-3-PHOSPHATE DEHYDROGENASE PROMOTER

Güneş, Hande

M.S., Department of Chemical Engineering

Supervisor: Prof. Dr. Pınar Çalık

Co-Supervisor: Prof. Dr. Tunçer H. Özdamar

August 2015, 128 Pages

The aim of this study is to investigate effects of oxygen transfer conditions on recombinant glucose isomerase (r-GI) production by *Pichia pastoris* under glyceraldehyde-3-phosphate dehydrogenase promoter ( $P_{GAP}$ ). Two different sets of operation strategies were investigated in terms of oxygen transfer conditions. In the first one, aeration rate was kept constant at  $Q_O/V = 3$  vvm, 6 vvm, and 10 vvm while agitation rate was kept at  $N = 900$  rpm; and in the second one, dissolved oxygen concentration was kept constant at  $C_{DO} = 5\%$ , 10%, 15%, 20% and 40% air saturation throughout the bioprocesses. In the strategies where oxygen supplementation was relatively high,  $Q_O/V = 6$  vvm and 10 vvm, excessive abundance of oxygen at the earlier hours of the bioprocesses limited cell growth and GI activity. Regardless of the oxygen transfer conditions, the cell concentration and glucose isomerase activity profiles showed similar trends in each strategy with

different highest values. The highest cell concentration was achieved when dissolved oxygen concentration was constant at 20% air saturation as  $44 \text{ g L}^{-1}$  at  $t = 9 \text{ h}$ , while the highest recombinant GI activity was achieved when dissolved oxygen concentration was kept constant at 15% saturation as  $4440 \text{ U L}^{-1}$  at  $t = 15 \text{ h}$ . The highest overall cell yield on substrate was obtained when the dissolved oxygen concentration was kept at 20% air saturation as  $0.48 \text{ g cell g}^{-1}$  substrate, which is the theoretical yield used for the calculation of substrate feeding rate. Lower GI activities were obtained by  $P_{GAP}$  compared to alcohol oxidase 1 promoter ( $P_{AOXI}$ ); however, decrease in fermentation time by more than 3-fold and elimination of methanol usage make  $P_{GAP}$  a favorable alternative to  $P_{AOXI}$ -driven expression systems.

**Keywords:** Glucose isomerase, *Pichia pastoris*, oxygen transfer conditions, GAP promoter.

## ÖZ

### OKSİJEN AKTARIM KOŞULLARININ *Pichia pastoris* İLE GLİSERALDEHİT-3-FOSFAT DEHİDROJENAZ PROMOTÖRÜ ALTINDA REKOMBİNANT GLUKOZ İZOMERAZ ÜRETİMİNE ETKİSİ

Güneş, Hande

Yüksek Lisans, Kimya Mühendisliği Bölümü

Tez Yöneticisi: Prof. Dr. Pınar Çalık

Ortak Tez Yöneticisi: Prof. Dr. Tunçer H. Özdamar

Ağustos 2015, 128 Sayfa

Bu çalışmanın amacı oksijen aktarım koşullarının *Pichia pastoris* ile gliseraldehit-3-fosfat dehidrojenaz promotörü ( $P_{GAP}$ ) altında rekombinant glukoz isomerase (r-GI) üretimine etkilerinin araştırılmasıdır. Oksijen aktarım koşullarının r-GI üretimine etkileri iki deney seti ile incelenmiştir. Birinci deney setinde  $N = 900 \text{ min}^{-1}$  karıştırma hızında  $Q_O/V = 3 \text{ vvm}$ ,  $6 \text{ vvm}$  ve  $10 \text{ vvm}$  hava giriş hızlarında; ikinci sette  $C_{DO} = \%5$ ,  $\%10$ ,  $\%15$ ,  $\%20$  ve  $\%40$  hava doygunluk değerindeki oksijen derişimlerinde araştırılmıştır. Tasarlanan stratejiler arasında yüksek oksijen aktarım hızlarında,  $Q_O/V = 6 \text{ vvm}$  ve  $10 \text{ vvm}$ , ortamdaki yüksek oksijen derişimleri hücre çoğalmasını ve r-GI üretimini inhibe etmiştir. Oksijen aktarım koşullarından bağımsız olarak, bütün stratejilerde hücre çoğalma ve r-GI üretim profilleri benzer trendler göstermiş fakat ulaşılan en yüksek değerler farklı olmuştur. En yüksek hücre derişimi çözülmüş oksijen derişimi  $\%20$  hava doygunluğunda  $44 \text{ g L}^{-1}$  olarak

t = 9 st'te; en yüksek GI aktivitesi %15 hava doygunluęunda 4440 U L<sup>-1</sup> olarak t = 15 st'te elde edilmiřtir. En yüksek toplam substrat tüketimei üzerinden hücre verimi 0.48 g hücre g<sup>-1</sup> glukoz olarak %20 hava doygunluk deęerinde elde edilmiřtir ve bu deęer substrat besleme hızı hesaplamak için kullanılan teorik deęere eřittir. Alkol oksidaz 1 promotörü (P<sub>AOXI</sub>) ile karşılařtırıldıęında P<sub>GAP</sub> ile yapılan deneyler sonucunda daha düşük GI aktivitesi elde edilmiř olmasına raęmen fermentasyon süresinin en az üç kat kısalması ve metanol kullanımına gerek olmaması, P<sub>GAP</sub>'i P<sub>AOXI</sub> yanında önemli bir alternatif haline getirmektedir.

**Anahtar Kelimeler:** Glukoz izomeraz, *Pichia pastoris*, oksijen aktarım kořulları, GAP promotör



*To my family*

## ACKNOWLEDGMENTS

I wish to express my deepest gratitude to my supervisor Prof. Dr. Pınar Çalık for her guidance, support and help in every aspect of this study.

I am also thankful to my co-supervisor, Prof. Dr. Tunçer H. Özdamar for his valuable advices and critics.

Financial support provided by Middle East Technical University Research Fund Projects and Scientific and Technical Council of Turkey (TÜBİTAK-211T065) are gratefully acknowledged.

I owe very much to my lab-mates in my research group at Industrial Biotechnology and Metabolic Engineering Laboratory; Özge Ata Akyol, Sibel Öztürk, Burcu Gökbudak, Aslan Massahi, Erdem Boy, Abdullah Keskin, Duygu Yalçınkaya, Damla Hücetoğulları, Bebeta Hoxha, and Endri Sollaku for their friendship, help, support and contribution in every possible way.

It is a great chance for me to meet Eti Ester Levi, Leman Güneş and especially Burak Çağrı Duran for helping me collect unforgettable memories. I am thankful to all them for just being in my life.

I wish to thank Zeynep Karakaş and Arzu Arslan for being much more than just colleagues, and making toughest situations more endurable with their friendship. I would also like to thank all academic, administrative and technical staff of Department of Chemical Engineering, METU, for their help and support throughout my education.

Above all, my deepest gratitude goes to my family, Anıl Güneş, Güner Güneş and Sakin Güneş for their love, support and encourage all through my life no matter what. I could not be where I am today without them.

H. Güneş

## TABLE OF CONTENTS

ABSTRACT .....	v
ÖZ .....	vii
ACKNOWLEDGMENTS .....	x
TABLE OF CONTENTS .....	xi
LIST OF TABLES .....	xv
LIST OF FIGURES .....	xvi
NOMENCLATURE.....	xix
1. INTRODUCTION .....	1
2. LITERATURE SURVEY .....	7
2.1. Enzymes .....	7
2.2. Product: Thermostable Glucose Isomerase .....	8
2.2.1. Structure and Characteristics of Glucose Isomerase .....	9
2.3. Selection of the Host Microorganism .....	15
2.4. The Host Microorganism: <i>Pichia pastoris</i> .....	16
2.4.1. Promoters of <i>Pichia pastoris</i> .....	18
2.4.2. Central Carbon Metabolism of <i>Pichia pastoris</i> .....	22
2.4.3. Post-Translational Modifications and Protein Secretion.....	23
2.4.4. Proteolytic Degradation .....	25
2.5. Medium Design .....	26
2.6. Bioreactor Operation Conditions .....	27

2.6.1. pH .....	27
2.6.2. Temperature .....	27
2.6.3. Dissolved Oxygen Concentration.....	28
2.7. Oxygen Transfer Characteristics .....	30
2.7.1. Experimental Determination of Volumetric Mass Transfer Coefficient..	34
2.7.2. Other Parameters Involving Oxygen Transfer Characteristics .....	36
2.8. Influence of Geometrical Parameters of the Bioreactor on Mass Transfer Coefficient and Mixing .....	38
2.9. Computation of Bioprocess Characteristics .....	40
2.9.1. Specific Cell Growth Rate.....	40
2.9.2. Specific Substrate Consumption Rate .....	43
2.9.3. Yield Coefficients .....	45
3. MATERIALS AND METHOD .....	47
3.1 Chemicals .....	47
3.2 Buffers and Stock Solutions.....	47
3.3 Microorganism .....	47
3.4.1 Solid Medium.....	48
3.4.2 Precultivation Medium.....	48
3.4.3 Production Media .....	49
3.5. Recombinant Glucose Isomerase Production.....	49
3.5.1. Precultivation .....	49
3.5.2. Production in Laboratory Scale Bioreactor .....	51
3.5.2.3. Feeding Strategies Applied in Bioreactor Experiments .....	54
3.6 Analyses .....	55

3.6.1. Cell Concentration .....	56
3.6.2. Glucose Concentration .....	56
3.6.3. Glucose Isomerase Activity .....	57
3.6.3. Sodium Dodecyl Sulfate-Polyacrylamide Gel Electrophoresis (SDS-PAGE) .....	57
3.6.4. Protease Activity Assay .....	58
3.6.5. Organic Acid Concentration .....	58
4. RESULTS AND DISCUSSION .....	61
4.1. GI Production with Constant Oxygen Transfer Condition .....	63
4.2. GI Production with Constant Dissolved Oxygen Concentration .....	67
4.3. Comparison of Constant Oxygen Transfer Condition and Constant Dissolved Oxygen Concentration Strategies .....	72
4.3.1. Cell Concentration and Specific Cell Growth Rate .....	72
4.3.2. Glucose Concentration and Specific Glucose Consumption Rate .....	74
4.3.3. GI Activity and Specific GI Activity .....	77
4.3.4. GI Monomer Concentration: SDS-PAGE .....	79
4.3.5. Proteolytic Activity .....	80
4.3.6. Organic Acid Concentrations .....	81
4.3.7. Oxygen Transfer Characteristics .....	87
5. CONCLUSION .....	97
REFERENCES .....	101
APPENDICES	
A. BUFFERS AND STOCK SOLUTIONS .....	115
B. CALIBRATION CURVE FOR GLUCOSE CONCENTRATION .....	117

C. SILVER STAINING PROCEDURE.....	119
D. CALIBRATION CURVES FOR ORGANIC ACIDS .....	121
E. ORGANIC ACID CONCENTRATIONS .....	125

## LIST OF TABLES

### TABLES

<b>Table 1.</b> Commercially important GI producers.....	9
<b>Table 2a.</b> Sequence of GI from <i>T. thermophilus</i> .....	11
<b>Table 2b.</b> Sequence of codon optimized GI from <i>T. thermophilus</i> .....	12
<b>Table 3.</b> Composition of YPD agar solid medium .....	48
<b>Table 4.</b> Composition of the precultivation medium, BMGY.....	49
<b>Table 5.</b> Composition of basal salts medium, BSM .....	50
<b>Table 6.</b> Composition of <i>Pichia</i> trace salts, PTM1 .....	50
<b>Table 7.</b> Geometric properties of the bioreactor.....	53
<b>Table 8.</b> Values of the parameters in Equation 34.....	54
<b>Table 9.</b> Strategies applied in bioreactor experiments.....	55
<b>Table 10.</b> HPLC operation conditions for organic acid analysis.....	59
<b>Table 11.</b> Variations of oxygen transfer characteristics with cultivation time.....	89
<b>Table 12.</b> Instantaneous and overall yield coefficients .....	94
<b>Table 13.</b> Organic acid accumulation with cultivation time. ....	125

## LIST OF FIGURES

### FIGURES

<b>Figure 1.</b> Isomerization reaction catalyzed by GI..	9
<b>Figure 2.</b> Crystal structure of glucose isomerase from <i>T. thermophilus</i>	13
<b>Figure 3.</b> Metal binding sites of GI from <i>S. rubiginosus</i>	14
<b>Figure 4.</b> Complete reaction mechanism	17
<b>Figure 5.</b> Glycolysis/Gluconeogenesis pathway of <i>P. pastoris</i>	21
<b>Figure 6.</b> Central carbon metabolism of <i>P. pastoris</i>	24
<b>Figure 7. (a)</b> Oxygen transfer from gas bubble into the cell <b>(b)</b> $C_{DO}$ profile along the oxygen transfer process.	33
<b>Figure 8.</b> Schematic representation of the gas-liquid interface according to two film theory	34
<b>Figure 9.</b> Change in $C_{DO}$ during the application of dynamic method.	37
<b>Figure 10.</b> Determination of $K_L a$ by dynamic method.	37
<b>Figure 11.</b> Typical microbial growth curve of a batch culture.	41
<b>Figure 12.</b> Schematic representation of lab scale bioreactor system together with precultivation steps.	52
<b>Figure 13.</b> Variation of dissolved oxygen concentration in the fermentation medium with cultivation time.	62
<b>Figure 14.</b> Variation of dissolved oxygen concentration in the fermentation medium with cultivation time.	63
<b>Figure 15.</b> Variations in cell concentration with the cultivation time in constant OTC bioprocesses.	64
<b>Figure 16.</b> Variations in glucose concentration with the cultivation time for constant OTC bioprocesses.	65
<b>Figure 17.</b> Variations in GI activity with the cultivation time for constant OTC bioprocesses.	66



<b>Figure 18.</b> Variations in protease activity with the cultivation time for constant OTC bioprocesses. ....	66
<b>Figure 19.</b> Comparative representation of the variations of protease and GI activities with the cultivation time for constant OTC bioprocesses. ....	67
<b>Figure 20.</b> Variations in cell concentration with the cultivation time for CDO bioprocesses .....	68
<b>Figure 21.</b> Variations in glucose concentration with the cultivation time for CDO bioprocesses .....	69
<b>Figure 22.</b> Variations in GI activity with the cultivation time. ....	70
<b>Figure 23.</b> Comparison of maximum activity reached in each CDO bioprocess. ....	70
<b>Figure 24.</b> Variations in protease activity with the cultivation time for CDO bioprocesses. ....	71
<b>Figure 25.</b> Comparative representation of variations in protease and GI activities with the cultivation time for CDO bioprocesses. ....	71
<b>Figure 26.</b> Variations in cell concentration with the cultivation time, comparison of all experiments .....	73
<b>Figure 27.</b> Variations in the specific growth rate with the cultivation time.....	74
<b>Figure 28.</b> Feeding profile of glucose solution according to Equation (34). ....	75
<b>Figure 29.</b> Variations in glucose concentration in the fermentation medium with the cultivation time.....	76
<b>Figure 30.</b> Variations in the specific substrate consumption rate with the cultivation time.....	76
<b>Figure 31.</b> Variations in GI activity with the cultivation time. ....	77
<b>Figure 32.</b> Variations in the specific GI activity with the cultivation time.....	78
<b>Figure 33.</b> Silver stained SDS-PAGE gel images .....	80
<b>Figure 34.</b> Variations in protease activity with the cultivation time. ....	81
<b>Figure 35.</b> Variations in organic acid concentrations with the cultivation time for OTC <sub>1</sub> strategy. ....	83
<b>Figure 36.</b> Variations in organic acid concentrations with the cultivation time for OTC <sub>2</sub> strategy.....	83

<b>Figure 37.</b> Variations in organic acid concentrations with the cultivation time for OTC <sub>3</sub> strategy. ....	84
<b>Figure 38.</b> Variations in organic acid concentrations with the cultivation time for CDO <sub>1</sub> strategy. ....	84
<b>Figure 39.</b> Variations in organic acid concentrations with the cultivation time for CDO <sub>2</sub> strategy. ....	85
<b>Figure 40.</b> Variations in organic acid concentrations with the cultivation time for CDO <sub>3</sub> strategy. ....	85
<b>Figure 41.</b> Variations in organic acid concentrations with the cultivation time for CDO <sub>4</sub> strategy. ....	86
<b>Figure 42.</b> Variations in organic acid concentrations with the cultivation time for CDO <sub>5</sub> strategy. ....	86
<b>Figure 43.</b> Calibration curve for glucose concentration .....	117
<b>Figure 44.</b> Calibration curve for gluconic acid concentration. ....	121
<b>Figure 45.</b> Calibration curve for malic acid concentration. ....	122
<b>Figure 46.</b> Calibration curve for citric acid concentration. ....	122
<b>Figure 47.</b> Calibration curve for lactic acid concentration. ....	123
<b>Figure 48.</b> Calibration curve for succinic acid concentration. ....	123
<b>Figure 49.</b> Calibration curve for fumaric acid concentration. ....	124

## NOMENCLATURE

a	Area	$\text{m}^2$
C	Concentration or Off-bottom clearance of the tank	$\text{g L}^{-1}$ , $\text{mol L}^{-1}$ or m
D	Impeller diameter	m
Da	Damköhler number	-
F	Mass flow rate	$\text{g h}^{-1}$
h	Impeller height	m
H	Average height of reactor working volume	m
j	Molar flux	$\text{mol m}^{-2} \text{s}^{-1}$
$K_L a$	Overall liquid phase mass transfer coefficient	$\text{s}^{-1}$
N	Agitation rate	rpm
OUR	Oxygen uptake rate	$\text{mol m}^{-3} \text{s}^{-1}$
OTR	Oxygen transfer rate	$\text{mol m}^{-3} \text{s}^{-1}$
OD	Optical density	$\square$
p	Partial pressure	atm
q	Specific formation/consumption rate	$\text{mol g}^{-1} \text{h}^{-1}$
Q	Volumetric flow rate	$\text{m}^3 \text{h}^{-1}$
r	Formation/consumption rate	$\text{mol h}^{-1}$
t	Time	h
T	Tank diameter or temperature	m or $^{\circ}\text{C}$
V	Volume	$\text{m}^3$
Y	Yield	$\text{g g}^{-1}$

## Greek Letters

$\eta$	Effectiveness factor (OUR/OD)	
$\mu$	Specific growth rate	$\text{h}^{-1}$
$\mu_0$	Pre-determined specific growth rate	$\text{h}^{-1}$
$\lambda$	Wavelength	nm

## Superscripts and Subscripts

*	Value at equilibrium
0	Initial condition
AOX	Alcohol oxidase
DO	Dissolved oxygen
G	Gas side or glucose
GAP	Glyceraldehyde-3-phosphate dehydrogenase
Gly	Glycerol
i	Interface
L	Liquid side
O	Oxygen
P	Product
S	Substrate
X	Cell

## Abbreviations

DF	Dilution factor
FDA	Food and Drug Administration
GI	Glucose isomerase
GRAS	Generally recognized/regarded as safe
HPLC	High performance liquid chromatography
OTC	Oxygen transfer condition

P	Promoter
PPP	Pentose phosphate pathway
r	Recombinant
SDS-PAGE	Sodium dodecyl sulfate-polyacrylamide gel electrophoresis
TCA	Tricarboxylic Acid



## **CHAPTER 1**

### **INTRODUCTION**

Industrial biotechnology uses microorganisms and enzymes for the production of biomolecules and has a wide range of applications that can be divided into seven subgroups; pharmaceutical biotechnology industry (production of vitamins, vaccines, antibiotics and therapeutic proteins), basic biochemical industry (production of organic acids, amino acids and alcohols), enzyme production industry (production of industrial and restriction enzymes), classical biotechnology industry (yeast production), bioenergy and biofuel industry (production of biogases; ethanol, butanol and biodiesels), agricultural biotechnology and waste treatment by biotechnological processes. As industrial biotechnology uses renewable materials and innovative methodologies to reduce greenhouse gas emission, it is accepted to be a promising approach for lowering the impacts of climate change resulting from chemical engineering industries and related sectors. Along with environmental benefits, it can enhance the performance of industries and product value as it focuses on increasing the efficiency of the processes. Producing biomolecules in organisms other than their native source is now enabled with the developments in recombinant DNA technology. It is done by cloning the gene responsible for the expression of desired biomolecule into the genome of a different organism, known as the host organism. These host organisms are chosen for their ability of overexpression, harmlessness to environment, or for reducing production costs. By being able to choose the optimum host organism, one can increase product value, lower production cost and decrease the environmental pollution caused by the process. As this technology matures,

industrial biotechnology will be able to propose more innovative solutions to climatic and economic problems.

D-glucose isomerase (GI, E.C. 5.3.1.5), also known as D-xylose isomerase or D-xylose ketol-isomerase, is an enzyme catalyzing the reversible isomerization reaction of D-glucose to D-fructose and D-xylose to D-xylulose. Conversion of D-glucose to D-fructose is used in the production of high fructose corn syrup (HFCS), while isomerization of D-xylose to D-xylulose is an important step for the conversion of xylan containing biomass into ethanol. Production of monosaccharides by GI is becoming more popular due to its potential health and medical benefits (Jokela *et al.*, 2002).

According to the report “Industrial Enzymes Market” by Markets and Markets (2014), the global demand for industrial enzyme production would reach \$ 6 billion by 2018. According to Turkish Chamber of Food Engineers (2011), HFCS is produced 12.5 million tons since 2006 in the world, and 400 thousand tons are produced since 2010 in Turkey. The world market of HFCS is expected to reach over 153 million tons.

Industrial protein production for commercial purposes is done with the help of genetic and metabolic engineering. Proteins can be expressed in various cell cultures such as mammals, plants, insects, bacteria, molds and yeasts. Large proteins are usually expressed in eukaryotic systems while prokaryotic systems are used for smaller ones. Choosing the right expression system is the most important step for r-protein production. As reported by Sanchez and Demain (2012), 45% of recombinant proteins produced in the USA and Europe come from mammalian cells, 40% from bacteria, whose 39% is from *Escherichia coli*, and 15% come from yeasts. Although bacterium *E. coli* is a popular host microorganism, yeast expression systems are gaining more attention due to their ability to do post-translational modifications and secretion which makes post-fermentation purification and modifications easier and also decreases cost (Liu et al, 2012). The most commonly used yeasts for industrial



protein production are *Saccharomyces cerevisiae*, *Kluyveromyces lactis*, *Pichia pastoris* and *Hansenula polymorpha* (Schmidt, 2004).

Commercial GI market is dominated by *Actinoplanes missouriensis*, *Bacillus coagulans* or *Streptomyces* species which are generally not thermostable. Therefore, commercial isomerization reaction cannot be carried out at temperatures above 60-65°C (Wang *et al.* 2011). Isolating thermostable *xylA* gene encoding GI from thermostable bacteria such as *Thermotoga neapolitana*, *Thermus thermophilus* or *Thermus flavus* enables the production of thermostable recombinant GI which results in higher enzymatic activity and thermostability (Wang *et al.* 2011).

For the production of thermostable GI, *E. coli* and *Bacillus* species are the most popular expression hosts. Lee *et al.* (1990) cloned thermostable *Clostridium thermosulfurogenes* GI gene into *E. coli* and *B. subtilis* and compared their expression levels. Both expression levels were higher than that in the native source. The highest GI activity was reported to be reached as 1.54 U mg<sup>-1</sup> protein in *B. subtilis* and 0.46 U mg<sup>-1</sup> protein in *E. coli*. In another study, Dekker *et al.* (1991) cloned thermostable *T. thermophilus* GI gene into *E. coli*. 450 U L<sup>-1</sup> GI yield was achieved by the expression in *E. coli*, which is 45-fold higher GI yield compared to the expression in *T. thermophilus*. Thermostable *T. thermophilus* GI encoding *xylA* gene was cloned to *E. coli* and *B. brevis* by the same research group in another study (Dekker *et al.* 1992). *B. brevis* yielded more than 1 g L<sup>-1</sup> thermostable GI and reported to be more productive than *E. coli* in terms of GI production. Park *et al.* (1997) cloned *xylA* gene from *T. flavus* into *E. coli* and produced thermostable GI whose optimum temperature is 90°C and reached 55% yield from the isomerization reaction of glucose. In a more recent study, Angardi and Çalık (2013) expressed thermostable GI from *T. thermophilus* in *E. coli*. The highest GI activity was obtained as 16400 U L<sup>-1</sup>. Afterwards, Akdağ and Çalık (2014) achieved 35260 U L<sup>-1</sup> thermostable GI activity from *T. thermophilus* by using untreated beet molasses as the substrate for expression in *E. coli*.

*xylA* gene from *T. thermophilus* was successfully cloned and expressed in *S. cerevisiae* for ethanolic fermentation of xylose. The highest specific activity was reached as 1 U mg<sup>-1</sup> (Walfridsson *et al.* 1996). Kuyper *et al.* (2005), isolated *xylA* gene from the fungus *Piromyces* sp. and cloned to *S. cerevisiae* for anaerobic xylose fermentation. In this study, GI activity or concentration was not determined but specific xylose consumption rate was determined as 1.1 g xylose g<sup>-1</sup> biomass h<sup>-1</sup> which was reported as the highest specific xylose consumption rate among all published data on metabolically engineered *S. cerevisiae* strains. de Figueiredo Vilela *et al.* (2013) expressed *Burkholderia cenocepacia* GI in *S. cerevisiae* for ethanol production. *xylA* gene insertion increased xylose consumption by 5-fold, and ethanol production more than 1.5-fold.

*P. pastoris* is a methylotrophic yeast reported to be suitable for heterologous protein expression system (Cos *et al.* 2006). Its ability to reach high cell densities on cheap, minimal media, to perform post-translational modifications like glycosylation, disulfide bond formation and proteolytic activity and secrete proteins to extracellular medium have made *P. pastoris* expression systems desirable for recombinant protein production (Cereghino and Cregg, 2000). In their review, Cos *et al.* (2006) reported several different inducible and constitutive promoters of *P. pastoris* which have successfully been used for heterologous protein expression. The most widely studied promoter of *P. pastoris* is alcohol oxidase 1 promoter (P<sub>AOX1</sub>), which is a tightly regulated, inducible promoter. It is fully repressed in the presence of glycerol and derepressed in the presence of methanol. Therefore, in expression systems of *P. pastoris* under P<sub>AOX1</sub>, methanol is not only used as the carbon source but also as the inducer of the promoter expressing the target gene (Cereghino and Cregg, 2000; Ata *et al.* 2015; Güneş *et al.* 2015). However, usage of methanol as the carbon source for the fermentation raises environmental and health concerns because of handling issues and toxic nature of methanol and the by-products of fermentation such as formaldehyde and hydrogen peroxide, especially when the targeted protein is going to be used in food or drug related industries. Because of these problematic issues,

using an alternative expression system without the need for methanol usage has gained attention in recent years (Çalık *et al.* 2015). As a result, glyceraldehyde-3-phosphate dehydrogenase promoter  $P_{GAP}$  has become a popular choice for constitutive, methanol-free recombinant protein expressions in *P. pastoris* (Zhang *et al.* 2009). Because of the constitutive nature of the  $P_{GAP}$ , protein expression is coupled with cell growth. This coupling eliminates the need for a several-phased fermentation process, as needed in inducible expressions since a certain cell growth should be achieved to start the induction of the promoter for protein expression (Çalık *et al.* 2015). In several studies, depending on the fermentation mode and the protein expressed,  $P_{GAP}$  is reported as a strong constitutive promoter with comparable expression levels with the ones done under  $P_{AOXI}$  (Cos *et al.* 2005; Zhang *et al.* 2009; Çalık *et al.* 2015).

*xylA* gene from *T. thermophilus* was firstly cloned into pPICZ $\alpha$ -A expression vector in our research group by Ata (2012). Then, pPICZ $\alpha$ -A::*xylA* vector was cloned into *AOXI* locus of *P. pastoris* for inducible expression of GI under *AOXI* promoter. The highest GI activity was reported as 203 U L<sup>-1</sup> for extracellular production. Afterwards, the effect of codon optimization and different feeding strategies on inducible thermostable GI expression were investigated and reported in Ata *et al.* (2015). The highest GI activity was determined as 32500 U L<sup>-1</sup> by keeping methanol concentration in the medium constant at 5 g L<sup>-1</sup>.

In this study, the objective is to investigate the effects of oxygen transfer conditions on recombinant GI production by *P. pastoris* under  $P_{GAP}$  using glucose as the carbon source. In the first three experiments, aeration rate was kept constant at  $Q_0/V = 3$  vvm, 6 vvm and 10 vvm, while agitation rate was  $N = 900$  rpm, and in the other experiments dissolved oxygen concentration in the bioreaction medium was kept constant at 5%, 10%, 15%, 20% and 40%, by using a cascade system to supply air and oxygen enriched air when necessary while agitation rate was  $N = 900$  rpm. Fermentation data for each strategy were analyzed in terms of cell concentration, glucose concentration, GI activity, GI monomer concentration, acidic protease

activity and organic acid concentration. Additionally, yield coefficients, the specific substrate consumption rates and oxygen transfer characteristics were calculated in order to understand fermentation characteristics more in-depth and to discuss the response of *P. pastoris* to different fermentation strategies.

## CHAPTER 2

### LITERATURE SURVEY

Structure and characteristics of the protein, selection of the host microorganism and its promoter, optimum bioprocess operation modes and parameters should be investigated to design an efficient recombinant protein production machinery. In this context, this chapter covers the literature survey done on the recombinant protein to be produced, glucose isomerase, and the host microorganism, *Pichia pastoris*, along with the inspection of bioprocess operation parameters and modes; and their effects on heterologous protein expression by *P. pastoris*.

#### 2.1. Enzymes

The biological catalysts, enzymes, increase the rate of biochemical reactions by interacting with the reactants and products to provide a more thermodynamically favorable pathway for transformation of reactants to products. To visualize, the rate of enzymatically catalyzed reactions usually  $10^6$ - $10^{12}$  times more than that of the uncatalyzed reactions and several orders of magnitude more than the corresponding ones that are chemically catalyzed (Voet *et al.* 2013).

Enzymes are divided into six subgroups according to the type of the reaction they catalyze. These subgroups are oxidoreductase, transferase, hydrolase, lyase, isomerase and ligase. Oxidoreductases catalyze oxidation/reduction reactions in which hydrogen and oxygen are gained or lost; transferases are responsible for the transfer of functional groups such as amino acid and phosphate groups; hydrolases catalyze hydrolysis reactions; lyases remove groups of atoms without hydrolysis;

isomerases catalyze isomerization reactions; and ligases are synthesis enzymes (Palmer *et al.* 2007).

Enzymes have three-dimensional substrate-specific structures. These three-dimensional structures have four types; primary, secondary, tertiary and quaternary structures. When amino acids have a linear sequence, then the structure is called primary structure; when the repeating structure has alpha helices and beta strands which are stabilized by hydrogen bonds, the structure is known as secondary structure; when the structure of the protein is determined by salt bridges, hydrogen bonds, hydrophobic interactions, disulfide bonds and post-translational modifications, the structure is tertiary structure, and when the structure results from the interactions of several proteins or polypeptides, known as subunits, and is determined by noncovalent interactions and disulfide bonds, the structure is known as quaternary structure. If the protein consists of two subunits, it is called as dimer; if there are three subunits, the protein is trimer; and if the protein is composed of four subunits, it is called as tetramer. If the subunits are the same polypeptides or proteins, then the multimers get the prefix homo-, if these subunits are different from one another, then they have the prefix hetero- (Raven *et al.*, 2013).

## **2.2. Product: Thermostable Glucose Isomerase**

Glucose isomerase (GI, E.C. 5.3.1.5), also known as D-xylose isomerase or D-xylose ketol-isomerase is an isomerization enzyme which catalyzes the reversible reaction of D-glucose to D-fructose and D-xylose to D-xylulose (Figure 1). The former reaction is important for high fructose corn syrup (HFCS) production while the latter is an essential step of ethanol production from biomass containing xylan.

Marshall and Kooi discovered an enzyme in *Pseudomonas hydrophila* that is capable of isomerization of glucose into fructose in 1957, and the microorganisms carrying glucose isomerase producing strains gained attention for their potential to be used in HFCS production (Bhosale *et al.* 1996). As the research on GI widened, it is seen that it is widely distributed in prokaryotes; especially bacteria and actinomycetes

have high capacity to produce GI. While several *Bacillus* species are good producers of GI, only fungus that is known to be capable of GI production is *Aspergillus oryzae* (Bhosale *et al.* 1996). In addition, GI production in the yeasts *Candida utilis* (Wang *et al.* 1980) and *Candida boidinii* (Vongauvanlert and Tani, 1988) has been reported. Some commercial GI producers are given in Table 1.

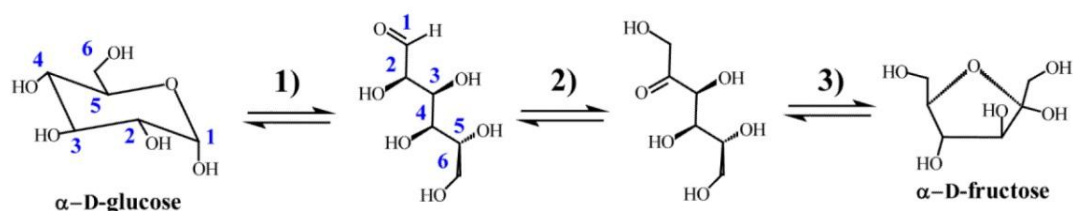


**Figure 1.** Isomerization reaction catalyzed by GI. (1) Ring opening, (2) isomerization, (3) ring closure (Kovalevsky *et al.* 2010).

**Table 1.** Commercially important GI producers (Bhosale *et al.* 1996)

Organism	Trade Name	Manufacturer
<i>Actinoplanes missouriensis</i>	Maxazyme	Gist Brocades and Anheuser-Busch Inc.
<i>Bacillus coagulans</i>	Sweetzyme	Novo-Nordisk
<i>Streptomyces rubiginosus</i>	Optisweet	Miles Kali-Chemie

### 2.2.1. Structure and Characteristics of Glucose Isomerase

GI from *T. thermophilus* is a homotetramer with identical, four subunits in its active form. Identical subunits are connected to each other with noncovalent bonds. Depending on the source microorganism, molecular weight of GI can vary between 44 and 191 kDa. Subunits of GI from *T. thermophilus* are composed of 387 amino acids and have a molecular weight of 44 kDa (Dekker *et al.*, 1991) (Table 2).

Chang *et al.* (1999) determined the crystal structure of thermostable GI from *T. thermophilus* and reported that the tertiary fold of the subunits are similar to glucose isomerases from other source organisms. The monomers are composed of two domains. Domain I, residues from 1 to 321, folds into  $(\beta/\alpha)_8$ -barrel, while Domain II, residues from 321 to 387, contacts with Domain I of the adjacent subunit. Each monomer of GI has ten  $\beta$ -strands, sixteen  $\alpha$ -helices, and five 310-helices (Figure 2). To understand the structural factors affecting thermostability of GI from *T. thermophilus*, they compared the structure with two other GIs from *Arthrobacter* B3728 and *Actinoplanes missouriensis* whose optimum reaction temperatures are 80°C and 75°C, respectively. Increase in ion pairs and ion pair networks, decrease in large inter-subunit cavities, removal of potential deamidation/isoaspartate formation sites and shortened loops have been speculated to increase thermostability of GI from *Thermus thermophilus* compared to two other GIs from *Arthrobacter* B3728 and *Actinoplanes missouriensis*.

Depending on the host microorganism, optimum temperature for thermostable GI ranges between 60°C and 90°C. Enzymes from thermophilic hosts are reported to be more stable at high temperatures compared to those from mesophilic sources (Bhosale *et al.*, 1996). Hlima *et al.* (2012) showed that the optimum temperature for GI from *Streptomyces* sp. SK is 80°C; while optimum temperature of GI from *Actinoplanes missouriensis* was reported to be 60°C (Lambeir *et al.* 1992). Using GI from thermophilic hosts are more desirable since increasing temperature is important because of its positive effect on the equilibrium concentration of fructose, and a higher reaction rate (Hlima *et al.* 2012).

Like temperature, optimum pH for GI activity depends on the host organism while it typically ranges between 6.5 and 8.5. Hlima *et al.* (2012) reported optimum pH for GI from *Streptomyces* sp. SK to be 6.5 and pH of the isomerization reaction with GI from *T. thermophilus* was reported as 7.0 by Dekker *et al.* (1991); also, Mishra and Debnath (2002) found the optimum pH to vary between 7.0 and 8.5 depending on the buffer solution used.



**Table 2a.** Sequence of GI from *T. thermophilus* (National Center for Biotechnology Information GenBank, Accession Number: D90256.1).

```

GTGTACGAGCCCAAACCGGAGCACAGGTTTACCTTTGGCCTTTGGACTGTGGGCAATGTG 60
GGCCGTGATCCCTTCGGGGACGCGGTTTCGGGAGAGGCTGGACCCGGTTTACGTGGTTCAT 120
AAGCTGGCGGAGCTTGGGGCCTACGGGGTAAACCTTCACGACGAGGACCTGATCCCGCGG 180
GGCAGGCCTCCTCAGGAGCGGGACCAGATCGTGAGGCGCTTCAAGAAGGCTCTCGATGAA 240
ACCGGCCTCAAGGTCCCCATGGTCACCGCCAACCTCTTCTCCGACCCTGCTTTCAAGGAC 300
GGGGCCTTCACGAGCCCGGACCCTTGGGTTTCGGGCCTATGCCTTGCGGAAGAGCCTGGAG 360
ACCATGGACCTGGGGGCAGAGCTTGGGGCCGAGATCTACGTGGTCTGGCCGGGCGGGGAG 420
GGAGCTGAGGTGGAGGCCACGGGCAAGGCCCCGAAGGTCTGGGACTGGGTGCGGGAGGCG 480
CTGAACTTCATGGCCGCCTACGCCGAGGACCAGGGATACGGGTACCGGTTTGCCCTCGAG 540
CCCAAGCCTAACGAGCCCCGGGGGGACATTTACTTCGCCACCGTGGGGAGCATGCTCGCC 600
TTTATTTCATACCCTGGACCGGCCCCGAGCGCTTCGGCCTGAACCCCGAGTTCGCCCACGAG 660
ACCATGGCCGGGCTTAACCTTTGTCCACGCCGTGGCCCAGGCTCTCGACGCCGGGAAGCTT 720
TTCCACATTGACCTCAACGACCAACGGATGAGCCGGTTTGACCAGGACCTCCGCTTCGGC 780
TCGGAGAACCTCAAGGCGGCCTTTTTCTGGTGGACCTCCTGGAAAGCTCCGGCTACCAG 840
GGCCCCCGCCACTTTGACGCCCACGCCCTGCGTACCGAGGACGAAGAAGGGGTTTGGGCC 900
TTCGCCCCGAGGCTGCATGCGTACCTACCTGATCTTAAAGGAAAGGGCTGAAGCCTTCCGC 960
GAGGATCCCGAGGTCAAGGAGCTTCTTGCCGCTTACTATCAAGAAGATCCTGCGGCCTTG 1020
GCCCTTTTGGGCCCCCTACTCCCGCGAGAAGGCCGAAGCCCTCAAGCGGGCGGAGCTTCCC 1080
CTCGAGGCCAAGCGGCGCCGGGGTTATGCCCTGGAACGCCTGGACCAGCTGGCGGTGGAG 1140
TACCTCCTGGGGGTGCGGGGG 1164

```

**Table 2b.** Codon-optimized sequence of GI from *T. thermophilus*. Altered codons are in black. Altered Kex2 cleavage sites are highlighted in yellow (Ata *et al.* 2015; National Center for Biotechnology Information GenBank Accession Number: AB981659).

```

ATGTACGAGCCAAAACCAGAGCACAGATTTACCTTTGGTCTTTGGACTGTGGGTAAATGTG 60
GGTAGAGATCCAATTCGGTGACGCTGTTAGAGAGAGACTGGACCCAGTTTACGTGGTTCAT 120
AAGCTGGCTGAGCTTGGTGCCTACGGTGTTAACCTTCACGACGAGGACCTGATCCCAAGA 180
GGTACTCCTCCTCAGGAGAGAGACCAGATCGTGAGAAGATTCAAGAAGGCTTTGGATGAA 240
ACTGGCTTGAAGGTCCAATGGTCACCGCCAACTTGTTCTCCGACCCTGCTTTCAAGGAC 300
GGTGCCTTCACTTCTCCAGACCCTTGGGTAGAGCCTATGCCTTAGAAAGTCTCTGGAG 360
ACCATGGACCTGGGTGCAGAGCTTGGTGCCGAGATCTACGTGGTCTGGCCAGGTAGAGAG 420
GGAGCTGAGGTGGAGGCCACTGGTAAGGCCAGAAAGGTCTGGGACTGGGTGAGAGAGGCT 480
CTGAACTTCATGGCCGCTACGCCGAGGACCAGGGATACGGTTACAGATTTGCCTTGGAG 540
CCAAAGCCTAACGAGCCAAGAGGTGACATTTACTTCGCCACCGTGGTTCTATGTTGGCC 600
TTTATTTCATACCCTGGACAGACCAGAGAGATTCGGTCTGAACCCAGAGTTCGCCCACGAG 660
ACCATGGCCGGTCTTAACTTTGTCCACGCCGTGGCCCAGGCTTTGGACGCCGGTAAGCTT 720
TTCCACATTGACTTGAACGACCAAAGAATGTCTAGATTTGACCAGGACTTGAGATTCGGT 780
TCTGAGAACTTGAAGGCTGCCTTTTTCTGGTGGACTTTGCTGGAATCTTCCGGTTACCAG 840
GGTCCAAGACACTTTGACGCCCACGCCCTGAGAACCGAGGACGAAGAAGGTGTTTGGGCC 900
TTGCCAGAGGTGTCATGAGAACCTACCTGATCTTAAAGGAAAGAGCTGAAGCCTTCAGA 960
GAGGATCCAGAGGTCAAGGAGCTTCTTGCCGCTTACTATCAAGAAGATCCTGCTGCCTTG 1020
GCCCTTTTGGTCCATACTCCAGAGAGAAGGCCGAAGCCTTGAAGAAGGCTGAGCTTCCA 1080
TTGAGAGCCAAGAGAGAAGAGGGTTATGCCCTGGAAAGACTGGACCAGCTGGCTGTGGAG 1140
TACTTGCTGGGTGTGAGAGGT 1164

```

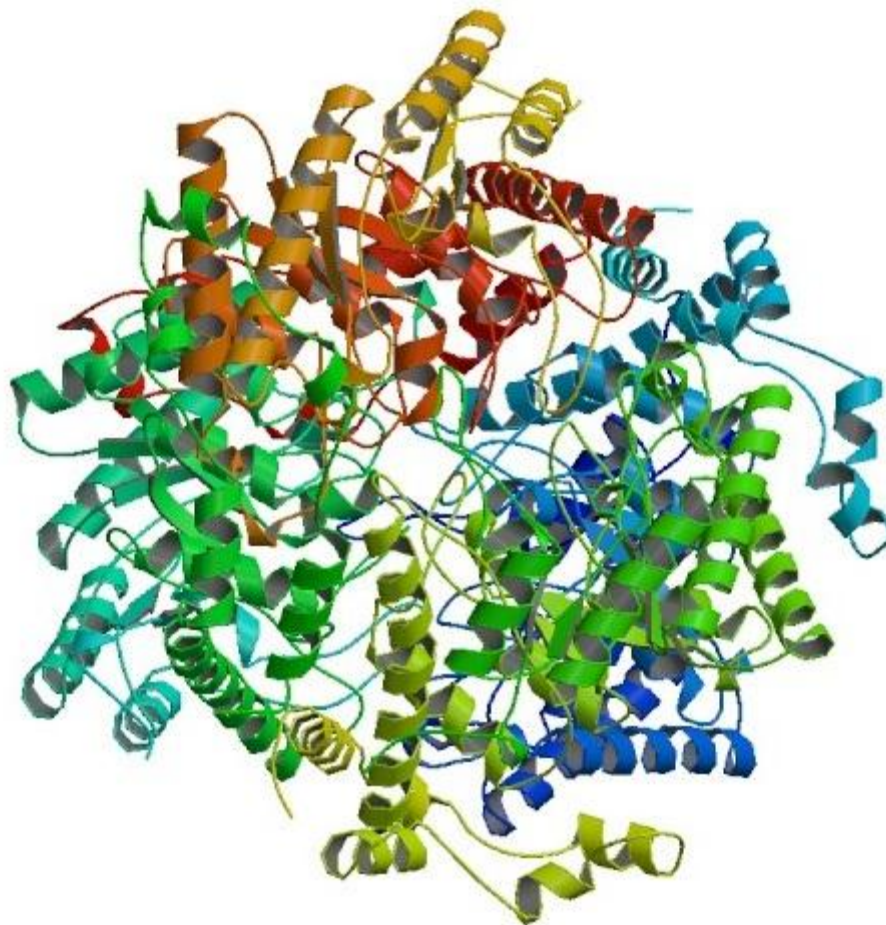


**Figure 2.** Crystal structure of glucose isomerase from *T. thermophilus*, determined by X-ray crystallography. Protein chains are colored from the N-terminal to C-terminal using a rainbow color gradient (RCSB Protein Data Bank, Accession Number: 1BXB).

Kovalevsky *et al.* (2010) investigated the metal ion roles on the isomerization reaction catalyzed by GI from *Streptomyces rubiginosus* by X-ray crystallography and neutron diffraction. Requirement for two divalent metal cations was reported to obtain a fully active GI. These metal binding sites were named as M1 and M2; where M1 is the structural metal sites for  $\text{Mn}^{2+}$ ,  $\text{Mg}^{2+}$ ,  $\text{Pb}^{2+}$ ,  $\text{Co}^{2+}$  and  $\text{Cd}^{2+}$  ions and M2 is the catalytic metal site showing larger variety of affinity for divalent metal cations, which may or may not inhibit the enzyme (Figure 3). Bhosale *et al.* (1996) stated that

ions with larger diameter than 0.8 Å inhibit the enzyme activity; *i.e.*,  $\text{Hg}^{2+}$ ,  $\text{Ag}^+$ ,  $\text{Cu}^{2+}$ ,  $\text{Ni}^{2+}$ , and  $\text{Zn}^{2+}$ .

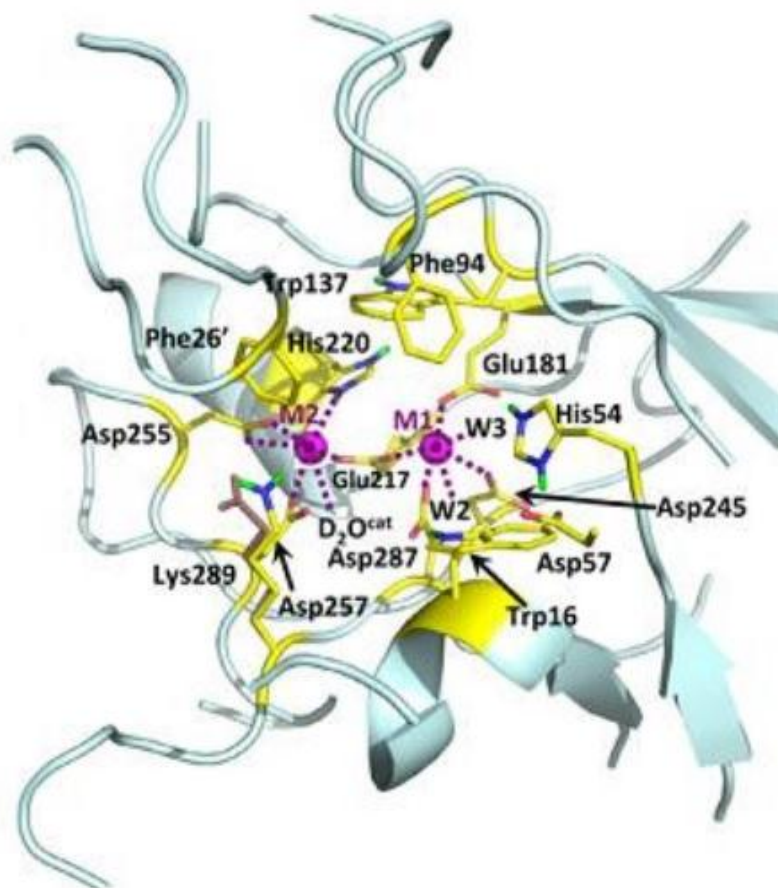


**Figure 3.** Metal binding sites of GI from *S. rubiginosus* (Kovalevsky *et al.* 2010). The residues coordinating metal cofactors, M1 and M2, are shown in magenta circles and lining cavity, Trp16, His54, Phe94, Trp137, and Phe26' are shown.

Identification of the location of the amino acids is essential to improve the catalytic activity of GI. Batt *et al.* (1990) identified the essential histidine residues in the active site of GI from *E. coli*, which are His-101 and His-271. Afterwards, Meilleur *et al.* (2006) located hydrogen atoms and showed that the initiation of reaction is

done by double protonation of His-53 at the active site and the reaction continued with the opening of the sugar ring via acid catalysis. As shown in Figure 1, isomerization reaction of glucose to fructose was proposed to be in three steps: ring opening, isomerization and ring closure (Kovalevsky *et al.* 2010).

Complete reaction mechanism proposed by Kovalevsky *et al.* (2010) is given in Figure 4. Some conformational changes take place in the active site during the time course of the reaction. For the initiation and implementation of the reaction, some amino acids play essential roles. In the first step, active site of the enzyme and reactive sugar cycle bind together where different arrangements of water molecules help the substrate to correctly bind to GI active site. The ring opening takes place in the next step where His-53 gives a proton to O5 temporarily, and takes it back after C1-O5 bond breaks. Within this step, neutral Lys-289 gets protonated and gives a proton to Asp-257. Then the isomerization step begins with the correct placement of O1 by Lys-183. During isomerization, a proton is transferred to C1 and O1 from C2 and O2, respectively.

Effect of codon optimization on the glucose isomerase production by *P. pastoris* was investigated by Ata *et al.* (2015). About 30% of the codons were changed according to codon usage bias of *P. pastoris* and Arg356, Arg365, Arg366 and Arg367 were replaced with Lys to prevent the cleavage of GI by Kex2 protease. (Table 2b) and 2.4-fold higher GI activity was obtained. It was also noted that the codon optimization did not affect optimum pH or temperature of thermostable GI.

### **2.3. Selection of the Host Microorganism**

Selection of the host microorganism is a crucial step for recombinant protein production. Depending on the targeted protein; several parameters should be considered when selecting the host microorganism such as high productivity, accessibility, limited production of by-products, being GRAS (generally recognized as safe), ability to do overexpression; post-translational modifications; intra- or extracellular production; and to grow in moderate conditions (Kirk and Othmer,

1994). Generally microorganisms are preferred for industrial protein production over plant and animal cell lines due to their ease of cultivation and fast rate of multiplication.

For recombinant GI production, *E. coli* and *Bacillus* species are the most widely-used expression systems (Bhosale *et al.* 1996). Other microorganisms used for GI production are as follows: *Schizosaccharomyces pombe* (Chan *et al.* 1986), *Streptomyces lividans* (Tan *et al.* 1990), *S. cerevisiae* (Moes *et al.* 1996; Walfridsson *et al.* 1996), and *P. pastoris* (Ata *et al.* 2015).

Yeasts are eukaryotic cells that can reach high cell densities in cheap, defined media, do post-translational modifications such as glycosylation, and disulfide bond formation and they can do extracellular protein expression. Because of these advantages, yeasts are suitable hosts for heterologous protein expression (Cos *et al.* 2006).

#### **2.4. The Host Microorganism: *Pichia pastoris***

*P. pastoris* is a facultative anaerobe methylotrophic yeast, widely used in biochemical and genetic research as well as industrial biotechnology (Kurtzmann, 2009). It is a eukaryote with oval-shaped cells which are 1 – 5 µm wide and 5 – 30 µm long. It lives in moderate temperatures (Macauley-Patrick *et al.* 2005) and has a broad pH range between 3 – 7 (Cereghino and Cregg, 2000). Cos *et al.* (2006) reported that over 600 proteins have been expressed in *P. pastoris* up today.

In 1970s, *P. pastoris* was firstly introduced by Philips Petroleum for the production of single cell proteins (SCP) as animal feed additive due to its ability to reach high cell densities in the presence of methanol as the only carbon source. They developed the first protocols for growth and media composition. But the oil crisis in 1973 increased methanol prices and made this process unfeasible (Ahmad *et al.* 2014). Afterwards, Cregg *et al.* (1985) developed *P. pastoris* expression system for heterologous protein expression under strong and tightly regulated inducible alcohol oxidase 1 promoter, P<sub>AOX1</sub>.

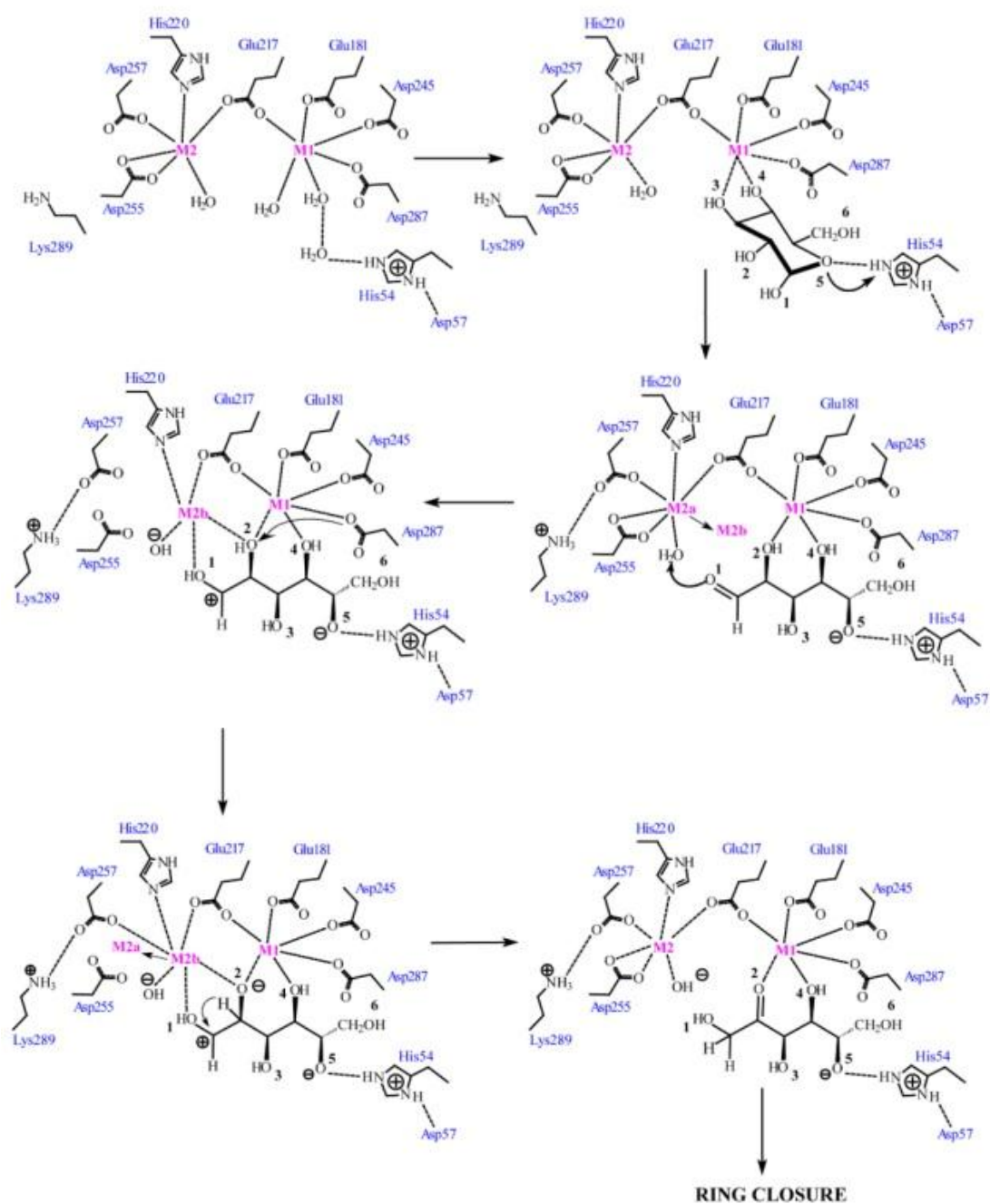


**Figure 4.** Complete reaction mechanism, as proposed by Kovalevsky *et al.* (2010).

From that day, *P. pastoris* expression system has been used for several different recombinant protein productions. So far, one of the most important breakthroughs in terms of *P. pastoris* being important for pharmaceutical industries is the FDA (Food and Drug Administration) approval of the recombinant pharmaceutical kallikrein inhibitor, Kalbitor® (Ahmad *et al.* 2014; Thomson, 2010).

*P. pastoris* has many advantages over other microorganisms. Due to its ability to perform post-translational modifications that higher eukaryotes perform, *P. pastoris* can be used to express proteins as biologically active molecules that would become inactive inclusion bodies in bacterial systems. It provides rapid growth in defined media with few endogenous protein secretion, has a good protein secretion capacity, and it is cheaper than using higher eukaryotes. Due to its physiological similarity to *S. cerevisiae*, which is the most widely-used yeast for protein expression, its metabolic manipulation and expression protocols are simple and readily available (Cereghino *et al.* 2002; Jahic *et al.* 2006).

However, there are some disadvantages of *P. pastoris* expression systems such as high proteolytic activity and non-native glycosylation. There are also some additional disadvantages resulting from using  $P_{AOX1}$  and  $P_{AOX2}$  promoters and methanol usage as the carbon source. Its usage for food and pharmaceutical protein production is controversial because of flammable and toxic properties of methanol; also handling and transportation of large amounts of methanol is expensive and troublesome (Çalık *et al.* 2015).

#### **2.4.1. Promoters of *Pichia pastoris***

Promoters are the regions of DNA that starts the transcription of a particular gene. The first enzyme in the methanol assimilation pathway of *P. pastoris* is alcohol oxidase. There are two alcohol oxidase genes in *P. pastoris*;  $P_{AOX1}$  and  $P_{AOX2}$ .  $P_{AOX1}$  is responsible for 90% of the production of alcohol oxidase enzyme in the cell while the remaining 10% is produced from  $P_{AOX2}$ . They are both used for heterologous protein expressions by *P. pastoris*;  $P_{AOX1}$  yielding higher expression levels than  $P_{AOX2}$



(Cos *et al.* 2006).  $P_{AOX1}$  and  $P_{AOX2}$  promoters are tightly regulated and inducible. They are induced in the presence of methanol and repressed in the presence of glycerol. Other than  $P_{AOX1}$  and  $P_{AOX2}$ , there are other promoters that are induced with methanol, such as the promoters of dihydroxyacetone synthase ( $P_{DAS}$ ) (Tschopp *et al.* 1987) and formaldehyde dehydrogenase ( $P_{FLD1}$ ) (Shen *et al.* 1998). Other important inducible promoters of *P. pastoris* are of high affinity glucose transporter ( $P_{GL}$ , induced with glucose limitation), isocitrate lyase ( $P_{ICL1}$ , induced with ethanol) (Menendez *et al.* 2003); alcohol dehydrogenase ( $P_{ADH1}$ , induced with glycerol and ethanol); enolase ( $P_{ENO1}$ , induced with glycerol); and glycerol kinase ( $P_{GUT1}$ , induced with glucose, glycerol and ethanol) (Cregg and Tolstorukov, 2012).

Contrary to inducible promoters; when protein expression is done with constitutive promoters, protein production is accomplished along with cell growth; therefore, the need for carbon source shift is eliminated. The most commonly used constitutive promoter of *P. pastoris* is glyceraldehyde-3-phosphate dehydrogenase promoter,  $P_{GAP}$ . Some of novel constitutive promoters of *P. pastoris* are reported as: promoter of translation elongation factor 1 ( $P_{TEF1}$ ), (Ahn *et al.* 2007); 3-phosphoglycerate kinase ( $P_{PGK1}$ ), (de Almeida *et al.* 2005); and putative aldehyde dehydrogenase ( $P_{G6}$ ), (Prielhofer *et al.* 2013). Although  $P_{TEF1}$ ,  $P_{GL}$ ,  $P_{DAS}$  and  $P_{FLD1}$  have been reported to reach expression levels similar to  $P_{GAP}$  and  $P_{AOX1}$ ;  $P_{AOX1}$  is still the most widely used promoter of *P. pastoris*, followed by  $P_{GAP}$ .

#### **2.4.1.1. Promoter of Glyceraldehyde-3-phosphate Dehydrogenase: $P_{GAP}$**

Because of the potential hazards of using methanol as the carbon source, researchers have been focusing on alternative promoters that would utilize safer carbon sources for environment and health. One of the promoters of *P. pastoris* by which methanol is not used as the carbon source is the promoter of glyceraldehyde-3-phosphate dehydrogenase (GAPDH) encoding gene. GAPDH is a homotetrameric protein with 333 amino acid residues, located in glycolysis pathway of *P. pastoris* metabolism (Figure 5).

Several heterologous proteins have been expressed at high levels under the promoter of GAPDH encoding gene,  $P_{GAP}$ , through fine-tuning bioreactor operation parameters, fermentation strategies and genetic manipulation. Glyceraldehyde-3-phosphate dehydrogenase gene was firstly isolated by Waterham *et al.* (1997) and its promoter was used for the expression of  $\beta$ -lactamase by using glucose as the carbon source. Higher expression levels were reached with  $P_{GAP}$  than with  $P_{AOXI}$ . In this expression system, proteins are expressed along with cell growth as long as the targeted protein is not toxic to the cell since toxic proteins would inhibit cell proliferation (Çalık *et al.* 2015). Generally, the highest expression levels were reached when glucose is used as the carbon source. In some cases, glycerol can be used as the carbon source and comparable expression levels with glucose can be reached.

#### **2.4.1.2. Comparison of glyceraldehyde-3-phosphate dehydrogenase and alcohol oxidase 1 promoters**

Several research groups compared the performances of  $P_{GAP}$ - and  $P_{AOXI}$ -driven expression systems. Some authors reported that  $P_{GAP}$  expression system is more efficient than  $P_{AOXI}$ ; while others reported the opposite. As mentioned before, Waterham *et al.* (1997) compared  $\beta$ -lactamase expression levels of  $P_{GAP}$  and  $P_{AOXI}$  and reported that  $P_{GAP}$  is a successful alternative to  $P_{AOXI}$  as they attained 1.7-fold higher enzyme activity by  $P_{GAP}$ -driven expression.

Similarly, Menéndez *et al.* (2004) reported fructose-releasing exo-levanase (LsdB) expression level of *P. pastoris* with  $P_{GAP}$  and  $P_{AOXI}$  and obtained 26.6 U ml<sup>-1</sup> LsdB under  $P_{GAP}$ , corresponding to 1.3-fold higher LsdB than obtained under  $P_{AOXI}$ . Moreover, they achieved more than 3.1-fold higher productivity while the process time is shortened by almost 2.5-fold. Although similar productivities were obtained for the production of human chitinase; higher protein titers were reported by Goodrick *et al.* (2001). On the other hand; Boer *et al.* (2000) obtained 5-fold higher cellobiohydrolase

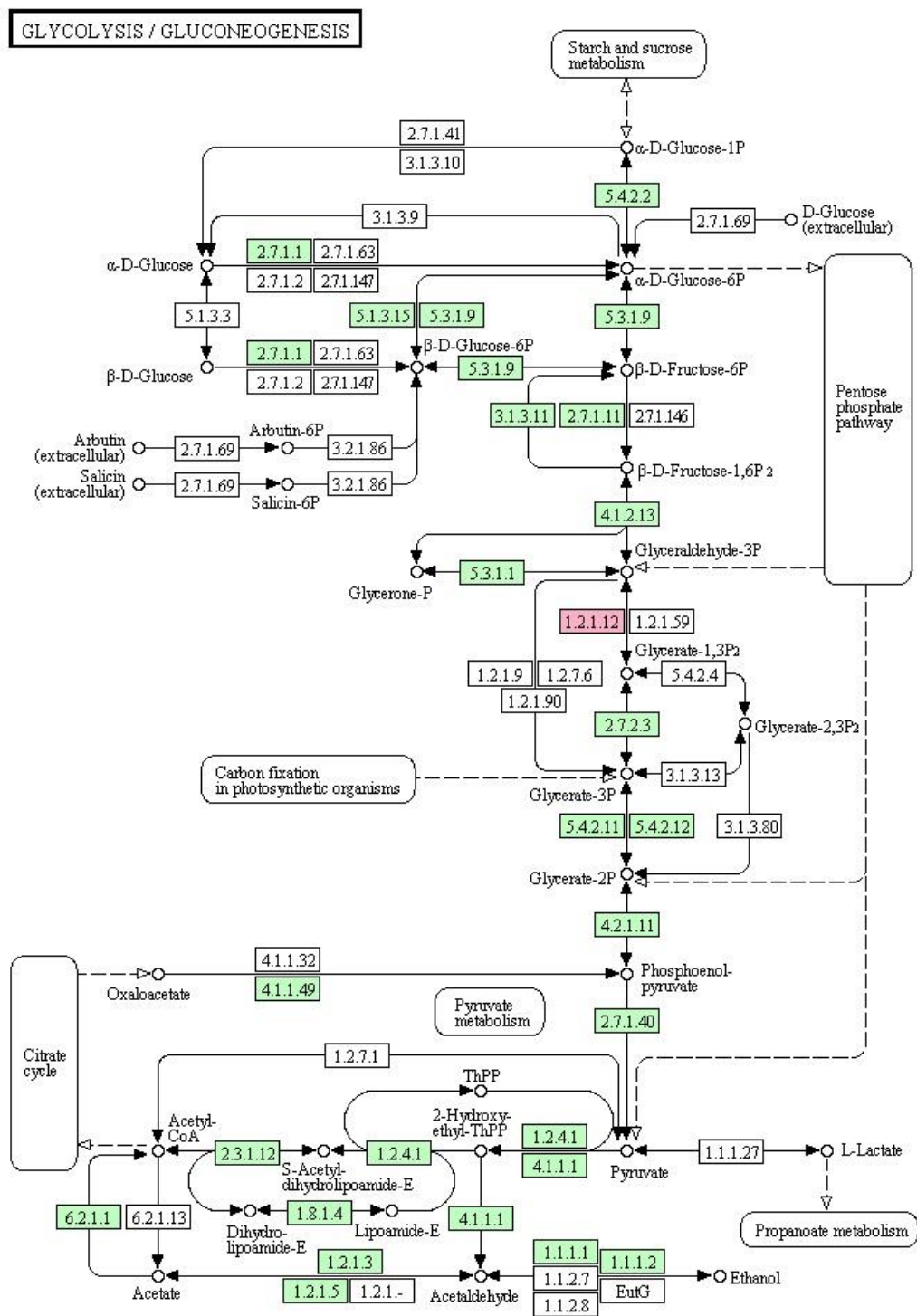


**Figure 5.** Glycolysis/Gluconeogenesis pathway of *P. pastoris*, GAPDH enzyme indicated with pink (GenomeNet Database, KEGG)

production with  $P_{AOXI}$  than  $P_{GAP}$ . Similarly, Vassileva *et al.* (2001) and Sears *et al.* (1998) obtained 1.4- and 8-fold higher recombinant protein expressions under  $P_{AOXI}$ , respectively.

#### **2.4.2. Central Carbon Metabolism of *Pichia pastoris***

Overexpression of heterologous proteins directly affects the metabolism of the cells. *P. pastoris* can produce energy by fermentation of sugars; *i.e.*, fructose and glucose, and sugar alcohols; *i.e.*, mannitol and sorbitol, and by oxidation of fermentation products; glycerol, ethanol and lactate. Being a methylotrophic yeast, *P. pastoris* can utilize sources with only one carbon atom, such as methanol. Unlike *S. cerevisiae*, *P. pastoris* lacks invertase gene so it cannot metabolize sucrose (Çalık *et al.* 2015). Schematic representation of central carbon metabolism of *P. pastoris* is given in Figure 6.

There is a specific order for the uptake of the carbohydrates with intermittent lag phases as the genes responsible for transporters are tightly regulated by the glucose concentration in the medium. Limited glucose uptake rates prevent *P. pastoris* metabolism from overflow, resulting in lower cell yield and targeted product formation.

Although glucose and glycerol enter the carbon metabolism from glycolysis pathway, they have different regulations. In *S. cerevisiae*, glucose addition to the cultivation medium in which cells are growing on glycerol causes rapid changes in the pattern of protein phosphorylation and transcriptional state of the genome. Zaman *et al.* (2008) reported that more than 40% of the genes change their expressions by at least 2-fold minutes after the addition of glucose to the medium containing glycerol for cell growth. The comparative effect of glucose and glycerol has not been investigated yet in *P. pastoris*; however, its response can be expected to be similar to some extent with *S. cerevisiae*.

Heyland *et al.* (2011) investigated the effect of recombinant protein overexpression on the cells' metabolism growing on glucose. TCA cycle is found to have the highest

response to recombinant protein overexpression since protein synthesis is an energy consuming process. Metabolic burden on the cell metabolism resulting from protein overexpression is compensated by decreasing the cell yield on ATP, specific cell growth rate, glucose consumption rate and byproduct formation rate. The limiting metabolic process is found to be the synthesis of energetically costly amino acids.

#### **2.4.3. Post-Translational Modifications and Protein Secretion**

One of the most important reasons for yeasts to be favorable host microorganisms is their ability to do some post-translational modifications such as correct protein folding, disulfide bond formation, glycosylation, and signal peptide development.

When heterologous proteins are overexpressed, they usually result in misfolded, inactive protein aggregates. Lack of disulfide bond formation and saturation of the cellular folding machinery can be the reasons for misfolded protein formation (Baneyx, 1999; Schlieker *et al.* 2002).

If a protein is misfolded, it causes stress to the cell by accumulating in the endoplasmic reticulum (ER). To reduce the stress, misfolded proteins are degraded by ER-associated degradation. When the stress is prevented, immature proteins are stabilized by the ER-resident chaperones and the help of disulfide isomerase and other proteins that facilitate protein folding to reduce stress and increase recombinant protein secretion (Idiris *et al.* 2010).

Some proteins require some hydrocarbons to be attached to certain amino acid groups for the correct folding, stability and solubility. This process is known as “glycosylation” and involves several enzymes to work concomitantly. There are two types of glycosylation (*O*- and *N*- linked) and *P. pastoris* is capable of doing both of them with some differences from mammalian cells. *P. pastoris* cells only add mannose residues while in mammalian cells oligosaccharides composed of galactose, *N*-acetylgalactosamine and sialic acid can be added as well (Cereghino and Cregg, 2000).

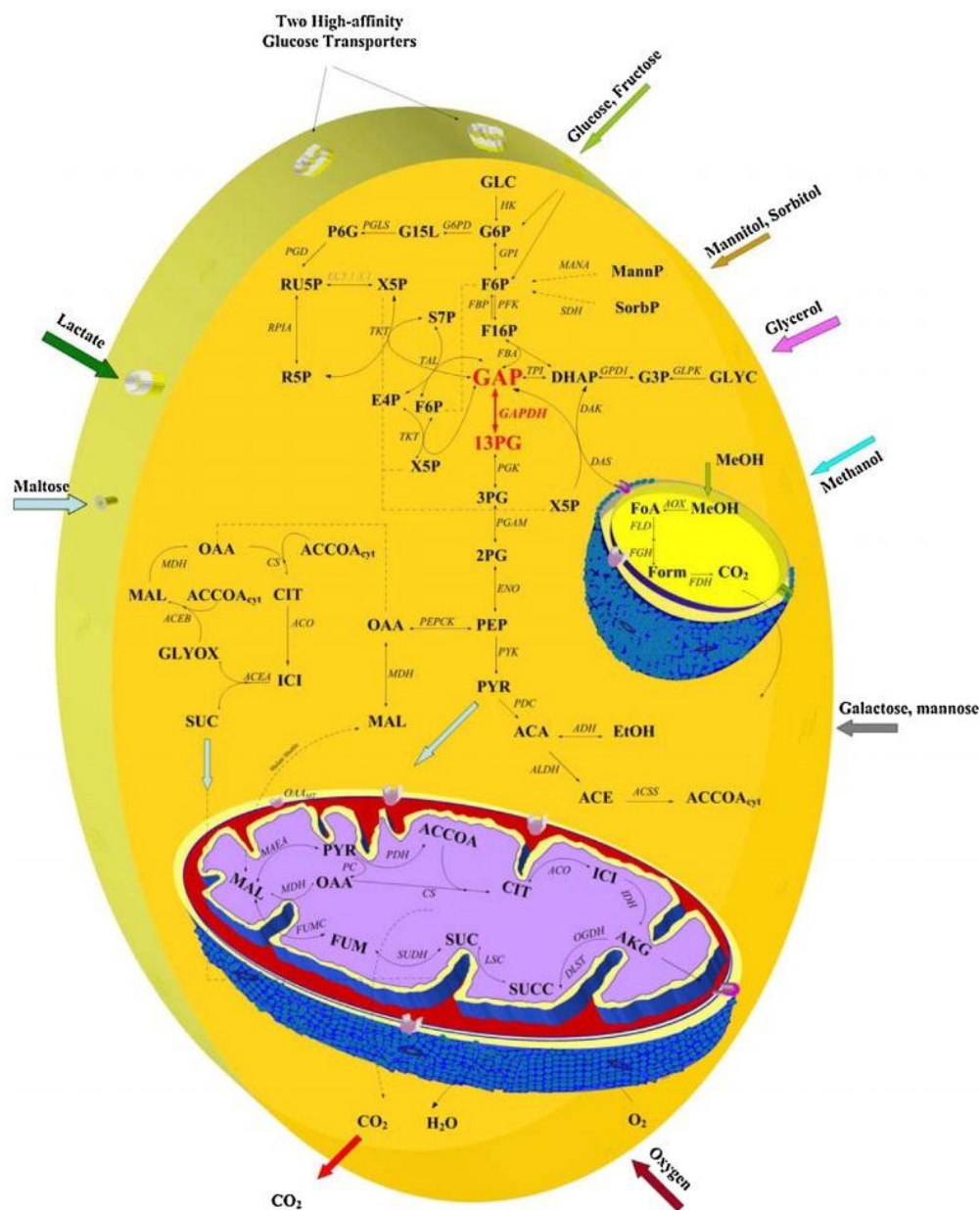


**Figure 6.** Central carbon metabolism of *P. pastoris* (Çalık *et al.* 2015).

Although the mode of production, extracellular or intracellular, mainly depends on the characteristics of the protein, extracellular production is usually more favorable because it reduces the cost of downstream processing. A signal sequence is necessary

in order to secrete proteins to the extracellular environment. Native signal sequences of proteins can be used as well as different signal sequences like alpha-mating factor pre-pro leader sequence ( $\alpha$ -MF) (Macauley-Patrick *et al.* 2005).

In *P. pastoris*, secretion of the proteins with  $\alpha$ -MF is conducted in three stages. First, protein is transported to ER where pre-domain is removed by signal peptidase, in the second stage pro-domain is removed in Golgi apparatus by dibasic endo-peptidase (*kex2*) activity. Lastly, the protein is packed to secretory vesicles and secreted to extracellular medium (Daly and Hearn, 2005).

#### **2.4.4. Proteolytic Degradation**

Degradation of the produced proteins by proteases is a major problem in *P. pastoris* expression system because it causes reduction in protein yield, protein activity, and contamination of the product by degradation intermediates (Idiris *et al.* 2010). Some reasons for high proteolytic activity are change in pH and temperature, carbon source shift, and foreign chemicals in the fermentation medium. Since *P. pastoris* can reach high cell concentrations, especially in fed-batch operations, accumulation of proteases in extracellular medium together with cell lysis are the main factors of proteolytic degradation in *P. pastoris* expression systems (Shen *et al.* 1998).

To prevent proteins from proteolytic degradation, adding casamino acids is known to be an effective method (Pal *et al.* 2006). Goodrick *et al.* (2001) speculates that in fed-batch processes, proteins produced are exposed to higher and higher concentration of proteolytic enzymes as fermentation time passes. Stabilization of the recombinant proteins and avoidance of proteolytic activity can be achieved by addition of casamino acids. Similarly, Pal *et al.* (2006) and Khasa *et al.* (2007) obtained higher yields of cell and recombinant protein concentration by the addition of casamino acids. However, development of protease-deficient strains to avoid proteolytic degradation is known to be the most effective strategy when changing the fermentation parameters fail to solve this problem.

## 2.5. Medium Design

Compared to inducible expression systems, where the inducer is also the carbon source in most cases, there are more variety of carbon sources in constitutive expression systems. Glucose, glycerol, methanol and oleic acid have been reported as the carbon sources for  $P_{GAP}$ -driven expression systems (Zhang *et al.* 2009); and fructose, sorbitol, mannitol and trehalose are also possible carbon sources as they can also be utilized by the carbon metabolism in glycolysis pathway (Çalık *et al.* 2015).

Waterham *et al.* (1997) compared glucose, glycerol, oleic acid and methanol as carbon sources and the maximum activity of  $\beta$ -lactamase was achieved in glucose; 73%, 45%, and 36% of activity with glucose was achieved with glycerol, oleic acid and methanol, respectively. Pal *et al.* (2006) compared the effect of glucose, glycerol and sorbitol for human granulocyte-macrophage colony-stimulating factor (hGM-CSF) production in shake-flasks. The results showed that maximum cell density was reached with glycerol but the highest recombinant protein concentration was achieved with glucose. Similarly, glucose yielded higher recombinant protein yield than glycerol in shake-flask experiments, as reported by Fei *et al.* (2009). On the other hand, Goodrick *et al.* (2001) reported higher recombinant human chitinase production with glycerol while cell concentration was higher with glucose in continuous expression. Then, Garcia-Ortega *et al.* (2013) used a strategy for human antigen-binding fragment (Fab) production such that glycerol was used as the carbon source for the batch phase, then the process was shifted to fed-batch with glucose as the carbon source. This strategy was reported as the most successful combination of the carbon sources for Fab production. By these results, it can be interpreted that there are several factors affecting the efficiency of the carbon source, such that the target protein, fermentation mode or the aim of fermentation; *i.e.*, aiming high cell concentration or recombinant protein yields. Therefore, the choice of the carbon source should be done according to these parameters.

As mentioned earlier, casamino acids can be used both to increase product yield and prevent proteolytic degradation. As reported by Fei *et al.* (2009), instead of casamino



acids, addition of precursor amino acids to the fermentation medium can increase the targeted protein yield as well. In these cases, amino acid composition of the targeted protein should be considered since rate-limiting amino acid may differ for each protein production. Proteolytic degradation of the recombinant protein should be taken into consideration as well as the amino acid composition. Addition of amino acids to the fermentation medium facilitates the metabolic network of *P. pastoris* to increase cell concentration and recombinant protein production (Çalık *et al.* 2015).

## **2.6. Bioreactor Operation Conditions**

After the designation of the expression system and feed medium components, bioreactor operation modes; *i.e.*, pH, temperature and oxygen transfer conditions should be investigated for optimum conditions.

### **2.6.1. pH**

As a rule of thumb, pH of the fermentation medium should not be close to the isoelectric point (pI) of the targeted protein in order to avoid precipitation. Therefore, pH value that the fermentation should be carried is dependent on the desired protein. Although *P. pastoris* is known to survive at a wide range of pH; values between 5.0 and 5.5 under pH-controlled conditions are reported to be optimum for recombinant protein expression and maintaining cell viability. In some cases, pH = 6.0 has also been reported to be the optimum such as methionine adenosyltransferase (MET) (Hu *et al.* 2008), *Yarrowia lipolytica* lipase LIP2 (Wang *et al.* 2012), and D-amino acid oxidase (Zheng *et al.* 2006) production.

### **2.6.2. Temperature**

In general, while higher temperatures result in protein denaturation, lower temperatures cause lower reaction rates. Therefore, bioprocesses should be carried out at controlled, isothermal and optimum temperatures. Although 30°C has been reported as the optimum temperature for *P. pastoris* by many studies (as cited in Cos *et al.* 2006; Çalık *et al.* 2015), there are some studies done in lower temperatures to increase the solubility of oxygen to enhance oxygen transfer rates at an expense of

lower reaction rates and metabolic fluxes. Dragosits *et al.* (2009) investigated the effect of decreasing the fermentation temperature to 20°C on the proteome of *P. pastoris*. In this study, while fluxes through TCA cycle were reduced, a 3-fold increase in recombinant protein production was observed.

### 2.6.3. Dissolved Oxygen Concentration

Oxygen concentration in the fermentation medium is related with its dynamics with cultivation time. Oxygen mass balance equation in the bioreactor liquid medium can be expressed as a verbal equation as follows:

$$(oxygen_{in}) - (oxygen_{out}) + (oxygen\ uptake\ rate) = (accumulation\ of\ oxygen) \quad (1)$$

Difference of the first two terms is equal to oxygen transfer rate (OTR) and it is balanced with oxygen uptake rate ( $r_O = OUR$ ) of *P. pastoris* cells. OUR is related with cell metabolism and the dynamics of intracellular reaction network. OTR and OUR are important fermentation characteristics for recombinant protein production rather than dissolved oxygen concentration ( $C_{DO}$ ).  $C_{DO}$  only shows the instantaneous accumulation of oxygen in the production medium and can be measured by an online oxygen probe attached to the bioreactor. Since oxygen transfer into the cell strongly affects cell metabolism and intracellular metabolic fluxes, to fine-tune bioreactor performance according to the physiology of the cells, the regulatory effect of oxygen transfer requires further investigation (Çalık *et al.* 2000)

In *P. pastoris*, dissolved oxygen is generally kept at 20-30% saturation by supplying air with a cascade system with constant agitation speed (Gasser *et al.* 2006; Zheng *et al.* 2006; Zhang *et al.* 2007; Fei *et al.* 2009; Çalık *et al.* 2015). Air is supplemented along with pure oxygen when feeding only air is not enough to meet desired dissolved oxygen concentration levels because oxygen consumption rate increases with increasing cell concentration.

*P. pastoris* fermentation strategies can also be dependent on constant oxygen transfer rate. In these processes, air flow rate is adjusted in a manner such that the aeration rate (volume air per reactor volume per minute, vvm) is kept constant throughout the

process. By its nature, this kind of process does not take the oxygen demand of the cells into account but supplies a constant oxygen flow per unit volume at all times.

Hu *et al.* (2008) reported MAT production by limited glycerol feeding with keeping dissolved oxygen (DO) at 50%, 25% and 0%. Lower DO values improved specific glycerol uptake rate ( $q_{\text{Gly}}$ ) and specific growth rate ( $\mu$ ). Keeping DO at 0% did not depress, but increased respiratory activity of the cells, resulting in higher  $q_{\text{Gly}}$  values. Baumann *et al.* (2008), reported similar results for Fab production with choosing glucose as the carbon source. Compared to limited-aerobic (10.91% DO) and fully-aerobic (20.97% DO) fermentation; hypoxic (5.97-8.39% DO) conditions resulted in 2-fold decrease in biomass, significant ethanol formation and 2.5-fold increase in specific product formation rate ( $q_p$ ). Similar to Hu *et al.* (2008), they showed that limitation on oxygen does not repress glucose consumption but results in a switch to an alternative metabolic pathway leading to increased specific substrate consumption rate and by-product formation as *P. pastoris* behaves facultative anaerobically in the presence of glucose. With these findings, they developed a feedback control system to keep ethanol concentration in the medium at 1% (v/v) for three different protein production while keeping  $C_{\text{DO}}$  at hypoxic levels and compared this new strategy with standard cultivation where glucose was fed with a constant rate of  $F = 161.7 \text{ g h}^{-1}$  while keeping oxygen concentration above 20% saturation. Compared to standard cultivation conditions, hypoxic fed-batch strategy and keeping ethanol concentration constant resulted in 13% higher product titer, reduced fermentation time by more than 3-fold and biomass concentration decreased by almost 1.5-fold. Again 2.5-fold increase in  $q_p$  was observed and  $\mu$  remained the same. They speculated that since glycolytic fluxes are higher in hypoxic conditions; glycolytic genes and promoters such as  $P_{\text{GAP}}$  are upregulated.

Later on, Baumann *et al.* (2010) examined the effect of  $C_{\text{DO}}$  on the interaction between the transcription of the genes and heterologous protein expression in *P. pastoris* cells. They used the data from the previous study (Baumann *et al.* 2008) and investigated the cellular adaptations on low oxygen concentrations and recombinant

protein production. Under hypoxia, most of the abundant proteins were involved in amino acid metabolism, glycolysis and general stress response while the proteins involved in TCA cycle, oxidative stress response and vitamin metabolism were expressed at lower levels. The increase in the transcription level of glycolytic genes under hypoxia supports their speculation in the previous study that Fab productivity increased under hypoxia as a result of the upregulation of the glycolytic genes, and the genes under the control of glycolytic promoters, such as  $P_{GAP}$ .

Since *P. pastoris* is a Crabtree-negative yeast, it is more vulnerable to changes in the availability of dissolved oxygen compared to the Crabtree-positive yeast *S. cerevisiae* (Baumann *et al.* 2010). Therefore, parameters related with oxygen transfer of microbial processes; such as oxygen transfer characteristics; oxygen uptake rate (OUR), oxygen transfer rate (OTR), and volumetric mass transfer coefficient ( $K_{La}$ ), along with bioreactor hydrodynamics for recombinant protein production by *P. pastoris* should be systematically studied in order to gain further insight about the bioprocess characterization.

## **2.7. Oxygen Transfer Characteristics**

As oxygen has low solubility in fermentation media (nearly 10 ppm), oxygen transfer is usually the rate limiting step for bioprocesses and determined the overall reaction rate.

The process of oxygen transfer from gas phase as an air bubble to the solid phase (into the cell) is divided into nine steps as explained by Whitman's (1923) two film theory (Garcia-Ochoa *et al.* 2010) as follows (Figure 7):

- (i) Transfer from the bubble to the gas liquid interface,
- (ii) Movement along the gas-liquid interface,
- (iii) Diffusion through the liquid film around the bubble,
- (iv) Movement through the bulk liquid (fermentation broth),
- (v) Diffusion through the stagnant liquid film around the cell,

- (vi) Movement along the liquid-cell interface and – if cells are within a flock, clump or a solid particle – diffusion through the solid and then to the cell,
- (vii) Transfer through the cytoplasm towards the reaction site,
- (viii) Reactions involving O<sub>2</sub> consumption and CO<sub>2</sub> formation,
- (ix) Transfer of the gases formed as a result of the reaction in the reverse direction.

Transportation of oxygen across the bulk liquid gets faster when the cells are homogeneously suspended in the well-mixed fermentation medium without any aggregation. Then, the second part of step (vi) is negligible and nonpolar molecules can be transported through the cell membrane by passive transportation (Campbell and Reece, 2011). Resistance to the transportation along the cytoplasm to the reaction site is generally neglected because of the small size of the microorganism (Nielsen and Villadsen, 1994). Stagnant liquid around the gas bubble represents the greatest limitation to mass transfer. In such a system, mass transfer can be modelled by Whitman's (1923) two film theory (Figure 8):

$$j^0 = k_G \cdot (p_G - p_i) = k_L \cdot (C_{DO,i} - C_{DO}) \quad (2)$$

$j^0$  is the molar flux of oxygen across the gas-liquid interface (mol m<sup>-2</sup> s<sup>-1</sup>),  $k_G$  and  $k_L$  are local (gas side and liquid side, respectively) mass transfer coefficients,  $p_G$  is the partial pressure of oxygen in gas bubbles,  $C_{DO}$  is the dissolved oxygen concentration in the liquid and subscript  $i$  represents the interface.

When overall mass transfer is considered, equation (2) can be written as:

$$J^0 = K_G \cdot (p_G - p^*) = K_L \cdot (C_{DO}^* - C_{DO}) \quad (3)$$

where  $p^*$  is the oxygen pressure in equilibrium with the liquid phase and  $C_{DO}^*$  is the oxygen saturation concentration in the bulk liquid in equilibrium with the bulk gas phase,  $K_G$  and  $K_L$  are overall mass transfer coefficients according to Henry's law,  $p^* = H \cdot C_{DO}^*$ .

Combining equations (2) and (3):

$$\frac{1}{K_L} = \frac{1}{H \cdot k_G} + \frac{1}{k_L} \quad (4)$$

Since solubility of oxygen in liquid broths is low, Henry's constant is large, therefore first term on the right hand side becomes negligible. Therefore overall mass transfer coefficient can be taken as equal to local mass transfer coefficient in liquid side,  $K_L = k_L$ . Oxygen transfer rate, (OTR,  $N_{O_2}$ ) can be obtained by multiplying overall molar flux,  $J^0$ , with interfacial area per unit volume of liquid,  $a$ :

$$OTR = N_{O_2} = J^0 \cdot a = K_L \cdot a (C_{DO}^* - C_{DO}) \quad (5)$$

Due to the difficulties of measuring  $k_L$  and  $a$  separately, the product of them,  $k_L a$  is reported and this parameter is named as volumetric mass transfer coefficient. Determination of this parameter is crucial as it is the key element to quantify the effects of dissolved oxygen and oxygen transfer characteristics on bioprocess performance.

Differential mass balance for dissolved oxygen in the bioreactor can be written as:

$$K_L a \cdot V (C_{DO}^* - C_{DO}) - q_{O_2} \cdot C_X \cdot V = \frac{d(C_{DO} \cdot V)}{dt} \quad (6)$$

If the reactor volume is constant and well-mixing is established, equation (6) becomes:

$$K_L a (C_{DO}^* - C_{DO}) - q_{O_2} \cdot C_X = \frac{dC_{DO}}{dt} \quad (7)$$

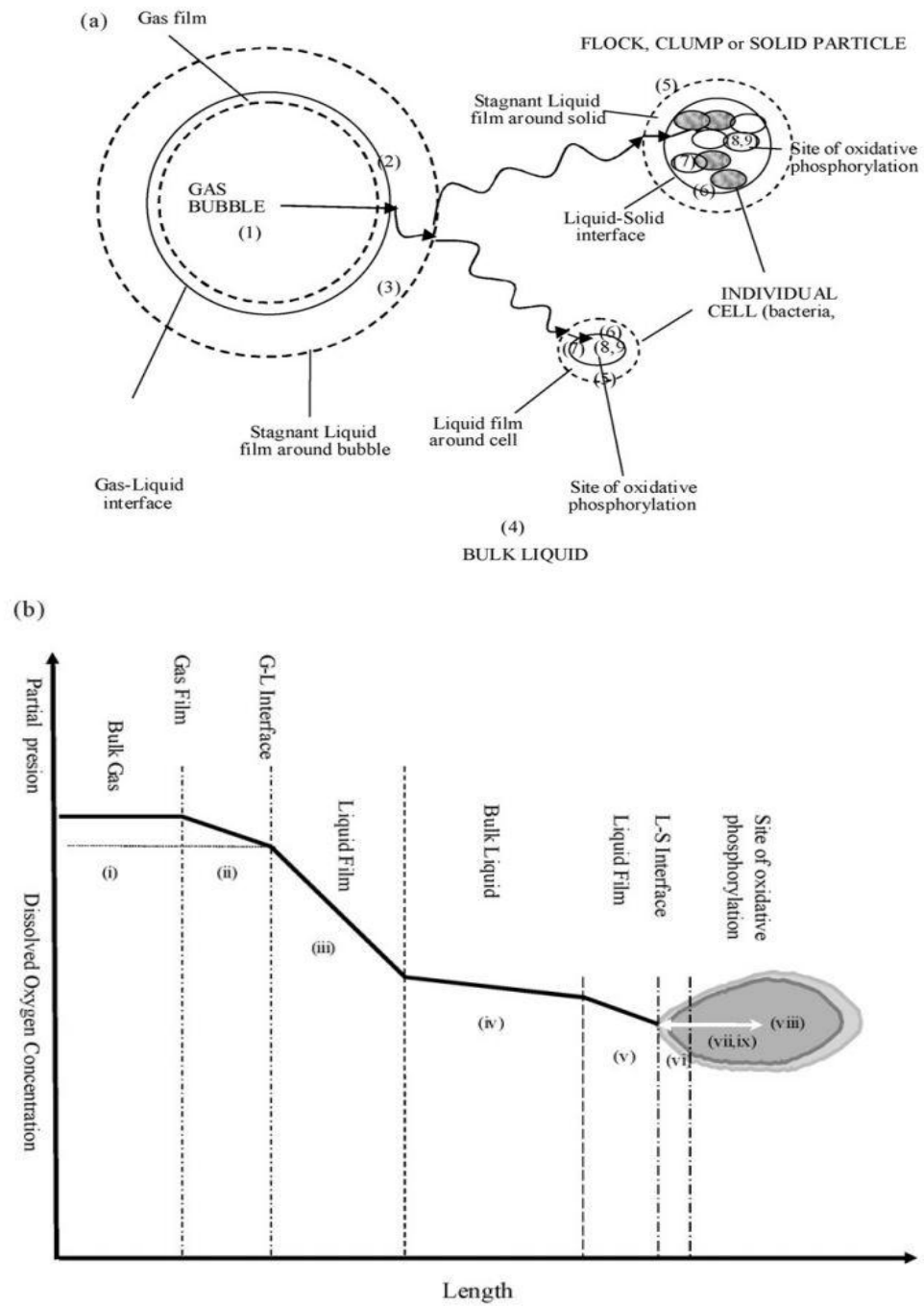


**Figure 7. (a)** Oxygen transfer from gas bubble into the cell **(b)**  $C_{DO}$  profile along the oxygen transfer process.

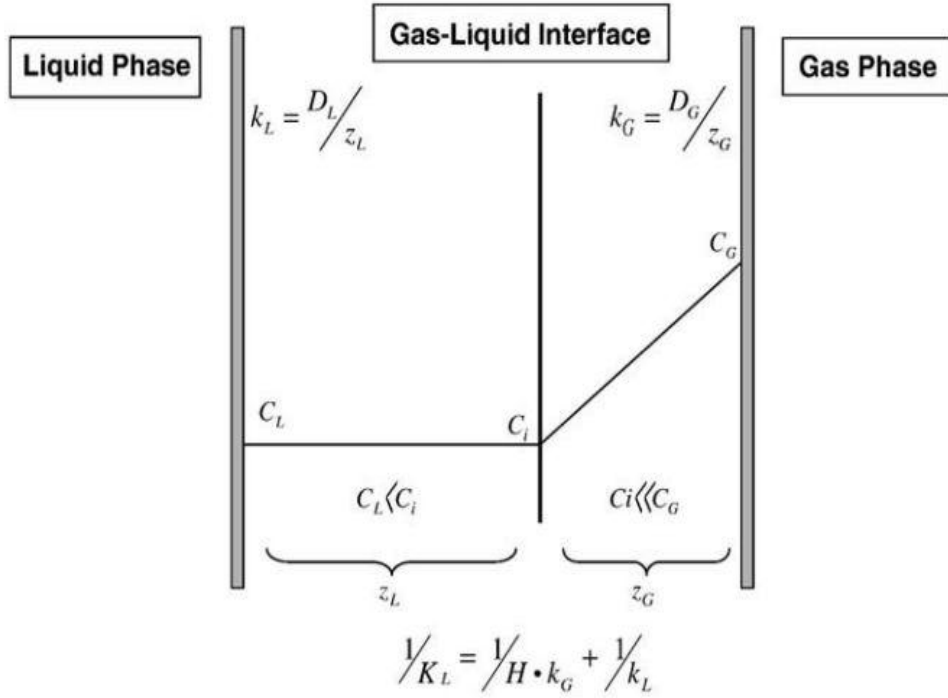


**Figure 8.** Schematic representation of the gas-liquid interface according to two film theory (Garcia-Ochoa and Gomez, 2009).

where  $\frac{dC_{DO}}{dt}$  term is the rate of oxygen accumulation in the liquid phase,  $K_L a \cdot (C_{DO}^* - C_{DO})$  term is OTR and  $q_{O_2} \cdot C_X$  term is OUR, where  $q_{O_2}$  is specific oxygen uptake rate and  $C_X$  is cell concentration.

$$OTR + OUR = \frac{dC_{DO}}{dt} \quad (8)$$

### 2.7.1. Experimental Determination of Volumetric Mass Transfer Coefficient

There are several methods to determine  $K_L a$  experimentally, which can be divided into two subgroups by one of which  $K_L a$  is measured in the absence of microorganisms or with nonviable cells to eliminate the effect of biochemical reactions ( $OUR = 0$ ); and in the other one, with the presence of microorganisms that



can utilize oxygen ( $OUR \neq 0$ ) (Garcia-Ochoa and Gomez, 2009). Some of these techniques are sodium sulfite oxidation method, oxygen balance method, static gassing-out method and glucose oxide method (Rainer, 1990).

OTR, OUR and  $K_La$  are usually measured by different methods for the same experiment but these values can be obtained simultaneously by applying dynamic method which is based on the respiratory activity of the microorganisms. In this method, firstly gas flow rate is set to zero and agitation rate decreased to the lowest possible value to eliminate surface aeration.  $C_{DO}$  is monitored by the oxygen probe. By eliminating the transfer of oxygen into the bioreactor, OTR is set equal to zero and equation (8) simply becomes:

$$OUR = \frac{dC_{DO}}{dt} \quad (9)$$

Before reaching critical  $C_{DO}$  level, oxygen supply is turned on again and agitation speed is set to normal bioreactor operation conditions to maintain the same oxygen transfer characteristics. In this time interval,  $C_{DO}$  increases until it reaches its steady value (Figure 9). By using the calculated OUR value from equation (9),  $K_La$  can be determined by using equation (8). Knowing  $C_X$  and calculating  $q_{O_2}$  from OUR, one can integrate equation (8) to get:

$$q_{O_2} \cdot C_X \cdot \Delta t + \Delta C_{DO} = K_La \cdot \int_{t_1}^{t_2} (C_{DO}^* - C_{DO}) \cdot dt \quad (10)$$

Equation (10) can be used to calculate  $K_La$  several times during one bioprocess by solving this equation for each data set of  $C_{DO}$  vs. time. Alternatively, Equation (8) can be used to plot the graph of  $C_{DO}$  vs.  $\frac{dC_{DO}}{dt} - r_{O_2}$ , whose slope gives  $-\frac{1}{K_La}$  (Figure 10).

The presence of microorganisms in the reaction medium as solid particles represents a physical resistance to mass transfer of oxygen. Therefore,  $K_L a_0$  is also determined by using the same method in order to interpret the effect of this resistance. This method is applied before cells are inoculated to the bioreaction medium. The only difference of this method from measuring  $K_L a$  is the supplementation of nitrogen to decrease  $C_{DO}$  as oxygen cannot be utilized in the absence of the viable microorganisms. Therefore, equation (7) simplifies to:

$$K_L a_0 (C_{DO}^* - C_{DO}) = \frac{dC_{DO}}{dt} \quad (11)$$

### 2.7.2. Other Parameters Involving Oxygen Transfer Characteristics

Although determination of OUR, OTR and  $K_L a$  are considered to be the major parameters to understand oxygen transfer characteristics of bioprocesses; other parameters such as maximum possible oxygen transfer rate ( $OTR_{max}$ ), maximum possible oxygen uptake rate ( $OUR_{max}$ , also known as oxygen demand,  $OD$ ), Damköhler number (Da), and effectiveness factor ( $\eta$ ) need to be calculated to gain a deeper insight of oxygen transfer characteristics and mass transfer limitations in bioprocesses (Çalık *et al.* 1998).

Maximum oxygen transfer rate can be obtained when the driving force, concentration difference, is the highest. For that reason, dissolved oxygen concentration in the fermentation medium should be equal to zero. Therefore:

$$OTR_{max} = J_{0,max} \cdot a = K_L a \cdot C_{DO}^* \quad (12)$$

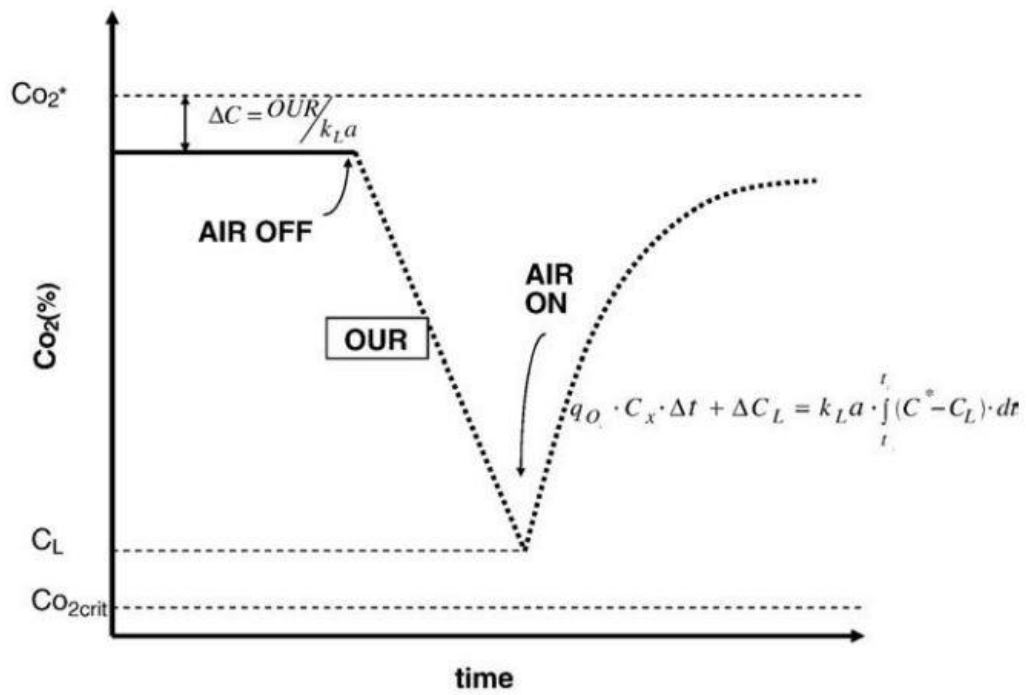


**Figure 9.** Change in  $C_{DO}$  during the application of dynamic method (Garcia-Ochoa and Gomez, 2009).

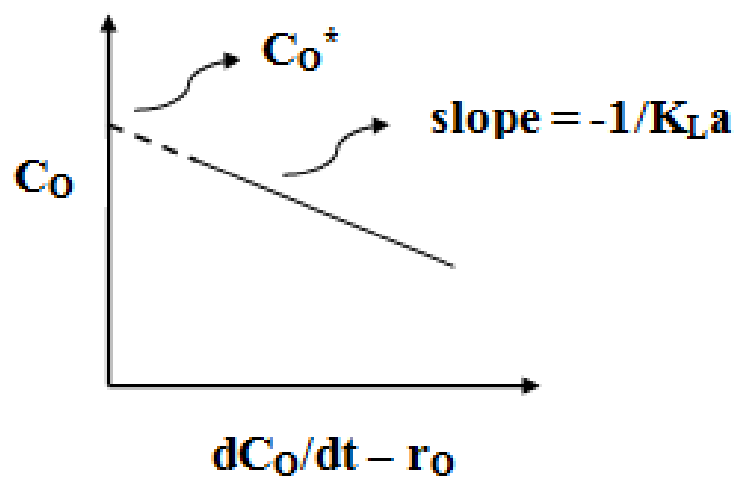


**Figure 10.** Determination of  $K_La$  by dynamic method.

Maximum oxygen utilization rate is equal to:

$$OUR_{\max} = -r_{O_2, \max} = \frac{C_X \cdot \mu_{\max}}{Y_{X/O_2}} \quad (13)$$

where  $\mu_{\max}$  is equal to maximum specific cell growth rate and  $Y_{X/O_2}$  represents the oxygen yield coefficient on cell, which is equal to mass of cell generated per unit mass of oxygen consumed.

Damköhler number (Da) is a dimensionless number defined as the ratio of reaction rate to mass transfer rate which characterizes if there is a reaction or mass transfer limitation in the system. In bioprocesses, a modified Damköhler number is defined as the ratio of maximum possible oxygen utilization rate to maximum oxygen transfer rate:

$$Da = \frac{OUR_{\max}}{OTR_{\max}} \quad (14)$$

To calculate the efficiency of the oxygen uptake rate facilitated by the bioprocess, the ratio of OUR to  $OUR_{\max}$  is defined as the effectiveness factor ( $\eta$ ):

$$\eta = \frac{OUR}{OUR_{\max}} \quad (15)$$

In literature Çelik *et al.* (2009) used these parameters to determine the oxygen transfer characteristics of recombinant human erythropoietin (rHuEPO) production by *P. pastoris* using  $P_{AOXI}$  and sorbitol as the co-substrate and Çalık *et al.* (1998, 2000) for serine alkaline protease (SAP) production by *B. licheniformis*.

## 2.8. Influence of Geometrical Parameters of the Bioreactor on Mass Transfer Coefficient and Mixing

Hydrodynamic conditions of the bioreactors strongly affect the gas-liquid mass transfer in bioprocesses which are determined by the properties of the culture, operation temperature and pressure, the presence of viable cells that can consume oxygen and geometrical characteristics of the bioreactor (Garcia-Ochoa and Gomez,

2009). Stirred tank bioreactors are widely used for bioprocesses as they provide excellent heat and mass transfer rates and mixing. Many parameters affect the mass transfer and mixing conditions but the most important ones are the stirrer speed, baffle type, impeller type, diameter and number.

Lu *et al.* (1997) investigated the effects of the width and number of baffles in stirred tanks with Rushton turbine impellers and showed that there is an optimum number of baffles for the improvement of mixing and mixing time. For the vessels having impeller over vessel diameter ( $D/T$ ) ratio larger than 0.2; when the baffle number was more than 8, mixing was interrupted by the sparging gas through the impeller and this increases mixing time. They found the optimum number of baffles to be 4 for mixing and oxygen dispersion.

Karimi *et al.* (2013) used three different impellers (Rushton turbine, pitched 4-blades and pitched 2-blades) with six configurations to investigate their effects on oxygen transfer. The results were reported to be in favor of twin Rushton turbine with 23% to 77% improvement on  $K_{La}$ . Compared to pitched 2- and 4-blades, Rushton turbine impellers were found to break and disperse air bubbles more effectively since they have larger cross sectional area.

Schaepe *et al.* (2013) tested the effects of different impeller types, diameters and different baffles on  $K_{La}$ . Rushton turbines and 6 blade concave disk impellers were used with different impeller diameters ( $D = 75$  mm and  $D = 105$  mm). When the effect of different number of impellers are compared, it was found that 2 impellers stimulated higher  $K_{La}$  values compared to 3 impellers. The results showed that mixing times are shorter with 2 impeller configuration. Because of the formation of flow compartments around impellers, top-to-bottom mixing gets retarded by fluid recirculation between impellers as number of impellers increases (Sieblist *et al.* 2011). Therefore, 2 impeller configuration is favorable both for better oxygen transfer and for mixing. To take the baffle size and type into account, three baffles were investigated; 15 mm and 30 mm standard baffle and 30 mm C-baffle. Higher

power consumptions were required with larger baffle sizes when the agitation rate was kept constant but their “energetic efficiency” with respect to mass transfer rates is smaller compared to narrower baffles. It is also important to note that antifoam agent consumption was significantly lower (-30%) with 30 mm baffle rods. Reducing the amount of antifoam agent used is important as they cause problems in downstream processing.

## **2.9. Computation of Bioprocess Characteristics**

Computation of bioprocess characteristics in terms of specific rates and yields is of the utmost importance. Here, the calculation procedures and derivations of the equations regarding specific cell growth and substrate consumption rates, as well as yield coefficients are given in this subsection.

### **2.9.1. Specific Cell Growth Rate**

Microbial growth can be divided into four phases: lag phase, exponential phase, stationary phase, and death phase (Figure 11).

Lag phase is the time when the cell culture adapts itself to the new environment and synthesize essential biomolecules for cell growth. In this phase, cells get more mature and gain the ability of division. This phase should be kept as short as possible by preparing production medium similar to precultivation medium to make the adaptation to the new environment easier.

Exponential phase is the time that the cell concentration increases with constant specific growth rate. The growth rate is defined as the number of new microorganisms appearing per unit time and it is proportional to the present population by equation (16) (Bailey and Ollis, 1986):

$$\mu \cdot C_x = \frac{dC_x}{dt} \quad (16)$$

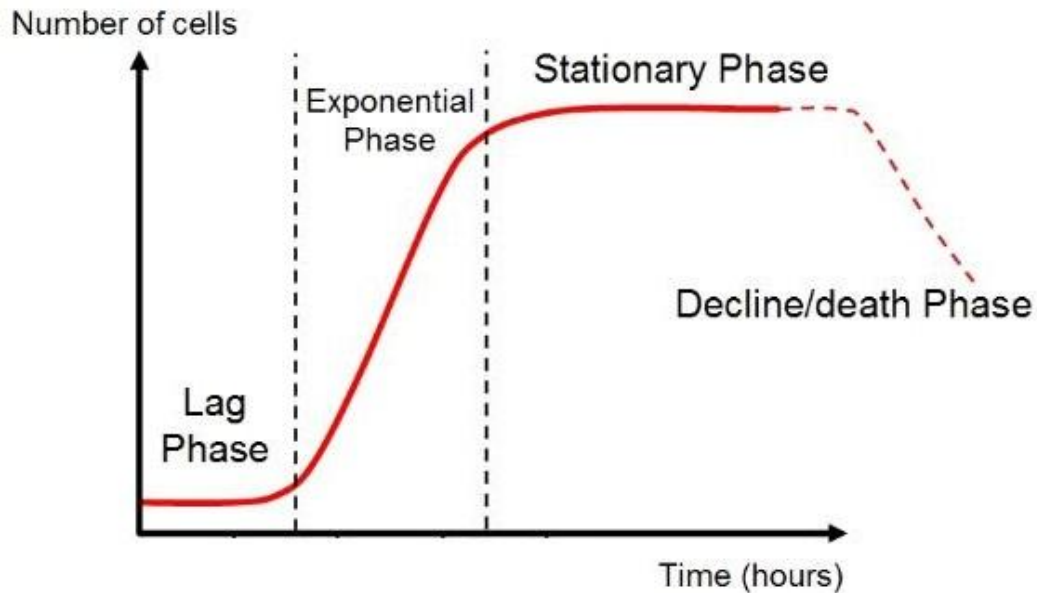


**Figure 11.** Typical microbial growth curve of a batch culture.

For the cells in the exponential phase, natural logarithm of the cells versus time curve is plotted. The slope of this curve gives the maximum number of division per cell per unit time,  $\mu_{\max}$ .

Exponential growth decelerates as the nutrients deplete and inhibitory by-products accumulate. When the exponential phase is finished, stationary phase starts. In this phase, cell concentration remains more or less the same as the cell formation and death rates are almost equal. In the processes where the target product is the secondary metabolites, stationary phase is desired where the exponential phase is only for the biomass accumulation and production of primary metabolites.

If the cells are not harvested during the stationary phase; death phase starts and the cell number rapidly decreases in a logarithmic trend because of the high death rate.

In fed-batch (semi-batch) processes, cells are inoculated into the medium at the start-up. If cells are assumed not to be lost by sampling, the process can be assumed to be batch-wise in terms of cells.

$$r_x \cdot V = \frac{d(C_x \cdot V)}{dt} \quad (17)$$

where V is the working volume and  $r_x$  is the cell generation rate which can be demonstrated as:

$$r_x = \mu \cdot C_x \quad (18)$$

Substitution of equation (18) into equation (17) and application of chain rule gives:

$$\mu \cdot C_x \cdot V = V \frac{dC_x}{dt} + C_x \frac{dV}{dt} \quad (19)$$

In fed-batch processes, volume increases with increasing time due to substrate feeding and this volume change can be shown as:

$$Q_s = \frac{dV}{dt} \quad (20)$$

where  $Q_s$  is the volumetric flow rate into the reactor.

Substitution of equation (20) into equation (19) gives:

$$\mu \cdot C_x \cdot V = V \frac{dC_x}{dt} + C_x \cdot Q_s \quad (21)$$

Rewriting equation (21):

$$\left( \mu - \frac{Q_s}{V} \right) C_x = \frac{dC_x}{dt} \quad (22)$$

By using equation (22), specific cell growth rate can be calculated in the rearranged form:

$$\mu = \frac{dC_x}{dt} \cdot \frac{1}{C_x} + \frac{Q_s}{V} \quad (23)$$

### 2.9.2. Specific Substrate Consumption Rate

For substrate point-of-view, the process is conducted in a fed-batch manner. Therefore, following mass balance equation can be used for the substrate.



$$Q_s \cdot C_{s_o} + r_s \cdot V = \frac{d(C_s \cdot V)}{dt} \quad (24)$$

where  $C_s$  is the substrate concentration in the fermentation medium,  $Q_s$  is volumetric substrate feeding rate,  $C_{s_o}$  is the concentration of substrate in the feeding medium (stock concentration) and  $r_s$  is the substrate consumption rate which can be expressed as:

$$-r_s = q_s \cdot C_x \quad (25)$$

where  $q_s$  is the specific substrate consumption rate.

Substitution of equation (25) into equation (24) results in:

$$q_s = \left( Q_s \cdot C_{s_o} - \frac{d(C_s \cdot V)}{dt} \right) \frac{1}{C_x \cdot V} \quad (26)$$

Applying chain rule and rearranging the terms:

$$q_s = \left( \frac{Q_s \cdot C_{s_o}}{V} - \frac{dC_s}{dt} - \frac{C_s}{V} \frac{dV}{dt} \right) \frac{1}{C_x} \quad (27)$$

The process can be regarded as pseudo-steady state in terms of substrate; therefore

$\frac{dC_s}{dt}$  can be taken as zero  $\left( \frac{dC_s}{dt} \approx 0 \right)$ .

Substitution of equation (20) into equation (27) results in:

$$q_s = \frac{Q_s}{C_x \cdot V} (C_{s_o} - C_s) \quad (28)$$

To be able to calculate specific substrate consumption rate ( $q_s$ ), volumetric substrate flow rate ( $Q_s$ ) should be known.

By taking  $\frac{dC_s}{dt} \approx 0$ , rate of substrate utilization is related only to cell formation:

$$-r_s = \frac{r_x}{Y_{x/s}} \quad (29)$$

where  $Y_{x/s}$  is the cell yield on substrate.

In this case, equation (25) can be rewritten by using equation (29):

$$q_s = \frac{r_x}{Y_{x/s} \cdot C_x} \quad (30)$$

Now equation (30) can be substituted into equation (28):

$$\frac{r_x}{Y_{x/s}} = \frac{Q_s}{V} (C_{s_o} - C_s) \quad (31)$$

Using equation (18) and rearranging:

$$Q_s (C_{s_o} - C_s) = \frac{V \cdot \mu \cdot C_x}{Y_{x/s}} \quad (32)$$

Knowing that the differentiation of equation (19) results in:

$$C_x \cdot V = C_{x_0} \cdot V_0 \cdot \exp(\mu \cdot t) \quad (33)$$

Substitution of equation (33) into equation (32):

$$Q_s = \frac{\mu_0 \cdot C_{x_0} \cdot V_0}{Y_{x/s} \cdot (C_{s_o} - C_s)} \cdot \exp(\mu_0 \cdot t) \quad (34)$$

Equation (34) is used for calculating the feeding profile of the substrate. This feeding strategy assumes that cells are always in the exponential phase and does not account for stationary phase of the cells. As glucose feeding increases exponentially regardless of cell concentration, when cells enter stationary phase glucose starts to accumulate in the medium and feeding becomes inefficient.

### 2.9.3. Yield Coefficients

In bioprocesses quantity of the biomass or product formation can be described by yield coefficients. These yield coefficients can be used to express the substrate or process efficiency for product and biomass formation. Overall yield coefficients are used to describe the formation of the products per the utilized substrate for the entire process (Equation (35)) while instantaneous yield coefficients are used to describe the instantaneous efficiency of the bioprocess (Equation (36)).

$$\begin{aligned}\bar{Y}_{x/s} &= \frac{\Delta C_x / \Delta t}{-\Delta C_s / \Delta t} \\ \bar{Y}_{p/s} &= \frac{\Delta C_p / \Delta t}{-\Delta C_s / \Delta t}\end{aligned}\tag{35}$$

$$\begin{aligned}Y_{x/s} &= \frac{r_x}{-r_s} = \frac{dC_x / dt}{-dC_s / dt} \\ Y_{p/s} &= \frac{r_p}{-r_s} = \frac{dC_p / dt}{-dC_s / dt}\end{aligned}\tag{36}$$

In aerobic processes, yield coefficients of cell and product on oxygen can also be calculated (Equation (37)).

$$\begin{aligned}Y_{x/o} &= \frac{r_x}{-r_o} \\ Y_{p/o} &= \frac{r_p}{-r_o}\end{aligned}\tag{37}$$



## CHAPTER 3

### MATERIALS AND METHOD

#### 3.1 Chemicals

Chemicals used in this study were analytical grade and obtained from Sigma, Merck and Fluka.

#### 3.2 Buffers and Stock Solutions

Preparation and formulation of the buffers and stock solutions are presented in APPENDIX A. Depending on the characteristics of the solution, sterilization was done either by autoclaving at 121°C for 20 minutes or by filtering through filters with 0.20 or 0.45 µm pore diameter (Sartorius Stedim Biotech GmbH, Germany)

#### 3.3 Microorganism

*P. pastoris* X-33 strain, carrying pGAPZ $\alpha$ -A::*xylA*<sub>Cd-Opt</sub> was used as GI producer. (Güneş and Çalık, *submitted*). Codon optimized *xylA* sequence was obtained from pPICZ $\alpha$ -A::*xylA*<sub>Cd-Opt</sub> plasmid constructed by Ata *et al.* (2015). The shuttle vector pGAPZ $\alpha$ -A was obtained from Invitrogen and propagated in *E. coli* DH5 $\alpha$  cells, grown in low salt Luria broth (LSLB) and purified. The purified pGAPZ $\alpha$ -A::*xylA*<sub>Cd-Opt</sub> plasmid was digested with *PagI* (Fermantas). Linearized plasmid was used for transfection of *P. pastoris* wild type X-33 host strain, using lithium chloride transformation method (Invitrogen).

### 3.4 Growth Media

All growth media were sterilized by autoclaving at 121°C for 20 minutes, then let to cool to about 50°C and necessary antibiotics, Zeocin™ or chloramphenicol, were added.

#### 3.4.1 Solid Medium

*P. pastoris* cells carrying pGAPZ $\alpha$ -A::xylA<sub>Cd-Opt</sub> gene, stored at -80°C in microbanks, were inoculated onto YPD agar plates whose composition is given in Table 3. Inoculated plates were incubated at 30°C for about 48 hours and stored at +4°C.

**Table 3.** Composition of YPD agar solid medium

Compound	Concentration (per liter)
Yeast extract	10 g
Peptone	20 g
Glucose*	20 g
Agar	20 g
Zeocin™	1 ml
dH <sub>2</sub> O	to 1 L

\* Sterilized by a filter with 0.20  $\mu$ m pore diameter and added to the medium after autoclaving.

#### 3.4.2 Precultivation Medium

*P. pastoris* cells carrying pGAPZ $\alpha$ -A::xylA<sub>Cd-Opt</sub> gene, grown on YPD agar plates were inoculated into the precultivation medium (buffered glycerol complex medium, BMGY), whose composition is given in Table 4 (Invitrogen). The precultivation was performed in 250 ml baffled, air-filtered shake bioreactors with 50 ml working volume for 15-20 hours. An orbital shaker (Sartorius, Germany) was used with agitation speed of 200 rpm and temperature of 30°C.

### 3.4.3 Production Media

Production of glucose isomerase with *P. pastoris* under  $P_{GAP}$  was done in two phases. In the first phase, basal salts medium (BSM) was used where glycerol is the carbon source (Table 5). In the second phase, 50% (w/v) glucose solution was used. In both phases, production medium also contains *Pichia* trace minerals (PTM1) (Table 6).

**Table 4.** Composition of the precultivation medium, BMGY

Compound	Concentration (per liter)
Yeast extract	10 g
Peptone	20 g
Potassium phosphate buffer (pH=6.0)	0.1 mol
Yeast nitrogen base (YNB)	13.4 g
Ammonium sulfate	10.0 g
Biotin*	$4 \cdot 10^{-5}$ g
Glycerol	10 g
Chloramphenicol (from 34 mg ml <sup>-1</sup> stock)*	1 ml
dH <sub>2</sub> O	to 1 L

\* Added after autoclaving.

## 3.5. Recombinant Glucose Isomerase Production

### 3.5.1. Precultivation

*P. pastoris* cells carrying pGAPZ $\alpha$ -A::xylA<sub>Cd-Opt</sub> gene are taken from the microbanks stored at -80°C, and transferred onto YPD-Agar plates. Plates were incubated at 30°C for 48 h in an incubator (Nüve, Turkey). Afterwards, a single colony was chosen and inoculated into 50 ml BMGY for precultivation. Precultivation was conducted at 200 rpm, 30°C for 15-20 h in laboratory scale baffled air-filtered shake flasks. Precultivation continued until OD<sub>600</sub> = 2-8, when cells are known to be in the exponential phase of their growth. When the desired cell concentration was reached, they were centrifuged at 1500 g and 4°C for 10 minutes. By this way, cells were separated from the supernatant containing precultivation medium. These cells were

dissolved in water and fed to the bioreactor containing BSM such that the initial OD<sub>600</sub> in the bioreactor is equal to 1.

**Table 5.** Composition of basal salts medium, BSM

Compound	Concentration (per liter)
85 % H <sub>3</sub> PO <sub>4</sub>	26.7 ml
CaSO <sub>4</sub> .2H <sub>2</sub> O	1.17 g
MgSO <sub>4</sub> .7H <sub>2</sub> O	14.9 g
KOH	4.13 g
K <sub>2</sub> SO <sub>4</sub>	18.2 g
Glycerol (100 %)	41.95 ml
Chloramphenicol (from 34 mg ml <sup>-1</sup> stock )*	1 ml
10% Antifoam*	1 ml
PTM1*	4.35 ml
dH <sub>2</sub> O	to 1 L

\*Added after autoclaving.

**Table 6.** Composition of *Pichia* trace salts, PTM1

Compound	Composition (per liter)
CuSO <sub>4</sub> .5H <sub>2</sub> O	6 g
NaI	0.08 g
MnSO <sub>4</sub> .H <sub>2</sub> O	3 g
Na <sub>2</sub> MoO <sub>4</sub> .2H <sub>2</sub> O	0.2 g
H <sub>3</sub> BO <sub>3</sub>	0.02 g
ZnCl <sub>2</sub>	20 g
FeSO <sub>4</sub> .7H <sub>2</sub> O	65 g
CoCl.6H <sub>2</sub> O	0.916 g
H <sub>2</sub> SO <sub>4</sub>	5 ml
Biotin	0.2 ml
dH <sub>2</sub> O	to 1 L



### **3.5.2. Production in Laboratory Scale Bioreactor**

For the production of glucose isomerase, a 3 L laboratory scale bioreactor (Braun CT2-2) was used with a working volume of 1-1.5 L. In this reactor; temperature, pH, dissolved oxygen, foam, agitation and feed inlet rates can be controlled. Schematic representation of the bioreactor is given in Figure 12.

#### **3.5.2.1. Bioreactor Operation Parameters**

Temperature was kept at  $30 \pm 0.1^\circ\text{C}$  using the PI controller of the bioreactor and by an external cooler, steam generator and a jacket. Agitation was done by a six-bladed Rushton turbine. To keep dissolved oxygen and pH in the bioreaction medium under control, oxygen and pH (Hamilton, Switzerland) probes were used. Oxygen supplement of the bioreactor was provided by an air compressor and a sparger. In the cases when supplying only air to keep the dissolved oxygen concentration at a desired value is not enough; air was enriched with increasing amounts of pure oxygen passing through a digital mass flow controller. pH of the bioreaction medium was maintained at  $5.5 \pm 0.1$  in the batch phase, and at  $5.0 \pm 0.1$  in the semi-batch phase using 25%  $\text{NH}_3\text{OH}$ . Foaming in the bioreactor was kept under control by adding 0.01% (v/v) antifoam solution (Y-30 emulsion, Sigma) to BSM at the beginning of batch phase, and minor amounts of 10% antifoam solution was added manually if needed throughout the bioprocess. Base and antifoam solutions and the feed solution of semi-batch phase were supplied through the inlet port of the bioreactor by peristaltic pumps.

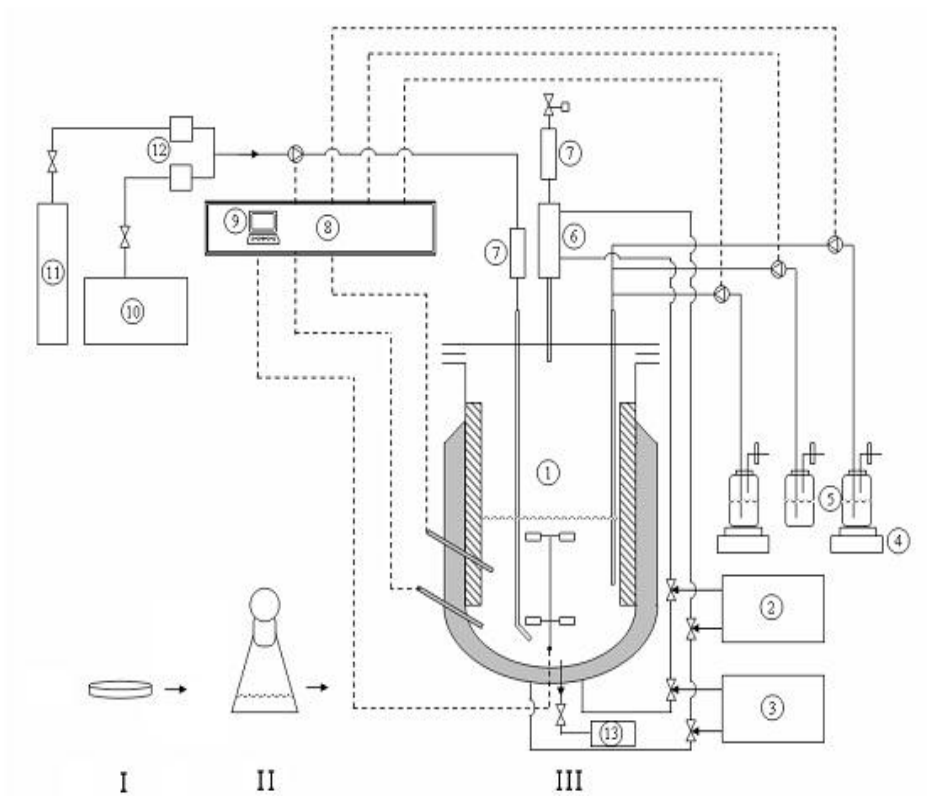


**Figure 12.** Schematic representation of lab scale bioreactor system together with precultivation steps. I. Solid medium containing inoculated cells from microbank. II. Precultivation medium II. Lab scale bioreactor system. (1) Bio-reaction vessel, Biostat CT2-2 (2) Cooling circulator (3) Steam generator (4) Balances (5) Feed, base and antifoam bottles (6) Exhaust cooler (7) Gas filters (8) Controller (9) Biostat CT Software (10) Air compressor (11) Pure O<sub>2</sub> tank (12) Digital mass flow controllers (13) Sampling bottle (Çelik, 2008)

**Table 7.** Geometric properties of the bioreactor

Property	Size
Tank diameter	$T = 12 \text{ cm}$
Impeller diameter	$D = T/2.4$
Impeller height	$h = T/12$
Off-bottom clearance	$C = T/6$
Average height of working volume	$H = 0.667T$

### 3.5.2.2. Production Phases

Cells harvested from the precultivation medium are inoculated to the bioreactor in such a manner that  $OD_{600}$  is equal to 1, which is equivalent to  $0.275 \text{ g L}^{-1}$  cell concentration. As mentioned in previous sections, production of glucose isomerase under  $P_{GAP}$  was done in two phases; glycerol batch and glucose semi-batch phases.

**Glycerol Batch (GB) Phase:** The first phase was conducted batch-wise where BSM is used as the bioreaction medium. In this phase, cell growth is the main objective. Therefore, glycerol was used as the carbon source as it is known to enable higher cell densities than glucose (Çalık *et al.* 2015) This phase continued until all glycerol was depleted, which is signaled by cell concentration reaching  $15\text{-}20 \text{ g L}^{-1}$ . Therefore cell growth was monitored for an indication of glycerol depletion, which takes about 18-20 h.

**Glucose Fed-Batch (GFB) Phase:** The main objective of the second phase of the production is to produce recombinant GI together with cell growth. Therefore, a non-repressive carbon source, glucose, was used for expressions under the constitutive  $P_{GAP}$ . The feed solution consists of 50% (w/v) glucose and  $12 \text{ ml L}^{-1}$  PTM1. Carbon source was supplied by the feed solution while a basic solution, 25%  $\text{NH}_3\text{OH}$ , was

used as nitrogen source, as well as to adjust pH. Glucose solution containing PTM1 was fed to the bioreactor continuously, according to predetermined exponential feed rate. The equation used to calculate the feeding rate using predetermined exponential cell growth rate is given in Equation (34) while the parameters of the equation are given in Table 8.

**Table 8.** Values of the parameters in Equation 34

Parameter	Glucose feed
$\mu_0$	$0.15 \text{ h}^{-1}$
$Y_{x/s}$	$0.48 \text{ g cell g}^{-1} \text{ glucose}$
$C_{s_0}$	$500 \text{ g L}^{-1}$

### 3.5.2.3. Feeding Strategies Applied in Bioreactor Experiments

In all of the experiments, precultivation and the first phase of the bioprocesses were carried out exactly the same while different strategies were applied in the second phase of the bioprocesses. In those experiments, glucose feeding was done the same using predetermined exponential feeding rate of  $\mu_0 = 0.15 \text{ h}^{-1}$ , as optimized in a previous study (Keskin, 2014) while different oxygen transfer strategies were applied in each experiment. Strategies followed can be divided into two groups: experiments based on constant oxygen transfer condition (OTC), and constant dissolved oxygen concentration ( $C_{DO}$ ). All of the strategies applied are given in Table 9.

**Table 9.** Strategies applied in bioreactor experiments

Strategy		Dissolved Oxygen	Aeration Rate	Agitation Rate,
		(C <sub>DO</sub> ), %	(Qo/V), vvm	(N) rpm
1.	OTC <sub>1</sub>	Variable	3	900
2.	OTC <sub>2</sub>	Variable	6	900
3.	OTC <sub>3</sub>	Variable	10	900
4.	CDO <sub>1</sub>	5	Variable	900
5.	CDO <sub>2</sub>	10	Variable	900
6.	CDO <sub>3</sub>	15	Variable	900
7.	CDO <sub>4</sub>	20	Variable	900
8.	CDO <sub>5</sub>	40	Variable	900

### 3.6 Analyses

During the experiments, a sample from the bioreaction medium was taken in every three hours. Firstly, cell concentration was determined from this sample, then it was centrifuged at 1500 g and +4°C for 10 minutes to separate pellets and supernatant. Supernatants were used to determine glucose concentration, GI activity and monomer concentration by SDS-PAGE. Some of the supernatant was then filtered with filters having 0.20 µm pore diameter and these filtrates were used in organic acid concentration determination via HPLC.

### 3.6.1. Cell Concentration

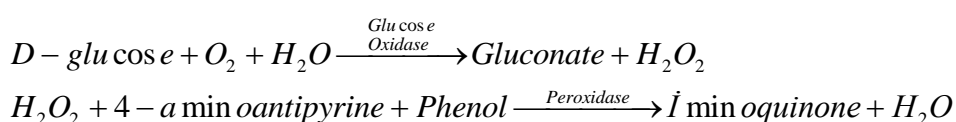
A UV-Vis Spectrophotometer (Thermo Spectronic, Helios $\alpha$ ) was used at 600 nm to determine *P. pastoris* cell concentration as dry cell weight per liter. In order to stay in the accurate measurement range of the UV-Vis Spectrophotometer (0.1-0.8 Å), samples were usually diluted with distilled water. Following equation was used to calculate cell concentration from OD<sub>600</sub> (Orman, 2007):

$$C_x = 0.275 \cdot OD_{600} \cdot DF \quad (38)$$

Where  $C_x$  cell concentration in DCW L<sup>-1</sup> is,  $OD_{600}$  is the optical density determined at 600 nm and DF is the dilution factor.

### 3.6.2. Glucose Concentration

Glucose concentration was determined by using a glucose analysis kit (Biasis, Ankara) based on glucose oxidation method (Boyacı, 2005). In this method, a series of reactions takes place where the conversion of glucose to gluconate and hydrogen peroxide is the first step of the reaction in the presence of glucose oxidase catalyst. Then, hydrogen peroxide reacts with 4-aminoantipyrine and phenol with peroxidase catalysis, to produce iminoquinone and water. The concentration of the last product, iminoquinone, having a reddish-pink color and being equimolar with glucose in the reaction medium, was measured by UV-Vis Spectrophotometer at 505 nm.



While conducting the experiment, first 2 ml of dH<sub>2</sub>O was added to reaction tubes, followed by the addition of 400 µl of buffer solution containing phenol and potassium dihydrogen phosphate. Then, 50 µl of sample solution was added to the tubes. Lastly, 50 µl of glucose reactive mixture containing glucose oxide, 4-aminoantipyrin and peroxidase, was added to the tubes and reaction started with the addition of the glucose reactive mixture. Reaction tubes were placed in a water bath

at 37°C for 20 minutes to obtain the red color resulted from the formation of iminoquinone. OD<sub>505</sub> of iminoquinone was measured with UV-Vis Spectrophotometer at 505 nm. Standard glucose solutions were used to obtain the calibration curve given in APPENDIX B to determine the glucose concentration of the reaction samples in g L<sup>-1</sup>.

### 3.6.3. Glucose Isomerase Activity

Supernatants of samples centrifuged at 1500 g, +4°C for 10 minutes were used to determine the extracellular glucose isomerase activity.

To determine the GI activity, 50 µl supernatant was added to 50 µl freshly prepared activity buffer of 0.02 M potassium phosphate buffer (pH=7.0) at 80°C, containing 0.4 M D-glucose and 10 mM MnCl<sub>2</sub>. The solution was incubated at 80°C for 10 minutes. After 10 minutes, the reaction was stopped by terminated by adding 60 µl of this mixture to 540 µl 0.1 M HCl solution. D-fructose produced was analyzed by the method described by Dische and Borenfreund (1951), known as carbazole-cysteine-sulfuric acid method. In this method, 1.8 ml 70% (v/v) sulfuric acid was added to test tubes containing the reaction mixture and 0.1 M HCl. Then 60 µl of freshly prepared 1.5% cysteine in 37% HCl and 60 µl of freshly prepared 0.12% (w/v) carbazole in ethanol was added to the mixture in this order. The mixture was incubated at room temperature for 30 minutes and vortexed occasionally. After 30 minutes, produced D-fructose concentration was determined by measuring the absorbance at 560 nm, using a UV-Vis Spectrophotometer. 1 U of GI activity is defined as the formation of 1 µmol D-fructose per minute under this reaction conditions. Equation (39) was used to calculate GI activity in U L<sup>-1</sup> from the absorbance of D-fructose.

$$A(UL^{-1}) = \frac{Abs(560nm) - 0.014}{50.94} \cdot 10^5 \quad (39)$$

### 3.6.3. Sodium Dodecyl Sulfate-Polyacrylamide Gel Electrophoresis (SDS-PAGE)

SDS-PAGE technique was used to determine the monomer concentration of GI secreted to extracellular medium. For that reason, 20 µl supernatants of the samples

were added to 10 µl loading buffer. Because of the homotetrameric physiology of GI, firstly heat denaturation was performed using a thermocycler at 95°C for 5 minutes to obtain GI monomers. SDS-PAGE procedure was conducted as described by Laemmli (1970); samples ran simultaneously with a prestained protein marker at a constant current of 40 mA. Silver staining was used to stain the gels. The staining procedure is given in APPENDIX C.

### 3.6.4. Protease Activity Assay

Extracellular acidic protease activity was determined by using supernatants of the samples. 2 ml 0.5% (w/v) Hammerstein casein in 0.05 M sodium acetate buffer (pH=5.0) was mixed with 1 ml diluted sample and incubated at 37°C for 20 minutes. After this time period, 10% trichloroacetic acid (TCA) was added to terminate the reaction. The solution was then centrifuged at 10500 g, +4°C for 10 minutes. After centrifugation, solution was incubated at room temperature for 5 minutes and the absorbance was measured at 275 nm in UV-Vis Spectrophotometer. 1 U of protease activity was defined by Moon and Parulekar (1991) as the formation of 4 nmol tyrosine per minute. The equation (40) was used in the calculation of protease activity.

$$A(UL^{-1}) = \left( \frac{Abs(275nm)}{0.8} \right) \left( \frac{1U}{4nmol\ min^{-1}} \right) \left( \frac{1}{20\ min} \right) \left( \frac{1000nmol}{1\ \mu mol} \right) (DF) \quad (40)$$

### 3.6.5. Organic Acid Concentration

Organic acid concentrations were measured by a High Performance Liquid Chromatography (HPLC, Waters, Alliance 2695). Concentration of each organic acid was calculated by using the calibration curves plotted by analyzing standard solutions' chromatograms. Filtered samples were used and diluted at least 5 times prior to analysis. Table 10 shows the operating conditions of HPLC for organic acid concentration analysis. Calibration curve for each organic acid is given in APPENDIX D.



**Table 10.** HPLC operation conditions for organic acid analysis (İleri and Çalık, 2006)

<b>Column</b>	Capital Optimal ODS
<b>Column dimensions</b>	4.6 mm x 250 mm x 5 µm
<b>System</b>	Reversed phase chromatography
<b>Mobile phase</b>	3.12% (w/v) NaH <sub>2</sub> PO <sub>4</sub> , 0.62·10 <sup>-3</sup> (v/v) H <sub>3</sub> PO <sub>4</sub>
<b>Flow rate of mobile phase</b>	0.8 ml min <sup>-1</sup>
<b>Column temperature</b>	30°C
<b>Detector type and wavelength</b>	Waters 2487 Dual Absorbance Detector, 210 nm
<b>Detector temperature</b>	30°C
<b>Injection volume</b>	5 µl
<b>Analysis period</b>	15 min
<b>Delay time</b>	5 min



## CHAPTER 4

### RESULTS AND DISCUSSION

In this study, effects of oxygen transfer conditions on thermostable glucose isomerase production by recombinant *Pichia pastoris* under  $P_{GAP}$  was systematically investigated. Eight different experiments were conducted which can be divided into two subgroups: (i) experiments done with constant oxygen transfer condition (OTC) and (ii) experiments done with constant dissolved oxygen concentration in the fermentation medium ( $C_{DO}$ ). In the first set of experiments, aeration rate was kept constant at  $Q_O/V = 3, 6$  and  $10$  vvm by altering the air flow rate into the bioreactor according to volume change while agitation speed was  $N = 900$  rpm. In the second set of experiments, dissolved oxygen was kept constant at  $C_{DO} = 5\%, 10\%, 15\%, 20\%$  and  $40\%$  saturation by a cascade system to supply air and, if necessary, oxygen-enriched air. In all of the experiments, glucose was used as the carbon source and it was fed with a precalculated exponential feed-stream flow rate (Equation (34)) using predetermined specific growth rate of  $\mu_0 = 0.15h^{-1}$ . Designed strategies were investigated and compared with each other in terms of the cell and glucose concentration, GI and protease activities, and organic acid concentrations. Oxygen transfer characteristics of each strategy were also investigated along with the bioprocess characteristics such as specific consumption rates and yield coefficients.

In all of the experiments, precultivation and glycerol batch phase of the production were done according to the methods given in Sections 3.5.1 and 3.5.2. Since the difference in the strategies are in the second phase of the production, glucose fed-batch phase, all of the comparisons were given for that phase and, although it is  $t \approx$

20 h of the overall production phase,  $t = 0$  h is taken as the beginning of this phase for the sake of simplicity in presentation and discussion of the results.

Variation of dissolved oxygen concentration in the fermentation medium with cultivation time is given in Figure 13. For constant OTC processes, it can clearly be seen that there is a strong connection between  $C_{DO}$  and  $C_X$ . As cell concentration increases,  $C_{DO}$  decreases and eventually drops to zero. Afterwards, when cells enter stationary phase,  $C_{DO}$  starts to increase again, even reaching higher concentrations than the starting values. For constant  $C_{DO}$  experiments, it was possible to keep  $C_{DO}$  constant at the desired value with  $\pm 0.02 \text{ mmol L}^{-1}$  ( $\sim 4 - 5\%$ ) deviation while this deviation is slightly higher in  $CDO_5$ . Maintaining 40% air saturation is not possible by only air supplementation, even at the earlier hours of the bioprocess. Introducing pure oxygen along with air causes some fluctuations, which causes deviations in  $C_{DO}$  levels.  $\pm 0.02 \text{ mmol L}^{-1}$  deviation might be acceptable for most of the processes but it is rather too much deviation for  $CDO_1$  strategy. A more robust control system is necessary if the process is to be conducted at low  $C_{DO}$  levels.

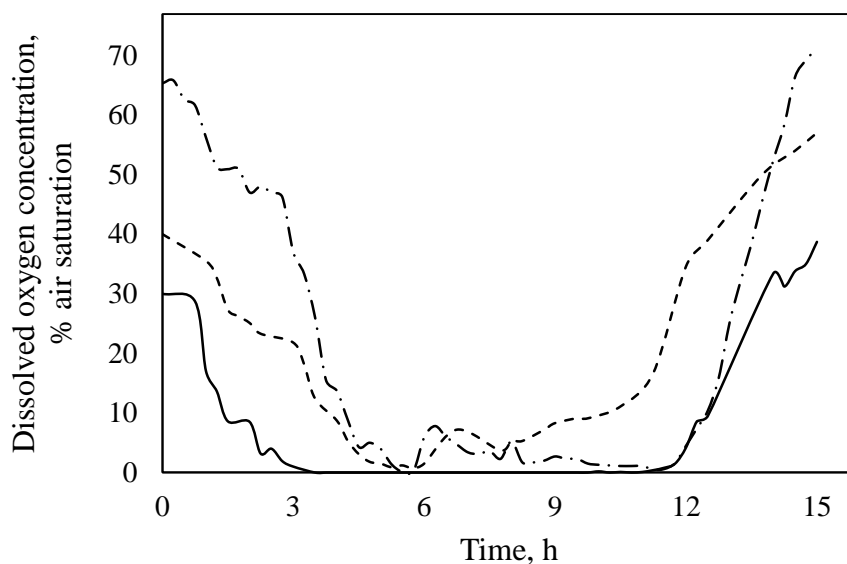


**Figure 13.** Variation of dissolved oxygen concentration in the fermentation medium with cultivation time. OTC<sub>1</sub> (solid line), OTC<sub>2</sub> (dashed line), OTC<sub>3</sub> (long dashed and dotted line).

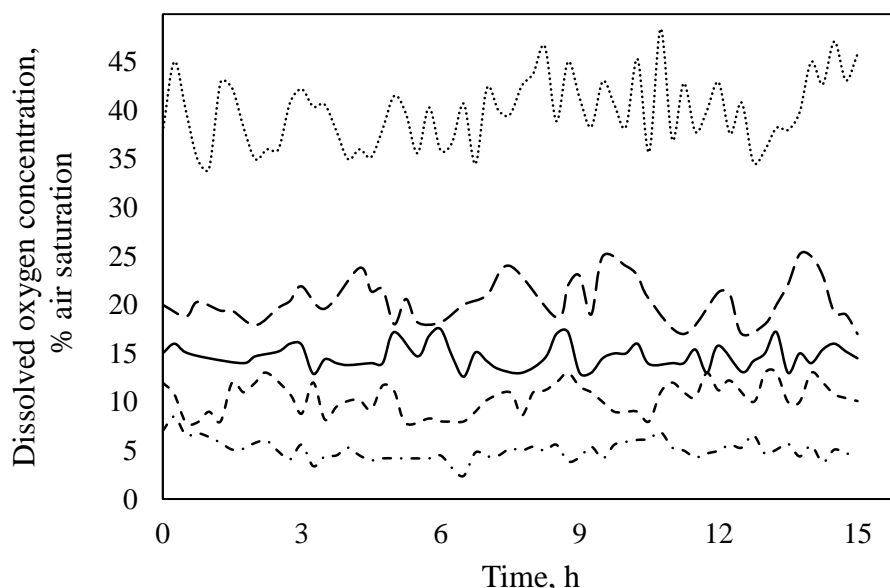


**Figure 14.** Variation of dissolved oxygen concentration in the fermentation medium with cultivation time. CDO<sub>1</sub> (dashed and dotted line), CDO<sub>2</sub> (square dotted line), CDO<sub>3</sub> (solid line), CDO<sub>4</sub> (long dashed line), CDO<sub>5</sub> (round dotted line).

#### 4.1. GI Production with Constant Oxygen Transfer Condition

Effects of constant OTC were investigated by three experiments (Table 9) and the operation conditions were compared with each other in terms of cell concentration, glucose accumulation, GI and protease activities.

The variations in cell concentration with cultivation time at constant OTC are presented in Figure 13. Among the applied strategies, the highest cell concentration was obtained in OTC<sub>1</sub> as 35 g L<sup>-1</sup>; whereas, the highest cell concentration decreased to 28 g L<sup>-1</sup> both in OTC<sub>2</sub> and OTC<sub>3</sub> with the increase in air flow rate. This can be explained by the excess amount of oxygen present in the fermentation medium, especially at the earlier hours of the process. High oxygen concentrations induce oxidative stress which can result in metabolism shift and retard cell growth (Baumann *et al.* 2011).

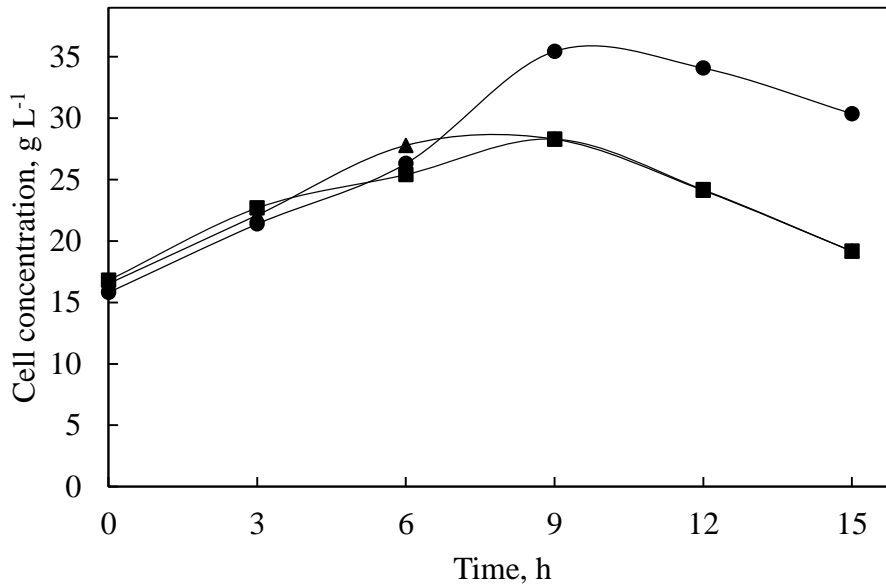


**Figure 15.** Variations in cell concentration with the cultivation time in constant OTC bioprocesses. OTC<sub>1</sub> (●), OTC<sub>2</sub> (■), OTC<sub>3</sub> (▲).

Glucose started to accumulate in the medium after  $t = 12$  h in OTC<sub>3</sub>,  $t = 9$  h in OTC<sub>1</sub>, and  $t = 6$  h in OTC<sub>2</sub> (Figure 16). As stated by Baumann *et al.* (2008) oxygen limitation did not directly decrease substrate consumption. Glucose concentration in the fermentation medium is related with specific glucose uptake rate of the cells. As a result of high oxygen availability, the highest glucose uptake rate of the cells was obtained in OTC<sub>3</sub>.

GI activity profiles of OTC<sub>1</sub>, OTC<sub>2</sub> and OTC<sub>3</sub> are given in Figure 17. The overall highest GI activity was achieved with OTC<sub>1</sub> strategy as  $3100 \text{ U L}^{-1}$  while the highest GI activity obtained in OTC<sub>3</sub> is considerably low,  $1200 \text{ U L}^{-1}$ . GI activity mainly depends on GI monomer production and the correct folding of GI subunits to obtain active GI homotetramer structure. As  $P_{GAP}$  is located in the glycolysis pathway, glucose isomerase production is directly related with the response of glycolysis pathway to environmental changes.

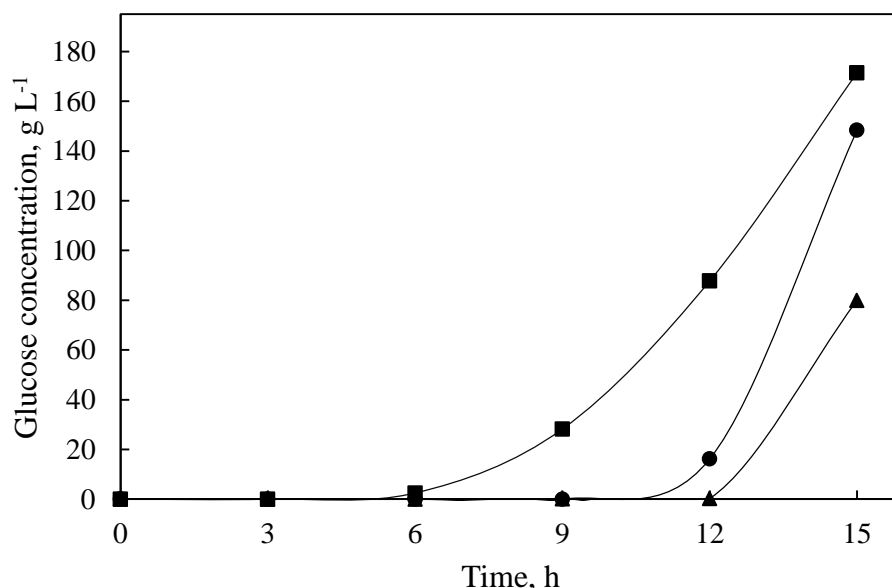


**Figure 16.** Variations in glucose concentration with the cultivation time for constant OTC bioprocesses. OTC<sub>1</sub> (●), OTC<sub>2</sub> (■), OTC<sub>3</sub> (▲).

In that context, oxygen limitation is reported to increase regulation of glycolytic genes and consequently the activity of  $P_{GAP}$  (Baumann *et al.* 2010). High oxygen concentrations resulting from high oxygen transfer conditions throughout the process may cause oxidative stress (Gasser *et al.* 2008) and decrease GI activity through unfolded protein response (UPR). Although GI is secreted as monomer subunits, it seems that it could not form its active conformation in the extracellular medium. Extreme pH, high osmolarity and dissolved oxygen concentration may result in problems during the formation of active GI configuration.

The highest acidic proteolytic activity was obtained as 143 U mL<sup>-1</sup> in OTC<sub>3</sub>, by which the lowest GI activity was attained (Figure 18). This was the expected result since protease activity is inversely related to GI activity. For OTC<sub>1</sub> and OTC<sub>2</sub>, a direct correlation could not be drawn between GI and protease activity since GI activity was higher in OTC<sub>1</sub> and protease activity was lower in OTC<sub>2</sub> because proteolytic activity is not the only factor affecting GI activity (Figure 19). However,

if proteolytic degradation could have been prevented, higher GI activities would have been obtained by using OTC<sub>1</sub> strategy.

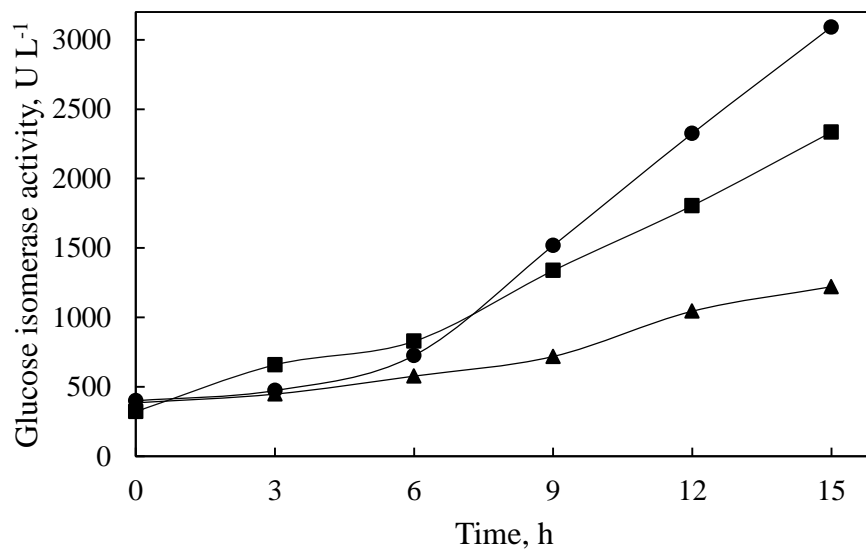


**Figure 17.** Variations in GI activity with the cultivation time for constant OTC bioprocesses. OTC<sub>1</sub> (●), OTC<sub>2</sub> (■), OTC<sub>3</sub> (▲).

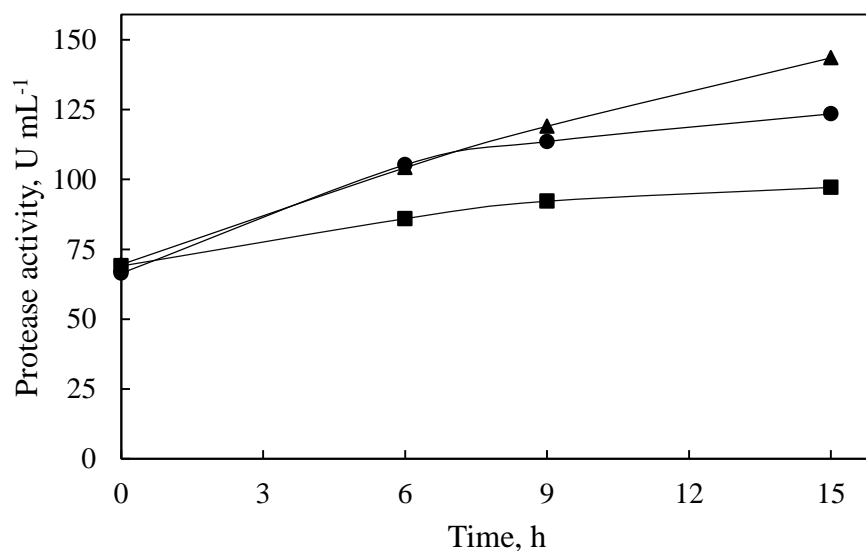


**Figure 18.** Variations in protease activity with the cultivation time for constant OTC bioprocesses. OTC<sub>1</sub> (●), OTC<sub>2</sub> (■), OTC<sub>3</sub> (▲).



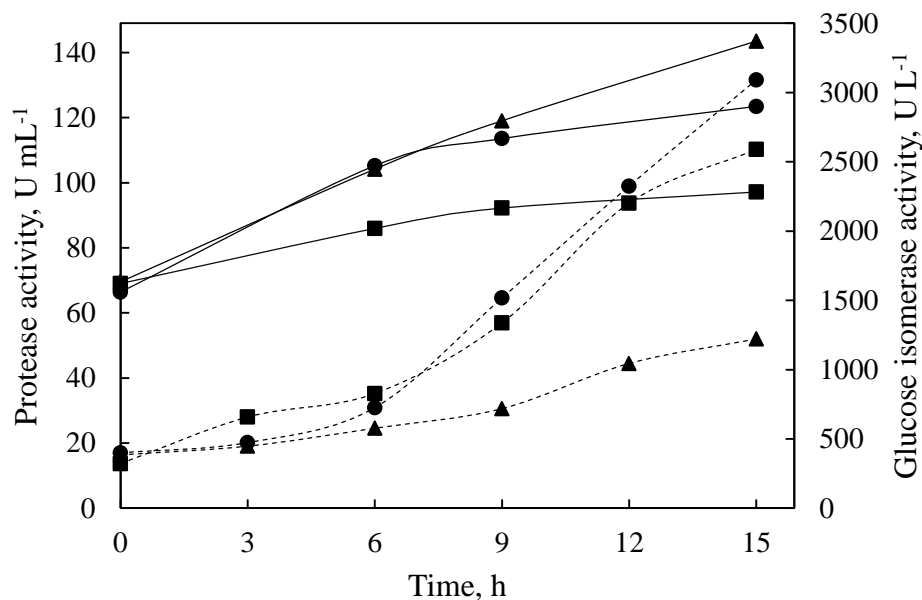


**Figure 19.** Comparative representation of the variations of protease (solid lines) and GI (dashed lines) activities with the cultivation time for constant OTC bioprocesses. OTC<sub>1</sub> (●), OTC<sub>2</sub> (■), OTC<sub>3</sub> (▲).

#### 4.2. GI Production with Constant Dissolved Oxygen Concentration

Figure 20 shows the cell concentration profiles of CDO<sub>1</sub>, CDO<sub>2</sub>, CDO<sub>3</sub>, CDO<sub>4</sub> and CDO<sub>5</sub>. Among the strategies based on dissolved oxygen concentration, the highest cell concentration was achieved with CDO<sub>4</sub> as 44 g L<sup>-1</sup> at t = 9 h. At all C<sub>DO</sub> conditions, the bioprocesses entered stationary phase between t = 9 – 12 h. Lower dissolved oxygen concentrations resulted in lower cell concentrations.

The highest glucose accumulation was observed in CDO<sub>1</sub> strategy (88 g glucose L<sup>-1</sup>), with CDO<sub>5</sub> being a close second with 85 g glucose L<sup>-1</sup> at t=15 h of the bioprocesses (Figure 21). Although the cell concentrations were relatively higher with higher DO, the glucose consumption rate decreased with increasing DO. The least glucose accumulation was obtained by CDO<sub>4</sub> strategy which was expected since the parameters of the glucose feeding strategy were optimized at dissolved oxygen concentration of 20% air saturation. As the cells were obviously not in the exponential growth phase after t = 12 h, glucose accumulation rate is the highest

between  $t = 12 - 15$  h. If the processes had been conducted for 12 h, negligible amounts of glucose would have been accumulated in all CDO strategies except for CDO<sub>1</sub>. Since the lowest cell concentration was obtained in CDO<sub>1</sub>, high concentrations of glucose in the fermentation media were expected.

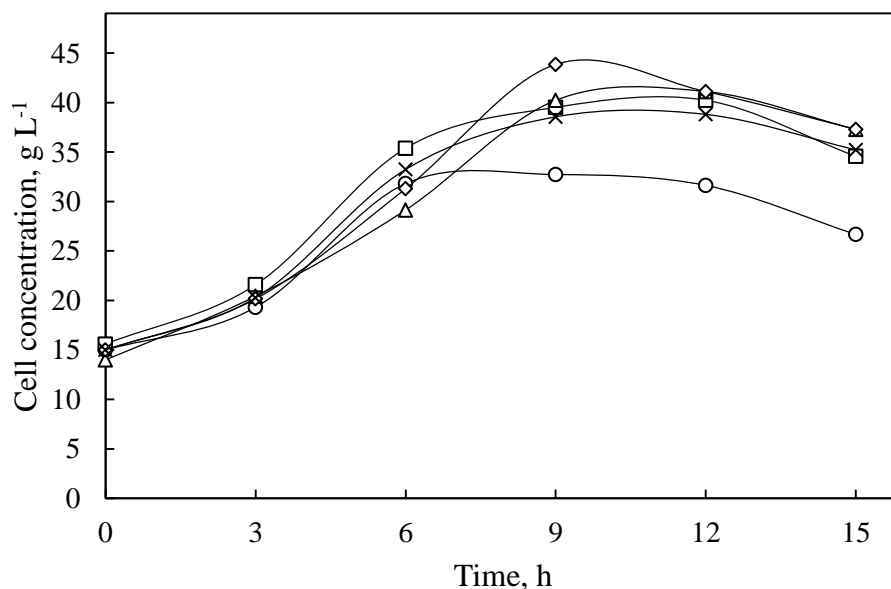


**Figure 20.** Variations in cell concentration with the cultivation time for C<sub>DO</sub> bioprocesses. CDO<sub>1</sub> (o), CDO<sub>2</sub> (□), CDO<sub>3</sub> (x), CDO<sub>4</sub> (◇), CDO<sub>5</sub> (Δ).

The highest GI activity was obtained when DO was kept constant at 15%, as 4440 U L<sup>-1</sup>. The lowest GI activity was obtained with the highest C<sub>DO</sub>, *i.e.*, CDO<sub>5</sub>. High oxygen supply to meet the oxygen demand may have caused oxidative stress on the cells and may have been resulted in unfolded or misfolded protein response. Similar to CDO<sub>5</sub>, keeping DO constant at 20% (CDO<sub>4</sub>) also resulted in rather low GI activity.

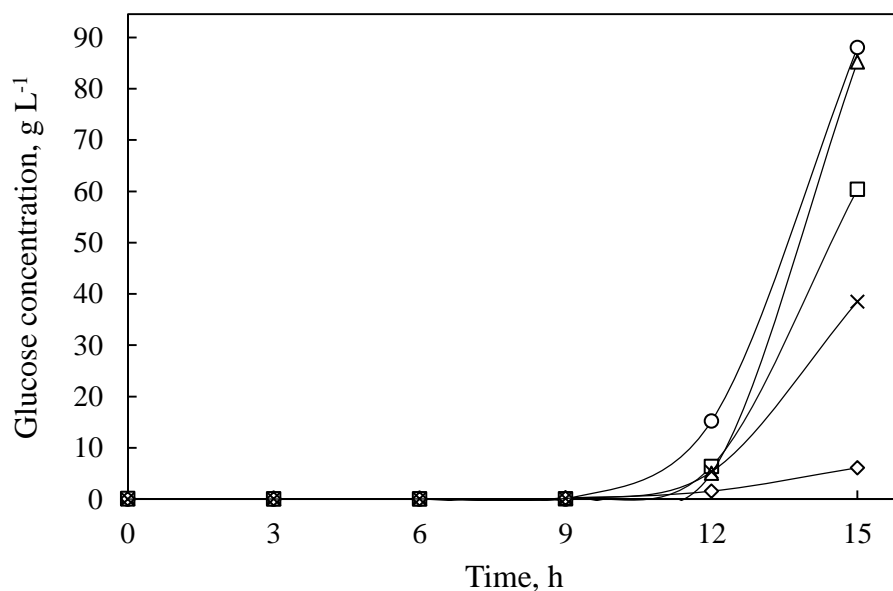


**Figure 21.** Variations in glucose concentration with the cultivation time for CDO bioprocesses. CDO<sub>1</sub> (o), CDO<sub>2</sub> (□), CDO<sub>3</sub> (x), CDO<sub>4</sub> (◇), CDO<sub>5</sub> (Δ).

Similar to constant OTC strategies, relatively low protease activities were obtained in DO-stat strategies (Figure 24). The highest protease activity was obtained as 147 U mL<sup>-1</sup> with C<sub>DO5</sub> while the second highest protease activity was 146 U mL<sup>-1</sup> with CDO<sub>1</sub>. The highest GI activity was obtained when proteolytic activity was minimum (CDO<sub>3</sub>), nonetheless, in the case of CDO<sub>5</sub>, GI activity was not relatively high when proteolytic activity was almost as low as in CDO<sub>3</sub>. It is clearly known that GI production is inversely proportional to proteolytic activity, however, a straightforward conclusion on the correlations between protease activity and GI activity could not be drawn (Figure 25).

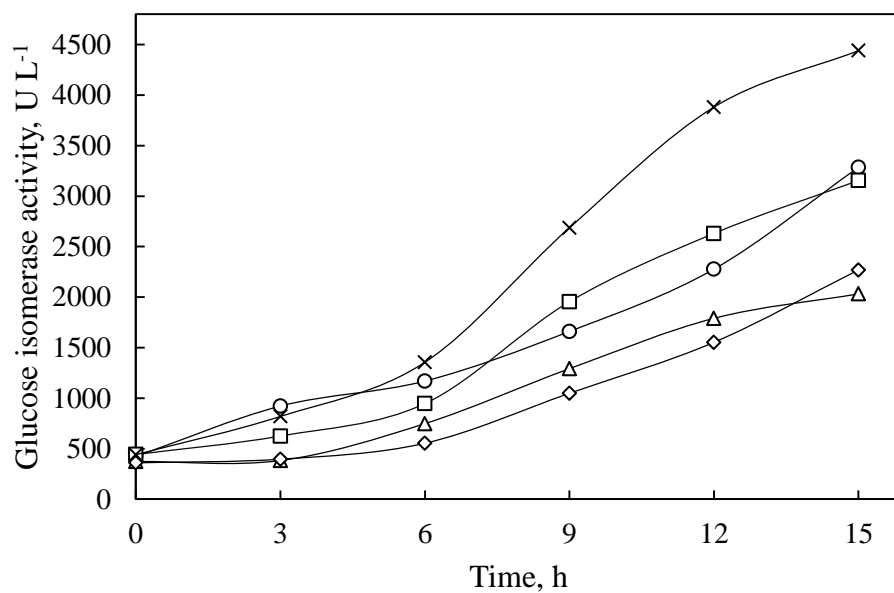


**Figure 22.** Variations in GI activity with the cultivation time for CDO bioprocesses. CDO<sub>1</sub> (o), CDO<sub>2</sub> (□), CDO<sub>3</sub> (x), CDO<sub>4</sub> (◇), CDO<sub>5</sub> (Δ).

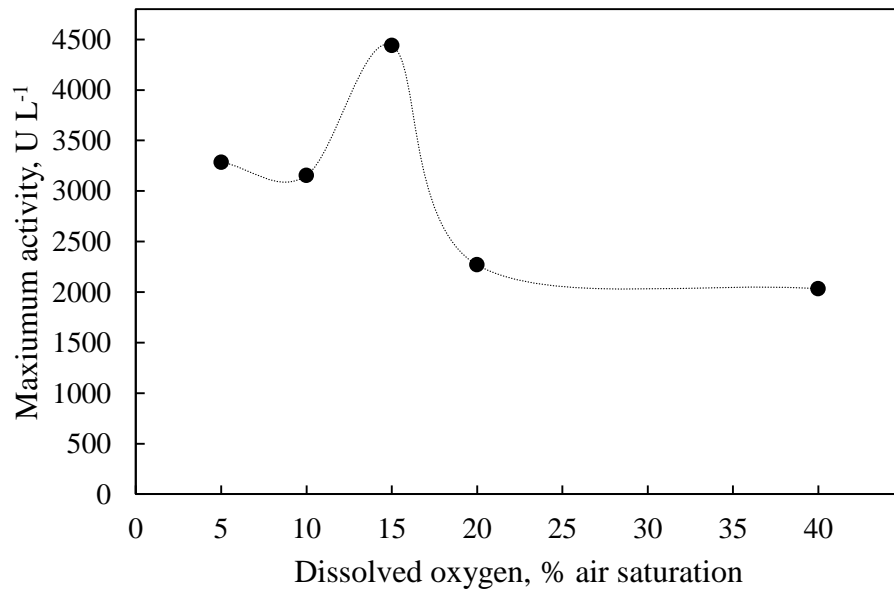


**Figure 23.** Comparison of maximum activity reached in each CDO bioprocess.

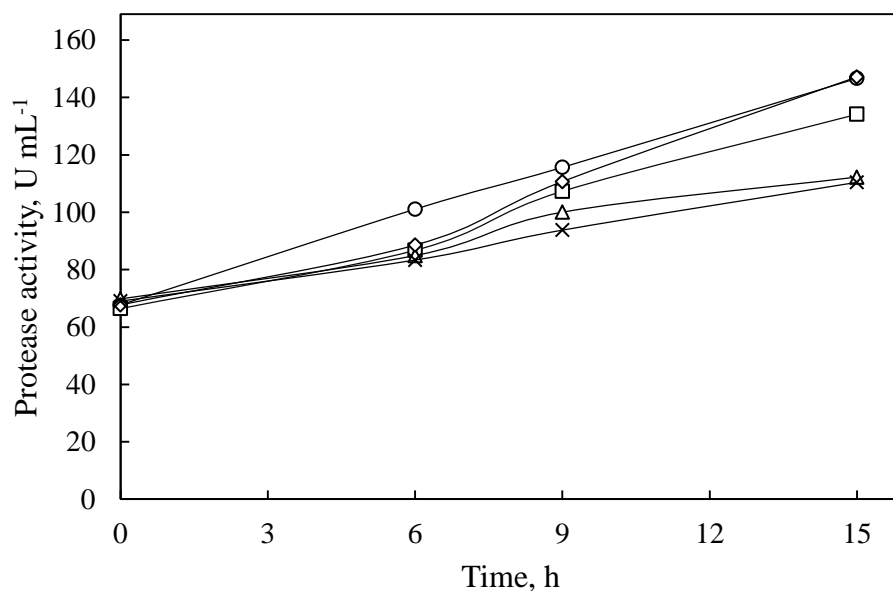


**Figure 24.** Variations in protease activity with the cultivation time for CDO bioprocesses. CDO<sub>1</sub> (o), CDO<sub>2</sub> (□), CDO<sub>3</sub> (x), CDO<sub>4</sub> (◇), CDO<sub>5</sub> (Δ).

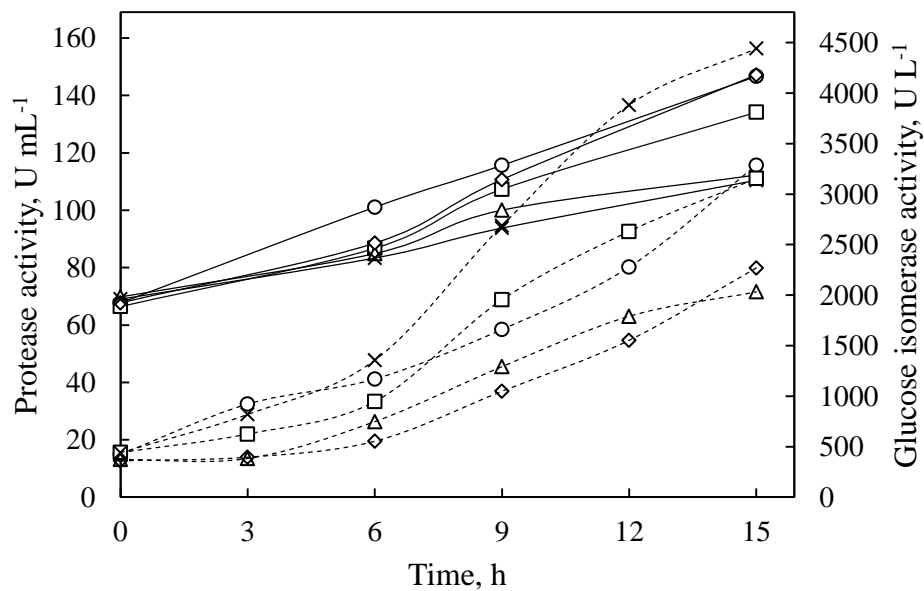


**Figure 25.** Comparative representation of variations in protease (solid lines) and GI (dashed lines) activities with the cultivation time for CDO bioprocesses. CDO<sub>1</sub> (o), CDO<sub>2</sub> (□), CDO<sub>3</sub> (x), CDO<sub>4</sub> (◇), CDO<sub>5</sub> (Δ).

### **4.3. Comparison of Constant Oxygen Transfer Condition and Constant Dissolved Oxygen Concentration Strategies**

To systematically investigate the effect of oxygen transfer conditions of GI activity and production, findings of all designed strategies were compared and the results are discussed throughout this section.

#### **4.3.1. Cell Concentration and Specific Cell Growth Rate**

Glucose fed-batch phase was started when glycerol is depleted in the production medium (BSM). This depletion was understood by monitoring the cell concentration since it reaches about 15-20 g L<sup>-1</sup> when glycerol is depleted. Therefore, glucose fed-batch phase was started more or less at the same cell concentration in all experiments. This is also important to be able to start the production while cells are at the same phase.

As shown in Figure 26, for the first three hours of the processes, the cell concentrations were approximately the same. These first three hours can be considered as the adaptation of the cells to the change of the carbon source to glucose. Since the initial cell concentrations were the same, their response to the shift of the carbon source can be evaluated to be roughly the same.

In all strategies, the highest cell concentrations were reached at  $t = 9$  h of the glucose fed-batch phase; the highest of which is 44 g L<sup>-1</sup> obtained in C<sub>DO4</sub> strategy. Since the predetermined specific growth rate was optimized according to the oxygen transfer conditions such that  $C_{DO} = 20\%$  at all times (Keskin, 2014), obtaining the highest cell growth rate in CDO<sub>4</sub> strategy was the expected result.

Although the cell concentration profiles were similar for the first three hours, the specific cell growth rate ( $\mu$ ) values differ for each strategy (Figure 27) even though the predetermined specific growth rate was the same in all strategies. The reason for this phenomenon is the behavior of the cells after the third hour of the process. Different increments in the increase of the cell concentrations after the third hour resulted in dissimilar differential values for the calculation of the specific cell growth

rate. Since overall cell concentrations were lower in constant OTC strategies, lower specific cell growth rates were obtained at the earlier hours of those bioprocesses.

Since the processes lasted as short as 15 h, the highest cell concentrations are lower than the cell concentrations obtained in the other strategies. Guan *et al.* (2013) obtained 75 g L<sup>-1</sup> cell concentration after 60 h of fermentation; whereas, 150 g L<sup>-1</sup> cell concentration was reached after 90 h of fermentation by Pepeliaev *et al.* (2011). On the other hand, Khasa *et al* (2007) obtained 33.5 g L<sup>-1</sup> after 40 h.

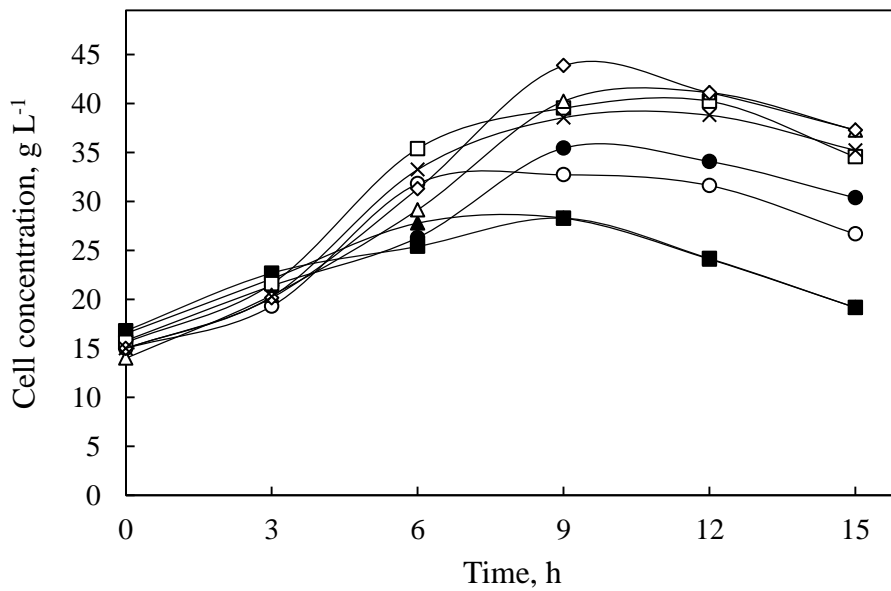


**Figure 26.** Variations in cell concentration with the cultivation time, comparison of all experiments. OTC<sub>1</sub> (●), OTC<sub>2</sub> (■), OTC<sub>3</sub> (▲), CDO<sub>1</sub> (○), CDO<sub>2</sub> (□), CDO<sub>3</sub> (x), CDO<sub>4</sub> (◇), CDO<sub>5</sub> (Δ).

At the earlier hours of the bioprocesses,  $\mu$  values changed between  $\mu = 0.13 - 0.16 \text{ h}^{-1}$  for CDO strategies while it was between  $\mu = 0.07 - 0.09 \text{ h}^{-1}$  for constant OTC strategies. Keeping in mind that predetermined specific cell growth rate was  $\mu = 0.15 \text{ h}^{-1}$ , the cells are theoretically expected to grow with that rate throughout the bioprocess. In CDO strategies, the cells tend to obey that predetermined value more than constant oxygen transfer condition strategies.

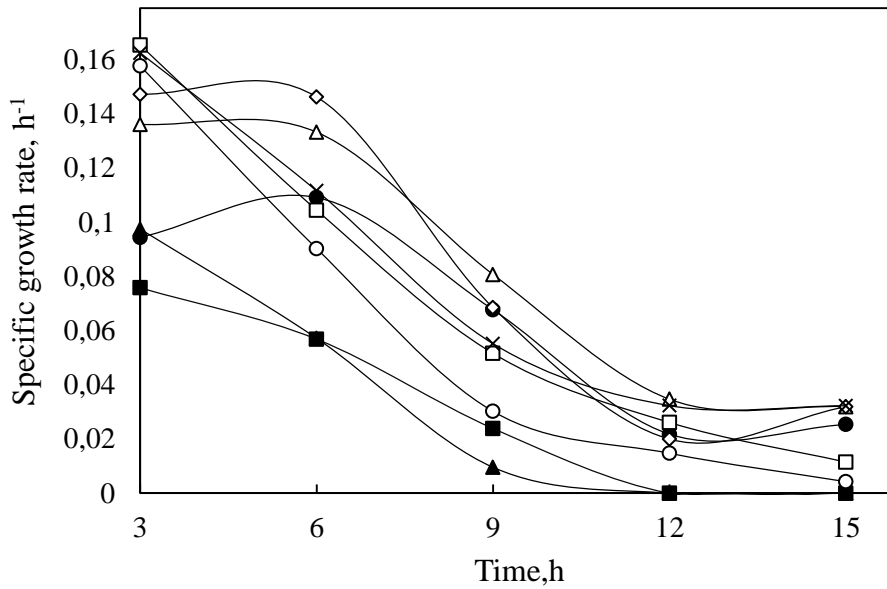


**Figure 27.** Variations in the specific growth rate with the cultivation time. OTC<sub>1</sub> (●), OTC<sub>2</sub> (■), OTC<sub>3</sub> (▲), CDO<sub>1</sub> (○), CDO<sub>2</sub> (□), CDO<sub>3</sub> (x), CDO<sub>4</sub> (◇), CDO<sub>5</sub> (Δ).

#### 4.3.2. Glucose Concentration and Specific Glucose Consumption Rate

Since the cell growth rates were closer to the theoretical value, no glucose accumulation was observed at the beginning of all strategies. The highest glucose concentration was obtained as 171 g L<sup>-1</sup> in OTC<sub>2</sub> strategy. Relatively higher glucose accumulations were observed in constant OTC strategies.

Glucose accumulation typically started when cells entered stationary phase, between  $t = 9 - 12$  h except for OTC<sub>2</sub>, where the highest glucose accumulation was detected. Interestingly, although OTC<sub>2</sub> and OTC<sub>3</sub> strategies showed similar cell growth trends, OTC<sub>2</sub> resulted in two-fold more glucose accumulation compared to OTC<sub>3</sub>, because of higher oxygen transfer rate in OTC<sub>3</sub>. The least glucose accumulation was obtained by C<sub>DO4</sub> as it is the most optimum oxygen condition for the parameters of the feeding profile (Figure 28).



Specific substrate consumption rates ( $q_s$ ) were similar at the beginning of all strategies since the parameters affecting were similar. The highest specific substrate consumption rate was obtained at  $t = 15$  h as  $q_s = 0.83$  g glucose  $g^{-1}$  cell  $h^{-1}$  with CDO<sub>4</sub> strategy.  $q_s$  values increased in CDO<sub>3</sub> and CDO<sub>4</sub> while they were more or less constant in CDO<sub>2</sub> around  $q_s = 0.30$  g glucose  $g^{-1}$  cell  $h^{-1}$  and decreased with cultivation time in other strategies.

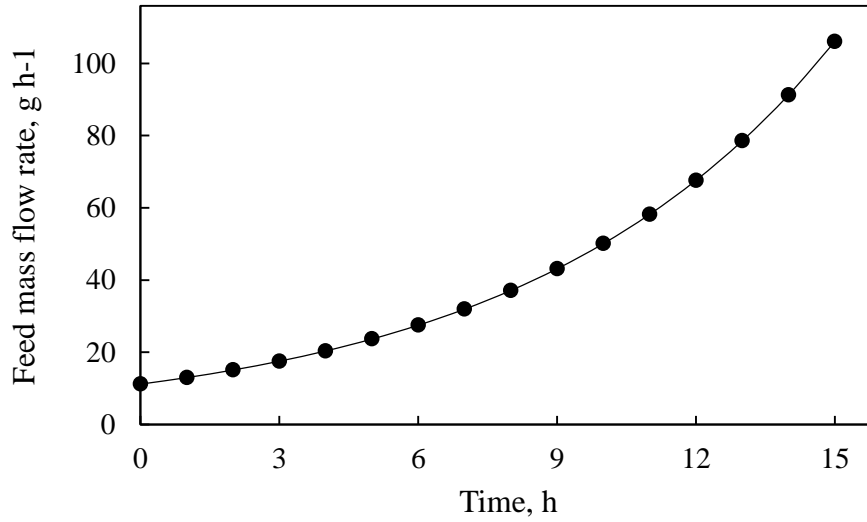


**Figure 28.** Feeding profile of glucose solution according to Equation 34.

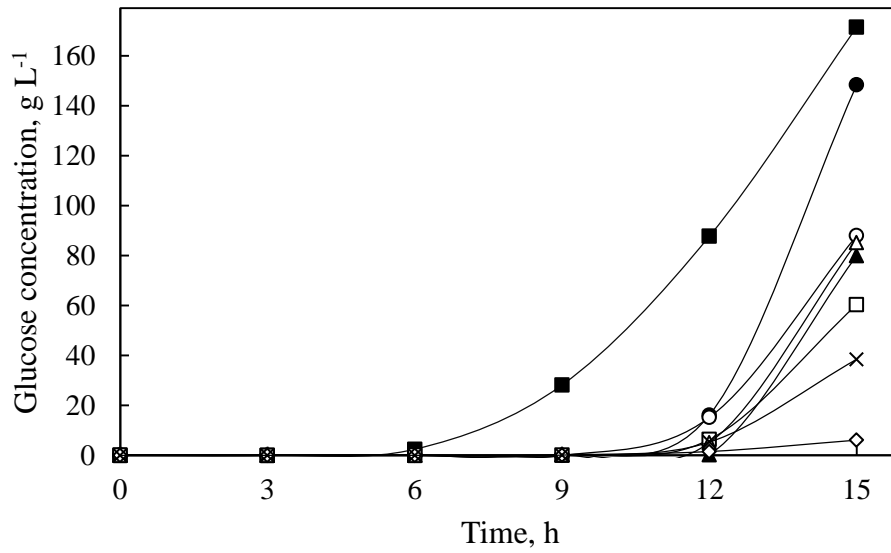


**Figure 29.** Variations in glucose concentration in the fermentation medium with the cultivation time. OTC<sub>1</sub> (●), OTC<sub>2</sub> (■), OTC<sub>3</sub> (▲), CDO<sub>1</sub> (○), CDO<sub>2</sub> (□), CDO<sub>3</sub> (x), CDO<sub>4</sub> (◇), CDO<sub>5</sub> (Δ).

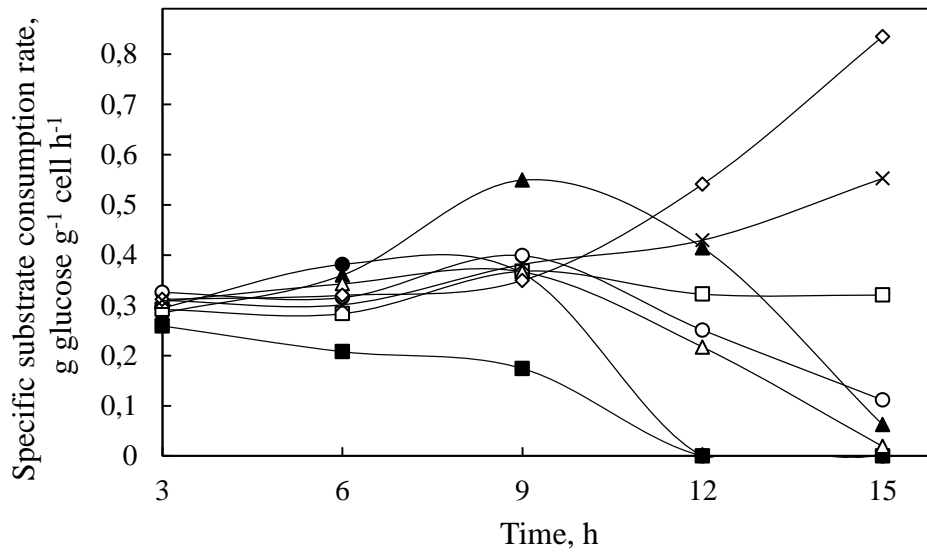


**Figure 30.** Variations in the specific substrate consumption rate with the cultivation time. OTC<sub>1</sub> (●), OTC<sub>2</sub> (■), OTC<sub>3</sub> (▲), CDO<sub>1</sub> (○), CDO<sub>2</sub> (□), CDO<sub>3</sub> (x), CDO<sub>4</sub> (◇), CDO<sub>5</sub> (Δ).

### 4.3.3. GI Activity and Specific GI Activity

Figure 31 shows variation in GI activity with the cultivation time for each strategy applied. The highest GI activity was obtained when dissolved oxygen concentration was kept constant at 15% air saturation, CDO<sub>3</sub>, as 4440 U L<sup>-1</sup>, being 1.4-fold higher than the second highest activity, which was obtained by CDO<sub>1</sub>. Comparable results were obtained for the strategies CDO<sub>1</sub>, CDO<sub>2</sub> and OTC<sub>1</sub>. Lower activity values were obtained in the strategies where oxygen concentrations were relatively higher; OTC<sub>2</sub>, OTC<sub>3</sub>, CDO<sub>4</sub> and CDO<sub>5</sub>. High oxygen transfer rate may cause oxidative stress within the cells, which eventually results in UPR and disturbs secretion of the proteins to extracellular medium (Sjöblom *et al.* 2008).

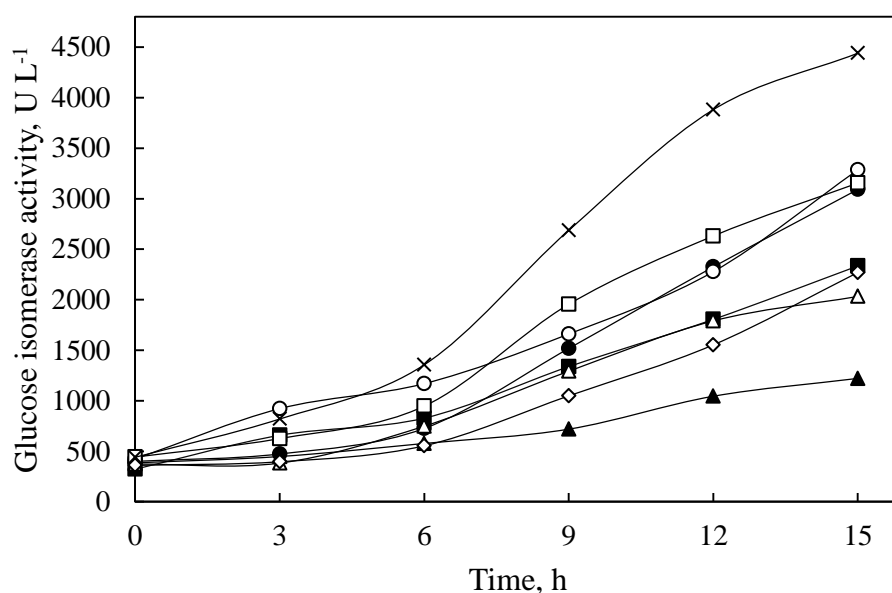


**Figure 31.** Variations in GI activity with the cultivation time. OTC<sub>1</sub> (●), OTC<sub>2</sub> (■), OTC<sub>3</sub> (▲), CDO<sub>1</sub> (○), CDO<sub>2</sub> (□), CDO<sub>3</sub> (×), CDO<sub>4</sub> (◇), CDO<sub>5</sub> (△).

Specific GI activity,  $q_{GI}$ , is defined as GI activity obtained per gram cell. This value is evaluated to gain an insight about the active GI production capacity of the cells.  $q_{GI}$  values for each strategy are given in Figure 32. When specific activities were compared, CDO<sub>1</sub>, CDO<sub>3</sub> and OTC<sub>2</sub> showed very similar peak values, followed by

OTC<sub>1</sub> and CDO<sub>2</sub>. The lowest specific activities were obtained from OTC<sub>3</sub>, CDO<sub>4</sub> and CDO<sub>5</sub>. The highest specific activity obtained was 126 U g<sup>-1</sup> cell by CDO<sub>3</sub> strategy.

In *P. pastoris* fermentations, dissolved oxygen concentration is conventionally kept constant at moderate conditions, around 20 – 30% saturation but recent findings showed that low oxygen availability and even hypoxia can enhance cells' metabolic pathway for recombinant protein production (Baumann *et al.* 2008). Results obtained in this study also support Baumann and her co-workers' findings in terms of recombinant protein production and oxygen availability.

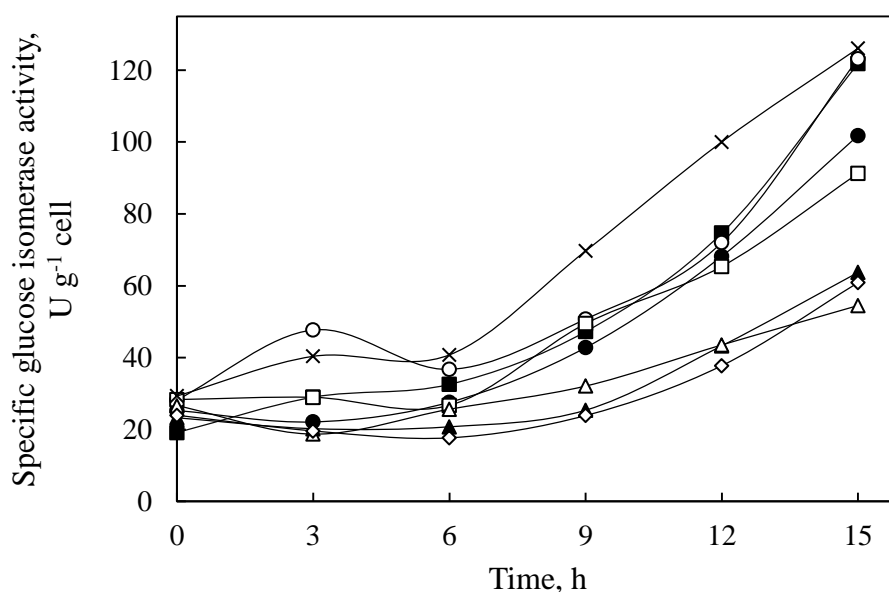


**Figure 32.** Variations in the specific GI activity with the cultivation time. OTC<sub>1</sub> (●), OTC<sub>2</sub> (■), OTC<sub>3</sub> (▲), CDO<sub>1</sub> (○), CDO<sub>2</sub> (□), CDO<sub>3</sub> (x), CDO<sub>4</sub> (◇), CDO<sub>5</sub> (Δ).

Ata *et al.* (2015) investigated the effect of feeding strategies on GI production by *P. pastoris* under P<sub>AOXI</sub> and obtained 32500 U L<sup>-1</sup> activity at t = 53 h while the specific activity was ca. 270 U g<sup>-1</sup> cell when methanol concentration in the medium was kept constant at 5 g L<sup>-1</sup>. Under P<sub>AOXI</sub>, GI activity was 7-fold and specific GI activity was 2-fold higher than the highest values obtained in this study, with an expense of longer cultivation time. Although 7-fold low GI activities were obtained under P<sub>GAP</sub>,

performances of individual cells, as evaluated by specific GI activity, only 2-fold lower. Performance of individual cells can be enhanced by fine-tuning the bioreactor operation parameters; which would result in higher specific GI activities. If more efficient feeding strategies are enabled in the future; comparable or even higher productivities can be obtained by  $P_{GAP}$ , than  $P_{AOXI}$  in more than 3-fold shorter fermentation times.

Akdağ and Çalık (2014) investigated the effect of untreated beet-molasses feeding strategies on GI production by sucrose-utilizing *E. coli*. The highest GI activity was obtained as  $35270 \text{ U L}^{-1}$  at  $t = 17 \text{ h}$ . Although high GI activities were obtained by *E. coli* at comparably early hours of the process; intracellular production of GI makes *E. coli* an undesirable host microorganism when downstream processing is taken into consideration.

#### **4.3.4. GI Monomer Concentration: SDS-PAGE**

To determine the effect of oxygen availability on GI monomer concentration, SDS-PAGE analysis was done. Figure 33 shows the comparison of GI monomers produced in each strategy on a silver stained SDS-PAGE gel. When the intensities are compared, it is seen that although GI activity is almost 2-fold higher in  $CDO_3$ , monomer concentration of GI produced by  $CDO_4$  is almost the same as that produced by  $CDO_3$ . This result indicates a problem with the formation of active homotetramer structure of the GI monomer after secretion to the extracellular medium. It can clearly be deducted that even though cells have a higher capacity of GI production with  $CDO_4$ , monomers produced and secreted remain as subunits instead of forming correct GI homotetramer conformation when dissolved oxygen concentration in the fermentation medium is high.

In  $OTC_3$  strategy, the cell concentration, GI activity and secreted GI monomer concentration remained at comparatively low levels. Although high substrate consumption rates were obtained, attaining low specific growth rate and low productivity can be the consequence of intracellular protein accumulation due to high

oxidative stress that might have been resulted from high oxygen transfer rates (Hohenblum *et al.* 2003).

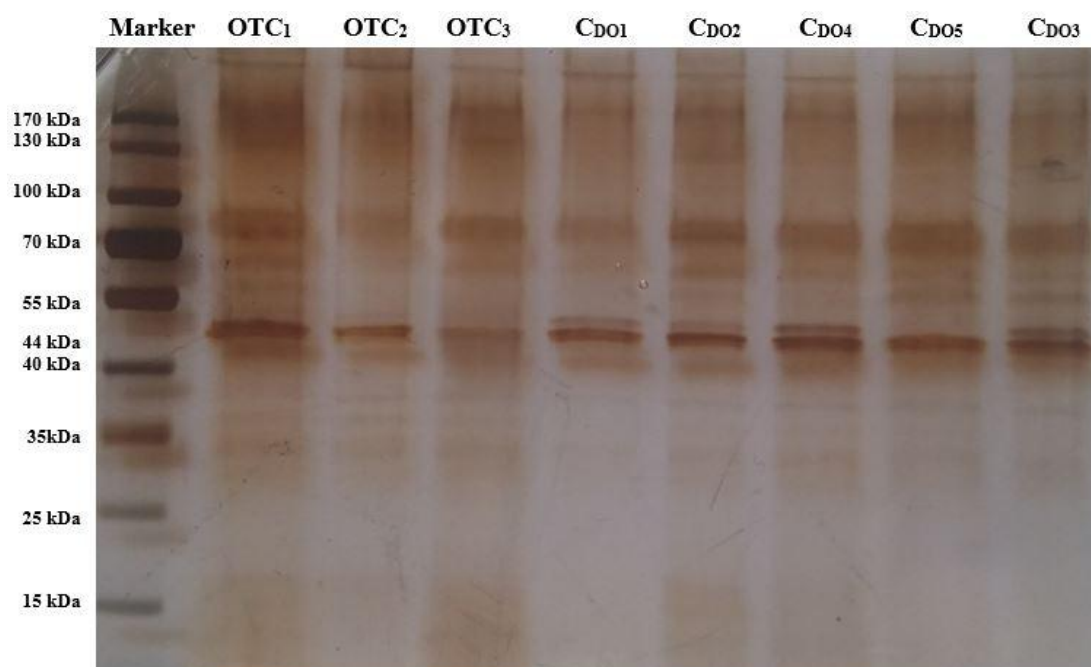


**Figure 33.** Silver stained SDS-PAGE gel images of the applied strategies at  $t = 15$  h. From left to right: Marker, OTC<sub>1</sub>, OTC<sub>2</sub>, OTC<sub>3</sub>, CDO<sub>1</sub>, CDO<sub>2</sub>, CDO<sub>4</sub>, CDO<sub>5</sub>, and CDO<sub>3</sub>.

#### 4.3.5. Proteolytic Activity

Protease activities with respect to the cultivation time are given in Figure 34. Only acidic protease activity was evaluated since bioprocesses were conducted within  $\text{pH} = 5.0 - 5.5$ . Analogous profiles were obtained in each process. The highest proteolytic activity was obtained as  $147 \text{ U mL}^{-1}$  in CDO<sub>4</sub>; being almost the same as OTC<sub>3</sub>. Evaluating proteolytic activity is important for the fermentation processes since the secretion of protease enzymes degrades produced recombinant proteins and decreases the final product yield.

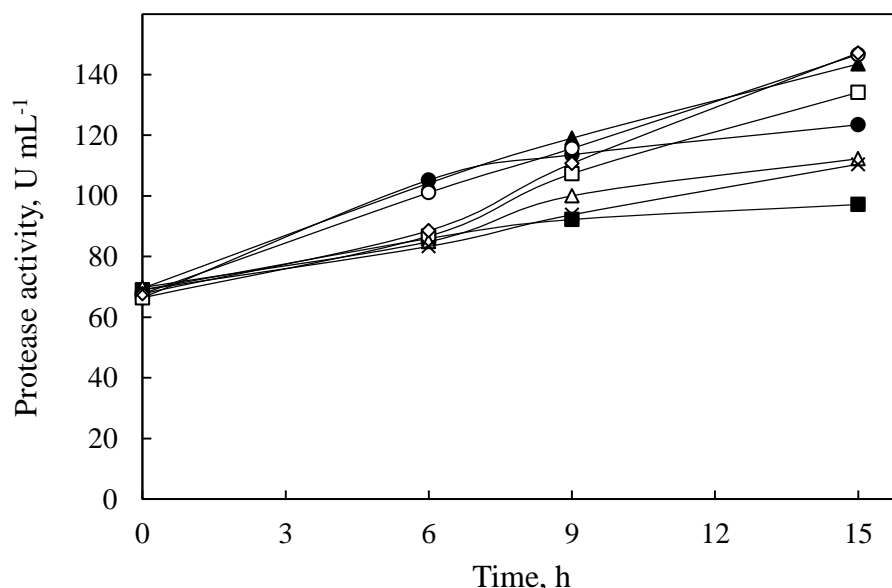


**Figure 34.** Variations in protease activity with the cultivation time. OTC<sub>1</sub> (●), OTC<sub>2</sub> (■), OTC<sub>3</sub> (▲), CDO<sub>1</sub> (○), CDO<sub>2</sub> (□), CDO<sub>3</sub> (x), CDO<sub>4</sub> (◇), CDO<sub>5</sub> (Δ).

In all strategies, the highest GI activities were obtained during the last hour of the cultivation. Even though cells enter stationary and/or death phase, GI production continues to increase and proteolytic degradation is negligible.

#### 4.3.6. Organic Acid Concentrations

Organic acid concentrations were analyzed for each strategy and are given in Figure 35 through Figure 42 and tabulated in APPENDIX E. The most excreted organic acid was acetic acid, which was present in various concentrations in every bioprocess. Pyruvic acid was hardly detected in all processes. In low-to-moderate oxygen transfer conditions; gluconic, lactic and the organic acids involved in TCA cycle show higher tendency of accumulation.

Gluconic acid could not be detected in the strategies where moderate oxygen transfer conditions were applied. It accumulated to rather high concentrations in OTC<sub>1</sub>, OTC<sub>2</sub> and CDO<sub>1</sub> strategies. Gluconic acid is used by pentose phosphate pathway (PPP) of

*P. pastoris* when oxygen and substrate availability is at moderate conditions. During starvation and hypoxia, gluconic acid cannot enter PPP and starts to accumulate. Therefore, incomplete glucose oxidation can be the reason for gluconic acid accumulation.

Lactic acid is produced during oxygen limitation because of the shift of pathway from fully-aerobic to anaerobic conditions. Lactic acid mostly accumulated in relatively lower oxygen transfer conditions whereas no lactic acid accumulation was observed in  $C_{DO4}$  and  $C_{DO5}$  strategies. Generally, lactic acid started to accumulate when DO dropped to almost zero for constant OTC strategies whereas it could be detected at all times with increasing concentration for CDO strategies where  $C_{DO}$  is comparatively low.

Pyruvic acid was almost never detected, indicating that fluxes through pyruvate node are high enough to prevent accumulation. Acetic acid was almost always detected in every strategy with increasing concentrations with cultivation time.

Other organic acids; citric-, malic-, succinic- and fumaric acids are involved in TCA cycle. Oxygen is essential for TCA cycle to be able to work properly. Similar to other oxygen-dependent metabolites, they accumulated less in higher oxygen availability, and more in rather low oxygen availability due to the low efficiency of aerobic respiration.



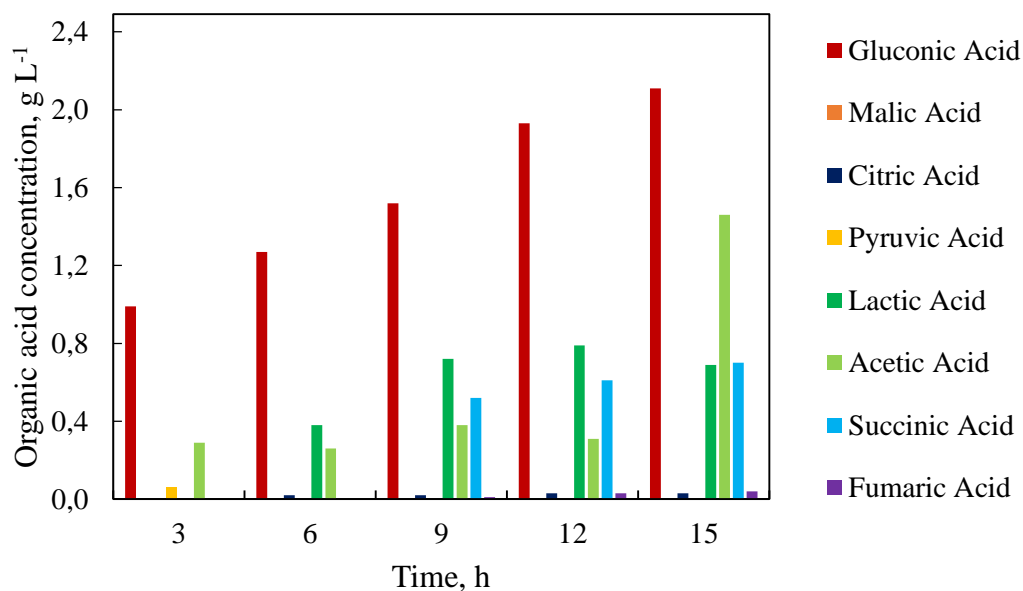


**Figure 35.** Variations in organic acid concentrations with the cultivation time for OTC<sub>1</sub> strategy.

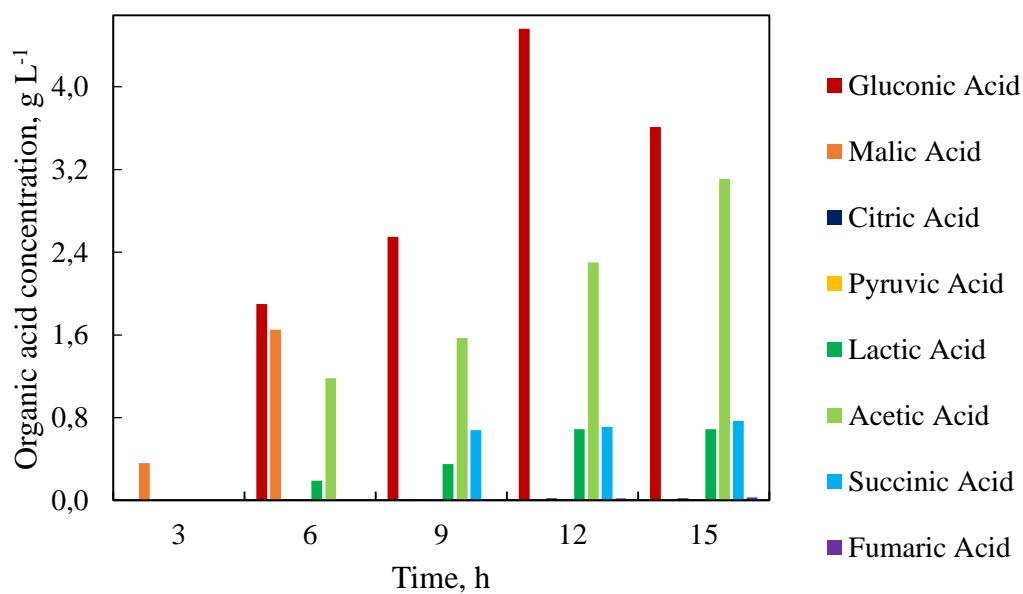


**Figure 36.** Variations in organic acid concentrations with the cultivation time for OTC<sub>2</sub> strategy.

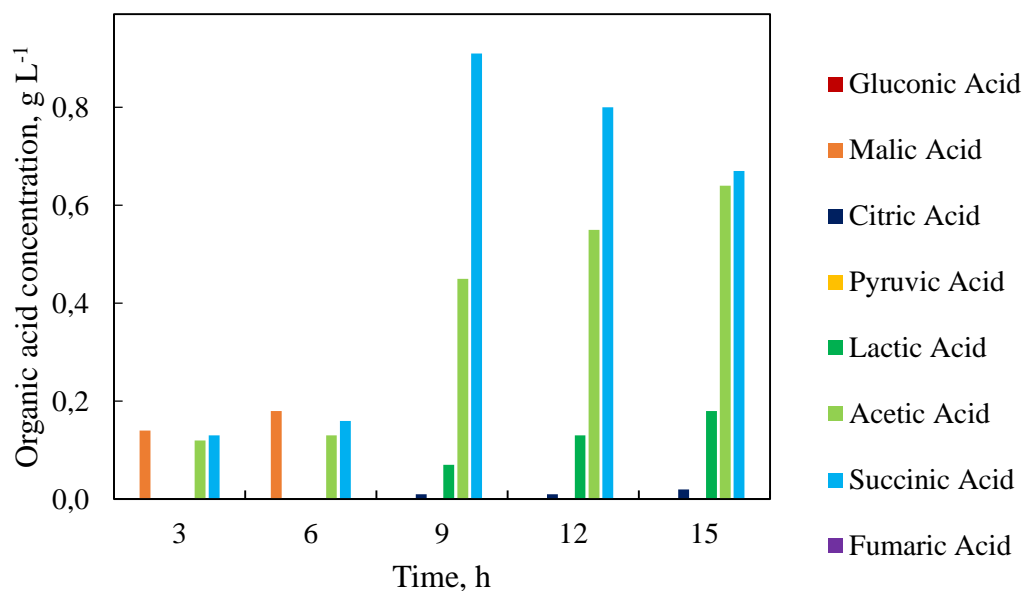


**Figure 37.** Variations in organic acid concentrations with the cultivation time for OTC<sub>3</sub> strategy.

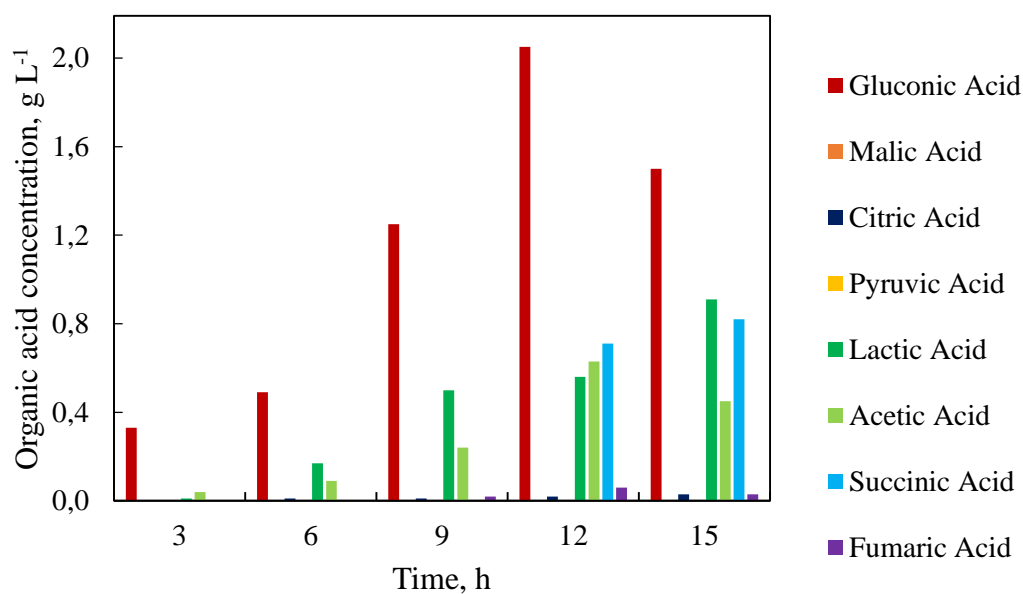


**Figure 38.** Variations in organic acid concentrations with the cultivation time for CDO<sub>1</sub> strategy.

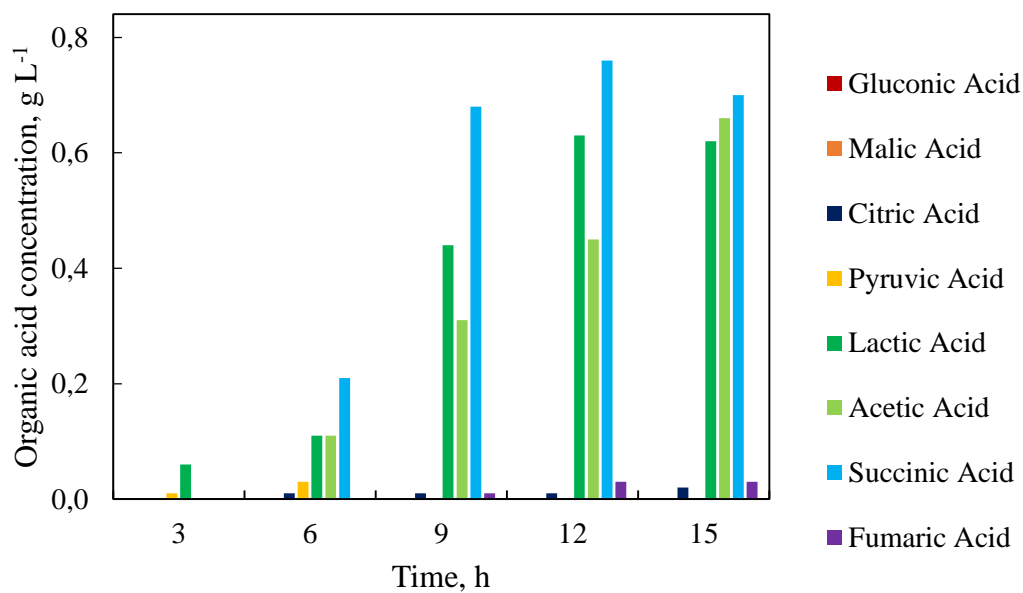


**Figure 39.** Variations in organic acid concentrations with the cultivation time for CDO<sub>2</sub> strategy.

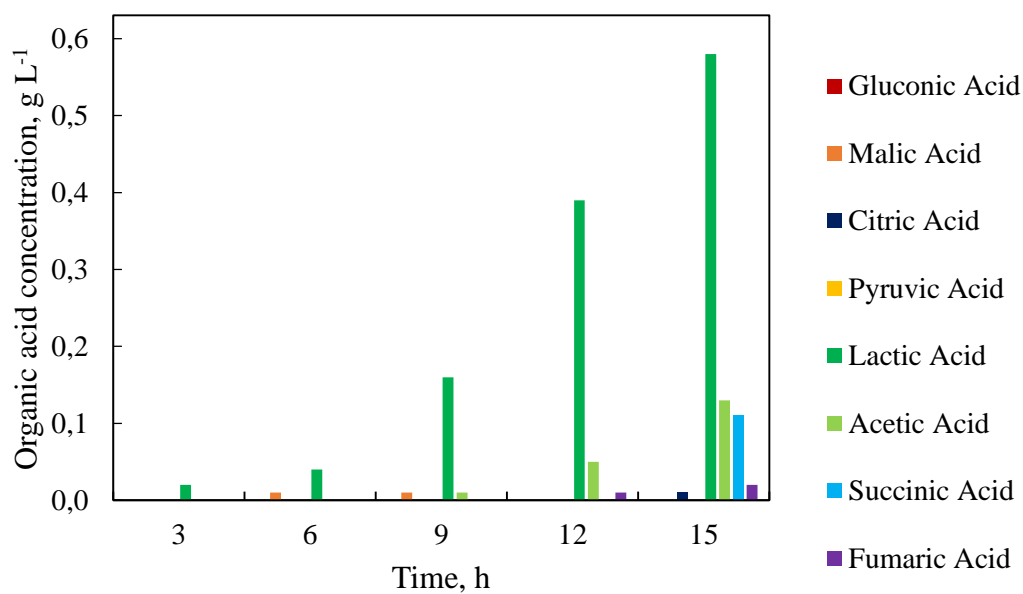


**Figure 40.** Variations in organic acid concentrations with the cultivation time for CDO<sub>3</sub> strategy.

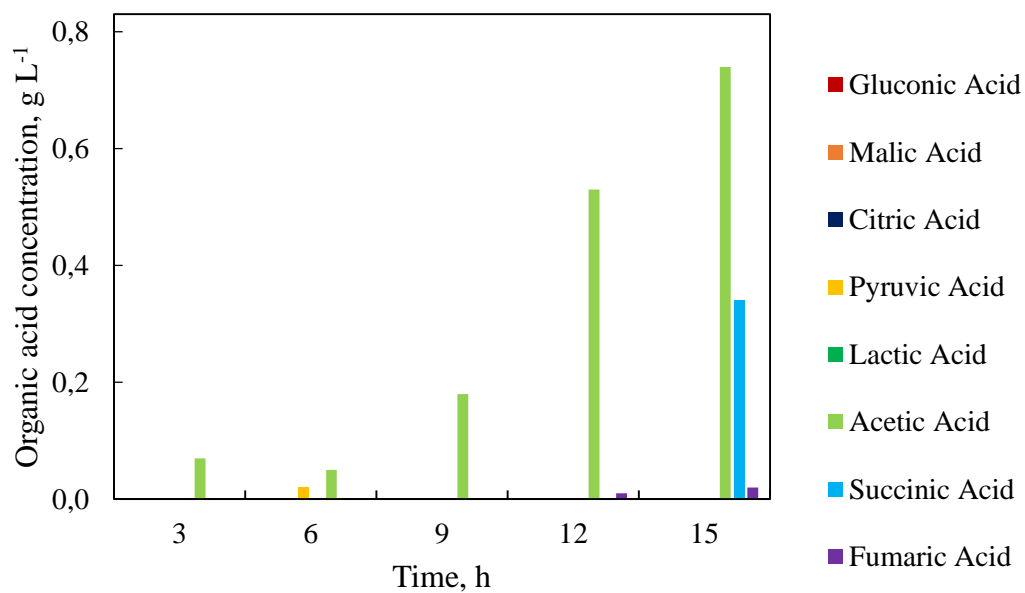


**Figure 41.** Variations in organic acid concentrations with the cultivation time for CDO<sub>4</sub> strategy.

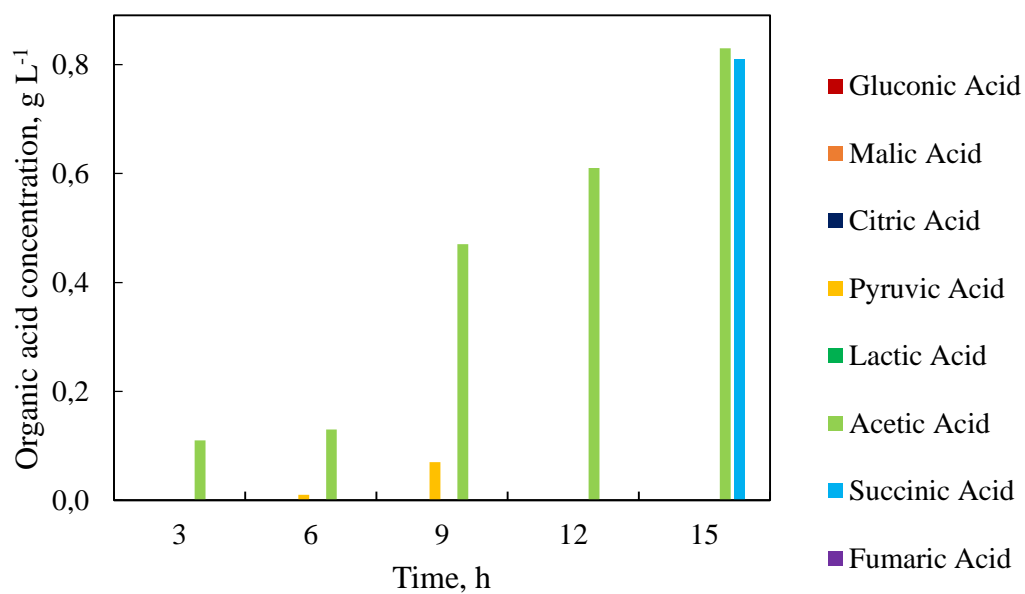


**Figure 42.** Variations in organic acid concentrations with the cultivation time for CDO<sub>5</sub> strategy.

Organic acid concentrations in the fermentation medium should be examined to gain a further understanding of the bioprocesses and possible limitations of the targeted protein production. Availability of organic acids is of utmost importance as most of the pathways, especially central carbon metabolism, is directly affected by their presence. Accumulation of these organic acids should be controlled by fine-tuning the bioreactor operation conditions for recombinant protein production since it may decrease the fluxes towards the recombinant protein production; furthermore, result in the waste of raw materials and lower specific cell growth rates as cell concentration cannot increase further.

#### **4.3.7. Oxygen Transfer Characteristics**

In order to investigate the effect of oxygen transfer characteristics on GI production, volumetric mass transfer coefficient, oxygen transfer rate, oxygen uptake rate, maximum possible oxygen transfer and uptake rates, Damköhler number, and effectiveness factor were calculated. Variation of oxygen transfer characteristics are given in Table 11. Parameters involved in oxygen transfer could only be calculated for the first six hours of the bioprocesses. Due to high demand of oxygen resulting from high cell concentrations, it was not possible to apply dynamic method to evaluate the parameters for the proceeding hours.

Volumetric mass transfer coefficient depends on superficial gas velocity, power input to the broth and medium properties such as viscosity. Therefore,  $K_{La}$  can be considered the same when aeration and agitation rates, and the broth composition are the same. By this assumption, all CDO experiments, at least for the zeroth hour, should perform the same oxygen transfer characteristics as aeration and agitation rates are almost the same, as well as cell concentration and fermentation medium composition. When Table 11 is analyzed, it is seen that this assumption is somewhat correct. In the case of constant OTC experiments, since air flow rate differs among the strategies, different  $K_{La}$  values were expected. Peculiarly, exactly the same  $K_{La}$  values were obtained at  $t = 0$  h for constant OTC strategies. For the consecutive

hours, the highest  $K_La$  values were obtained in OTC<sub>3</sub> strategy as  $0.054\text{ s}^{-1}$  and  $0.083\text{ s}^{-1}$  for  $t = 3\text{ h}$  and  $t = 6\text{ h}$  of the process, respectively. As cell concentration increases, volumetric uptake rate of oxygen, OUR, increases. The highest OUR was obtained from OTC<sub>3</sub> at  $t = 6\text{ h}$  as  $0.029\text{ mol m}^{-3}\text{ s}^{-1}$ .

The ratio of the oxygen uptake rate to oxygen demand is defined as the effectiveness factor. Closer its value gets to 1, more efficient the oxygen uptake process is. The highest effectiveness factor was obtained in CDO<sub>5</sub> strategy as  $\eta = 0.77$  at  $t = 0\text{ h}$ . Except from CDO<sub>5</sub>, at the beginning of the processes, all strategies showed similar efficiencies around 0.50 - 0.60 and typically decreased with cultivation time because of higher demand of oxygen.

In the cases where oxygen supply is high,  $Da$  is less than 1 for the first hours of the bioprocesses. As time passes and oxygen demand increases,  $Da$  becomes more than 1 in all strategies.

Specific oxygen uptake rate is defined as the mass of oxygen up-taken by unit cell per time. While  $q_O$  values increased with time for constant OTC processes, they stayed somewhat the same through the time course for CDO processes. This was the expected result since in CDO strategies, oxygen supply is controlled by the dissolved oxygen concentration readily in the broth, which indirectly connected to cell concentration. As cell concentration increases, oxygen supply increases accordingly, resulting in constant oxygen uptake rate by individual cells. On the other hand, oxygen is supplied at a constant rate, regardless of the cell concentration in constant OTC processes; resulting in increased  $q_O$  values.

**Table 11.** Variations of oxygen transfer characteristics with cultivation time.

		Time		
		0 h	3 h	6 h
OTC <sub>1</sub>	$K_L a$ $s^{-1}$	0.023	0.037	0.058
	$OTR \cdot 10^3$ $mol\ m^{-3}\ s^{-1}$	5.69	13.6	21.5
	$OTR_{max} \cdot 10^3$ $mol\ m^{-3}\ s^{-1}$	8.51	13.69	21.5
	$OUR \cdot 10^3$ $mol\ m^{-3}\ s^{-1}$	5.97	13.56	21.46
	$OUR_{max} \cdot 10^3$ $mol\ m^{-3}\ s^{-1}$	10.2	33.2	48.2
	$\eta$	0.59	0.41	0.45
	$Da$	1.19	2.42	2.25
	$q_o$ $g\ oxygen\ g^{-1}\ cell\ h^{-1}$	0.04	0.07	0.09
OTC <sub>2</sub>	$K_L a$ $s^{-1}$	0.023	0.038	0.054
	$OTR \cdot 10^3$ $mol\ m^{-3}\ s^{-1}$	5.11	11.0	19.7
	$OTR_{max} \cdot 10^3$ $mol\ m^{-3}\ s^{-1}$	8.51	14.1	20.0
	$OUR \cdot 10^3$ $mol\ m^{-3}\ s^{-1}$	5.11	11.0	19.7
	$OUR_{max} \cdot 10^3$ $mol\ m^{-3}\ s^{-1}$	8.70	34.9	107
	$\eta$	0.59	0.32	0.18
	$Da$	1.03	2.48	5.36
	$q_o$ $g\ oxygen\ g^{-1}\ cell\ h^{-1}$	0.04	0.06	0.09

**Table 11.** Continued.

		<b>Time</b>		
		<b>0 h</b>	<b>3 h</b>	<b>6 h</b>
<b>OTC<sub>3</sub></b>	<b>K<sub>L</sub>a</b> s <sup>-1</sup>	0.023	0.054	0.083
	<b>OTR</b> ·10 <sup>3</sup> mol m <sup>-3</sup> s <sup>-1</sup>	2.95	12.6	28.9
	<b>OTR<sub>max</sub></b> ·10 <sup>3</sup> mol m <sup>-3</sup> s <sup>-1</sup>	8.51	20.0	30.7
	<b>OUR</b> ·10 <sup>3</sup> mol m <sup>-3</sup> s <sup>-1</sup>	2.96	12.6	28.9
	<b>OUR<sub>max</sub></b> ·10 <sup>3</sup> mol m <sup>-3</sup> s <sup>-1</sup>	5.26	29.7	156
	<b>η</b>	0.56	0.42	0.19
	<b>Da</b>	0.62	1.49	5.07
<b>q<sub>o</sub></b> g oxygen g <sup>-1</sup> cell h <sup>-1</sup>		0.02	0.07	0.12
<b>CDO<sub>1</sub></b>	<b>K<sub>L</sub>a</b> s <sup>-1</sup>	0.018	0.031	0.045
	<b>OTR</b> ·10 <sup>3</sup> mol m <sup>-3</sup> s <sup>-1</sup>	5.94	10.83	15.9
	<b>OTR<sub>max</sub></b> ·10 <sup>3</sup> mol m <sup>-3</sup> s <sup>-1</sup>	6.66	11.47	16.65
	<b>OUR</b> ·10 <sup>3</sup> mol m <sup>-3</sup> s <sup>-1</sup>	5.94	10.83	15.9
	<b>OUR<sub>max</sub></b> ·10 <sup>3</sup> mol m <sup>-3</sup> s <sup>-1</sup>	12.4	14.92	45.3
	<b>η</b>	0.48	0.73	0.35
	<b>Da</b>	1.86	1.30	2.72
<b>q<sub>o</sub></b> g oxygen g <sup>-1</sup> cell h <sup>-1</sup>		0.05	0.06	0.06



**Table 11.** Continued.

		<b>Time</b>		
		<b>0 h</b>	<b>3 h</b>	<b>6 h</b>
<b>CDO<sub>2</sub></b>	<b>K<sub>L</sub>a</b> s <sup>-1</sup>	0.02	0.032	0.042
	<b>OTR</b> ·10 <sup>3</sup> mol m <sup>-3</sup> s <sup>-1</sup>	6.22	10.8	14.5
	<b>OTR<sub>max</sub></b> ·10 <sup>3</sup> mol m <sup>-3</sup> s <sup>-1</sup>	7.40	11.8	15.5
	<b>OUR</b> ·10 <sup>3</sup> mol m <sup>-3</sup> s <sup>-1</sup>	6.22	10.8	14.5
	<b>OUR<sub>max</sub></b> ·10 <sup>3</sup> mol m <sup>-3</sup> s <sup>-1</sup>	9.70	14.1	34.3
	<b>η</b>	0.64	0.76	0.42
	<b>Da</b>	1.31	1.19	2.21
	<b>q<sub>o</sub></b> g oxygen g <sup>-1</sup> cell h <sup>-1</sup>	0.05	0.06	0.05
	<b>K<sub>L</sub>a</b> s <sup>-1</sup>	0.02	0.028	0.045
	<b>OTR</b> ·10 <sup>3</sup> mol m <sup>-3</sup> s <sup>-1</sup>	3.15	8.70	13.7
<b>CDO<sub>3</sub></b>	<b>OTR<sub>max</sub></b> ·10 <sup>3</sup> mol m <sup>-3</sup> s <sup>-1</sup>	3.70	10.4	16.7
	<b>OUR</b> ·10 <sup>3</sup> mol m <sup>-3</sup> s <sup>-1</sup>	3.14	8.70	13.7
	<b>OUR<sub>max</sub></b> ·10 <sup>3</sup> mol m <sup>-3</sup> s <sup>-1</sup>	5.35	11.6	30.0
	<b>η</b>	0.59	0.75	0.46
	<b>Da</b>	1.45	1.12	1.80
	<b>q<sub>o</sub></b> g oxygen g <sup>-1</sup> cell h <sup>-1</sup>	0.04	0.05	0.05

**Table 11.** Continued.

		<b>Time</b>		
		<b>0 h</b>	<b>3 h</b>	<b>6 h</b>
<b>CDO<sub>4</sub></b>	<b>K<sub>L</sub>a</b> s <sup>-1</sup>	0.02	0.031	0.042
	<b>OTR</b> ·10 <sup>3</sup> mol m <sup>-3</sup> s <sup>-1</sup>	5.92	8.67	12.7
	<b>OTR<sub>max</sub></b> ·10 <sup>3</sup> mol m <sup>-3</sup> s <sup>-1</sup>	7.40	11.1	15.5
	<b>OUR</b> ·10 <sup>3</sup> mol m <sup>-3</sup> s <sup>-1</sup>	5.92	8.67	12.7
	<b>OUR<sub>max</sub></b> ·10 <sup>3</sup> mol m <sup>-3</sup> s <sup>-1</sup>	10.3	12.9	20.2
	<b>η</b>	0.57	0.67	0.63
	<b>Da</b>	1.39	1.16	1.30
<b>q<sub>o</sub></b> g oxygen g <sup>-1</sup> cell h <sup>-1</sup>		0.05	0.05	0.05
<b>CDO<sub>5</sub></b>	<b>K<sub>L</sub>a</b> s <sup>-1</sup>	0.02	0.03	0.044
	<b>OTR</b> ·10 <sup>3</sup> mol m <sup>-3</sup> s <sup>-1</sup>	4.61	6.40	10.4
	<b>OTR<sub>max</sub></b> ·10 <sup>3</sup> mol m <sup>-3</sup> s <sup>-1</sup>	7.40	11.1	16.3
	<b>OUR</b> ·10 <sup>3</sup> mol m <sup>-3</sup> s <sup>-1</sup>	4.61	6.40	10.4
	<b>OUR<sub>max</sub></b> ·10 <sup>3</sup> mol m <sup>-3</sup> s <sup>-1</sup>	6.02	10.4	18.5
	<b>η</b>	0.77	0.62	0.57
	<b>Da</b>	0.81	0.94	1.13
<b>q<sub>o</sub></b> g oxygen g <sup>-1</sup> cell h <sup>-1</sup>		0.04	0.04	0.04

#### 4.3.8. Yield Coefficients

Yield coefficients were calculated for the exponential phase of the bioprocesses. Overall and instantaneous yield with respect to each strategy are given in Table 12.

Since the highest cell concentration was reached in CDO<sub>4</sub> strategy, the highest overall  $Y_{X/S}$  is obtained by CDO<sub>4</sub> as well. Since the amount of glucose fed is the same for all experiments and the amount of the glucose utilized can be assumed to be the same for the first nine hour of the processes, the only parameter affecting the cell yield on substrate is the cell concentration. It is important to note that theoretical cell yield on glucose is  $0.48 \text{ g g}^{-1}$  (Cos *et al.* 2005) when  $C_{DO}$  is kept constant at 20% air saturation. Indeed  $Y_{X/S} = 0.48 \text{ g g}^{-1}$  was achieved by that strategy.

The highest  $Y_{X/O}$  value was obtained by OTC<sub>2</sub> strategy as  $5.45 \text{ g g}^{-1}$  at the beginning of the bioprocess. The highest  $Y_{X/O}$  values were all obtained at the beginning of the production due to increasing OUR values at the proceeding hours of the bioprocesses.

**Table 12.** Instantaneous and overall yield coefficients

Strategy	Time	$Y_{X/S}$	$Y_{X/O}$
	h	g cell g <sup>-1</sup> substrate	g cell g <sup>-1</sup> oxygen
OTC <sub>1</sub>	0	0.37	2.71
	3	0.28	1.12
	6	0.23	0.95
	9	0.24	-
	<b>Overall</b>	<b>0.33</b>	-
OTC <sub>2</sub>	0	0.21	3.34
	3	0.24	1.13
	6	0.18	0.41
	9	0.20	-
	<b>Overall</b>	<b>0.19</b>	-
OTC <sub>3</sub>	0	0.19	5.45
	3	0.30	1.29
	6	0.10	0.31
	9	0.01	-
	<b>Overall</b>	<b>0.19</b>	-
CDO <sub>1</sub>	0	0.15	2.10
	3	0.45	2.25
	6	0.22	1.22
	9	0.02	-
	<b>Overall</b>	<b>0.30</b>	-

**Table 12.** Continued.

Strategy	Time h	$Y_{X/S}$ g cell g <sup>-1</sup> substrate	$Y_{X/O}$ g cell g <sup>-1</sup> oxygen
<b>CDO<sub>2</sub></b>	0	0.28	2.79
	3	0.52	2.65
	6	0.30	1.79
	9	0.09	-
	<b>Overall</b>	<b>0.23</b>	-
<b>CDO<sub>3</sub></b>	0	0.20	4.86
	3	0.48	3.03
	6	0.30	1.92
	9	0.12	-
	<b>Overall</b>	<b>0.22</b>	-
<b>CDO<sub>4</sub></b>	0	0.16	2.53
	3	0.43	2.72
	6	0.39	2.70
	9	0.27	-
	<b>Overall</b>	<b>0.48</b>	-
<b>CDO<sub>5</sub></b>	0	0.21	4.04
	3	0.40	3.42
	6	0.33	2.74
	9	0.25	-
	<b>Overall</b>	<b>0.26</b>	-



## CHAPTER 5

### CONCLUSION

For aerobic organisms, oxygen transfer is essential and optimization of oxygen transfer conditions play a very important role to obtain high productivities. *P. pastoris* fermentations are conventionally conducted at 20 - 30% air saturation and more recent findings show that lower oxygen concentrations enabled higher product titers. The disagreement on oxygen transfer conditions in *P. pastoris* fermentations prompted us to investigate the effect of oxygen transfer conditions on glucose isomerase production by *P. pastoris* under  $P_{GAP}$ . To analyze the response of *P. pastoris* cells to oxygen transfer conditions; cell concentration, glucose accumulation, GI activity and monomer concentration, proteolytic degradation and organic acid profiles were presented. Designed and applied strategies were also analyzed in terms of oxygen transfer and bioprocess characteristics such as specific formation and consumption rates, as well as overall and instantaneous yields.

Among all strategies, the highest cell concentration was obtained in CDO<sub>4</sub> as 44 g L<sup>-1</sup> at  $t = 9$  h. Since the parameters determining the feeding rate of glucose was optimized according to 20% air saturation of the fermentation medium, obtaining the highest cell density by CDO<sub>4</sub> strategy was the expected result. Overall lowest cell concentrations were obtained in OTC<sub>2</sub> and OTC<sub>3</sub> strategies. It may be speculated that the excessive abundance of oxygen at the earlier hours of the bioprocesses result in a shift in metabolic pathway and represses cell growth.

During the exponential phase of cell growth, glucose accumulation was prevented since the glucose uptake rate was equal to glucose feeding rate; except for OTC<sub>2</sub>. The

highest specific glucose consumption rate was obtained as  $q_s = 0.80 \text{ g glucose g}^{-1} \text{ cell h}^{-1}$  by CDO<sub>4</sub> strategy.

The highest GI activity was achieved in CDO<sub>3</sub> strategy as  $4440 \text{ U L}^{-1}$ , which is 1.4-fold higher than the second highest GI activity achieved. The highest specific GI activity was also obtained by CDO<sub>3</sub> strategy as  $126 \text{ U g}^{-1} \text{ cell}$ . Lower activity values were obtained in the strategies where oxygen had higher abundance, such as OTC<sub>2</sub>, OTC<sub>3</sub>, CDO<sub>4</sub> and CDO<sub>5</sub> strategies. Lower oxygen availability probably increases transcription levels of the genes involved in glycolysis pathway which may be the reason for the increased productivities with low-to-moderate oxygen transfer conditions under  $P_{GAP}$ . Although the highest cell concentrations were reached at  $t = 9 \text{ h}$  of each strategy, GI activity continued to increase even at the stationary phase, reaching its peak at  $t = 15 \text{ h}$ . When the duration of bioprocesses was extended, GI activity decreased as well as cell concentration (data not shown), therefore the bioprocesses were kept as short as fifteen hours.

By CDO<sub>1</sub> strategy, the second highest GI activity was obtained. However, there is considerable amount of glucose accumulation due to high rates of glucose feeding. Since glucose accumulation may cause substrate inhibition to cells, glucose feeding rate should be decreased in order to prevent accumulation. If the parameters of predetermined exponential feeding equation are optimized, better results might be obtained in terms of both cell growth and GI activity. It is important to note that keeping dissolved oxygen concentration at low saturation levels such as 5% is challenging and a robust control system for the air flow is necessary such as a PID control system.

SDS-PAGE analysis showed that even though CDO<sub>4</sub> had almost the same GI monomer concentration as CDO<sub>3</sub>, the activity obtained from CDO<sub>3</sub> strategy was almost 2-fold higher than that from CDO<sub>4</sub>. Reasons for obtaining low GI activity in spite of having high monomer concentration should be studied deeper to overcome the problem and obtain higher productivities.



Organic acids involved in TCA cycle showed high abundance in the strategies with low-oxygen availability, which was the expected result as oxygen is essential for TCA cycle to work properly. Pyruvic acid was hardly detected during fermentation, indicating the fluxes going into and out of pyruvate node are high enough to prevent accumulation. Although organic acid concentrations give an insight about the central metabolism of the cells, doing metabolic flux analysis would be more beneficial in order to reduce speculation levels. Along with metabolic flux analysis, proteome and transcriptome studies would be valuable to have a deeper insight of the up and downregulations within the cells with changing oxygen transfer conditions.

The bioprocesses were analyzed in terms of oxygen uptake efficiencies. The highest oxygen uptake efficiency was achieved by CDO<sub>5</sub> strategy as 0.77 at the beginning of the bioprocess. Also in other strategies, the highest levels of efficiencies were obtained at the earlier hours of the processes and their values ranged between 0.50 – 0.60.

When overall cell yields on substrate were calculated for each strategy, it is seen that only CDO<sub>4</sub> reached the  $Y_{X/S}$  value used as the parameter of the substrate feeding equation. Different overall yields were obtained for different oxygen transfer strategies, indicating that  $Y_{X/S}$  parameter, along with other parameters, should be optimized in the feeding equation according to the oxygen transfer strategy to be applied.

Compared to  $P_{AOXI}$ -driven expression systems, using  $P_{GAP}$  for GI production considerably decreased cultivation time. Although as high GI activities could not be reached, constitutive nature of  $P_{GAP}$ , shortening of the cultivation time and elimination of methanol usage make  $P_{GAP}$  a favorable alternative to  $P_{AOXI}$  for recombinant protein production under *P. pastoris*.



## REFERENCES

- Ahmad, M., Hirz, M., Pichler, H., Schwab, H., 2014. "Protein expression in *Pichia pastoris*: Recent achievements and perspectives for heterologous protein production." *Applied Microbiology and Biotechnology* 98:5301-5317.
- Ahn, J., Hong, J., Lee, H., Park, M., Lee, E., Kim, C., Choi, E., Jung, J., Lee, H., 2007. "Translation elongation factor 1-alpha gene from *Pichia pastoris*: molecular cloning, sequence, and use of its promoter." *Applied Microbiology and Biotechnology* 74:601:608.
- Akdağ, B., Çalık, P., 2014, "Recombinant protein production by sucrose-utilizing *Escherichia coli* W: Untreated beet molasses-based feeding strategy development." *Journal of Chemical Technology and Biotechnology* 90(6):1070-1076.
- Angardi, V., Çalık, P., 2013, "Beet molasses based exponential feeding strategy for thermostable glucose isomerase production by recombinant *Escherichia coli* BL21 (DE3)." *Journal of Chemical Technology and Biotechnology* 88(5):845–852
- Ata, Ö, 2012. "Metabolical engineering of *Pichia pastoris* for extracellular thermostable glucose isomerase production." M.Sc. Thesis. Middle East Technical University, Turkey.
- Ata, Ö, Boy, E., Güneş H., Çalık, P., 2015. "Codon optimization of *xylA* gene for recombinant glucose isomerase production in *Pichia pastoris* and fed-batch feeding strategies to fine-tune bioreactor performance." *Bioprocess and Biosystems Engineering* 38:889-903.
- Bailey, J.E., Ollis, D.F., Biochemical engineering fundamentals. 2nd ed, McGraw-Hill Inc., New York, 1986.

- Baneyx, F., 1999. "Recombinant protein expression in *Escherichia coli*." *Current Opinion in Biotechnology* 10(5):411-421.
- Batt, C.A., Jamieson, A.C., Vandeyar, M.A., 1990. "Identification of essential histidine residues in the active site of *Escherichia coli* xylose (glucose) isomerase." *Proceedings of the National Academy of Sciences* 87:618-622.
- Baumann, K., Carnicer, M., Dragosits, M., Graf, A.B., Stadlmann, J., Jouhten, P., Maaheimo, H., Gasser, B., Albiol, J., Mattanovich, D., Ferrer, P., 2010. "A multi-level study of recombinant *Pichia pastoris* in different oxygen conditions." *BMC Systems Biology* 4:141.
- Baumann, K., Maurer, M., Dragosits, M., Cos, O., Ferrer, P., Mattanovich, D., 2008. "Hypoxic fed-batch cultivation of *Pichia pastoris* increases specific and volumetric productivity of recombinant proteins." *Biotechnology and Bioengineering* 100(1):177-183.
- Bhosale, S. H., Mala, B.L., Deshpande, V.V., 1996. "Molecular and industrial aspects of glucose isomerase." *Microbiological Reviews* 60(2):280-300.
- Boer, H., Teeri, T.T., Koivula, A., 2000. "Characterization of *Trichoderma reesei* cellobiohydrolase Cel7A secreted from *Pichia pastoris* using two different promoters." *Biotechnology and Bioengineering* 69:486-494.
- Boyacı, İ.H., 2005. "A new approach for determination of enzyme kinetic constants using response surface methodology." *Biochemical Engineering Journal*, 25:55-62.
- Çalık, P., Çalık, G., Özdamar, T.H., 2000. "Oxygen-transfer strategy and its regulation effects in serine alkaline protease production by *Bacillus licheniformis*." *Biotechnology and Bioengineering* 69(3):301-311.
- Çalık, P., Ata, Ö, Güneş, H., Massahi, A., Boy, E., Keskin, A., Öztürk, S., Zerze, G.H., Özdamar, T.H., 2015. "Recombinant protein production in *Pichia pastoris* under glyceraldehyde-3-phosphate dehydrogenase promoter: From carbon source

metabolism to bioreactor operation parameters.” *Biochemical Engineering Journal* 95:20-36.

Campbell, N.A., Reece, J.B., Biology. 6th ed., Pearson, Benjamin Cummings, San Francisco, 2001.

Carnicer, M., 2012. “Systematic metabolic analysis of recombinant *Pichia pastoris* under different oxygen conditions.” Ph.D. Thesis, Universitat Autònoma de Barcelona, Spain.

Çelik, E., 2008. “Bioprocess development for therapeutical protein production.” Ph.D. Thesis, Middle East Technical University, Turkey.

Cereghino, G.P.L., Cereghino, J.L., Ilgen, C., Cregg, J.M., 2002. “Production of recombinant proteins in fermenter cultures of the yeast *Pichia pastoris*.” *Current Opinion in Biotechnology* 13:329-332.

Cereghino, J.L., Cregg, J.M., 2000. “Heterologous protein expression in the methylotrophic yeast *Pichia pastoris*.” *FEMS Microbiology Reviews* 24:45-66.

Chan, E., Ueng, P.P., Chen, L., 1986. “D-xylose fermentation to ethanol by *Schizosaccharomyces pombe* cloned with xylose isomerase gene.” *Biotechnology Letters* 8(4):231-234.

Cos, O., Ramon, R., Montesinos, J.L., Valero, F. 2006. “Operational strategies, monitoring and control of heterologous protein production in the methylotrophic yeast *Pichia pastoris* under different promoters: A review.” *Microbial Cell Factories* 5(17).

Cos, O., Resina, D., Ferrer, P., Montesinos, J.L., Valero, F., 2005. “Heterologous production of *Rhizopus oryzae* lipase in *Pichia pastoris* using the alcohol oxidase and formaldehyde dehydrogenase promoters in batch and fed-batch cultures.” *Biochemical Engineering Journal* 26:86-94.

Cregg, J.M., Barringer, K.J., Hessler, A.Y., Madden, K.R. 1985. “*Pichia pastoris* as a host system for transformations.” *Molecular and Cellular Biology* 5:3376–3385.

Cregg, J.M., Tolstorukov, I., 2012. *P. pastoris* ADH promoter and the use thereof to direct expression of proteins. US Patent: 8,222,386

Daly R., Hearn, M.T.W., 2005. “Expression of heterologous proteins in *Pichia pastoris* and advances in protein production.” *Journal of Molecular Recognition* 18:119-138.

de Almeida, J.R.M., de Moraes, L.M.P., Torres, F.A.G., 2005. “Molecular characterization of the 3-phosphoglycerate kinase gene (*PGK1*) from the methylotrophic yeast *Pichia pastoris*.” *Yeast* 22:725-737.

de Figueiredo Vilela, L., de Mello, V.M., Reis, V.C.B., da Silva Bon, E.P., Torres, F.A.G., Neves, B.C., Eleutherio, E.C.A., 2013. “Functional expression of *Burkholderia cenocepacia* xylose isomerase in yeast increases ethanol production from glucose-xylose blend.” *Biosource Technology* 128:792-796.

Dekker, K., Sugiura, A., Yamagata, H., Sakaguchi, K., Udaka, S., 1992. “Efficient production of thermostable *Thermus thermophilus* xylose isomerase in *Escherichia coli* and *Bacillus brevis*.” *Applied. Microbiology and Biotechnology* 36:727-732.

Dekker, K., Yamagata, H., Sakaguchi, K., Udaka, S., 1991. “Xylose (glucose) isomerase gene from *Thermus thermophilus*: Cloning, sequencing, and comparison with other thermostable xylose isomerases.” *Journal of Bacteriology* 173(10):3078-3083.

Dragosits, M., Stadlmann, J., Albiol, J., Baumann, K., Maurer, M., Gasser, B., Sauer, M., Altmann, F., Ferrer, P., Mattanovich, D., 2008. “The effect of temperature on the proteome of recombinant *Pichia pastoris*.” *Journal of Proteome Research* 8:1380-1392.

Fei, L., Wang, Y., Chen, S., 2009. "Improved glutathione production by gene expression in *Pichia pastoris*." *Bioprocess and Biosystems Engineering* 32:729-735.

Garcia-Ochoa, F., Gomez, E., 2009. "Bioreactor scale-up and oxygen transfer rate in microbial processes: An overview." *Biotechnology Advances* 27:153-176.

Garcia-Ochoa, F., Gomez, E., Santos, V.E., Merchuk, J.C., 2010. "Oxygen uptake rate in microbial processes: an overview." *Biochemical Engineering Journal* 49(3):289-307.

Garcia-Ortega, X., Ferrer, P., Montesions, J.L., Valero, F., 2013. "Fed-batch operational strategies for recombinant Fab production with *Pichia pastoris* using the constitutive *GAP* promoter." *Biochemical Engineering Journal* 79:172-181.

Gasser, B., Saloheimo, M., Rinas, U., Dragosits, M., Rodriguez-Carmona, E., Baumann, K., Giuliani, M., Parrilli, E., Branduardi, P., Lang, C., Porro, D., Ferrer, P., Tutino, M.L., Mattanovich, D., Villaverde, A., 2008. "Protein folding and conformational stress in microbial cells producing recombinant proteins: a host comparative overview." *Microbial Cell Factories* 7:11.

GenomeNet Database, [http://www.genome.jp/kegg-bin/show\\_pathway?ppa00010](http://www.genome.jp/kegg-bin/show_pathway?ppa00010), last visited on July 2015.

Goodrick, J.C., Xu, M., Finnegan, R., Schilling, B.M., Schiavi, S., Hoppe, H., Wan, N.C., 2001. "High-level expression and stabilization of recombinant human chitinase produced in a continuous constitutive *Pichia pastoris* expression system." *Biotechnology and Bioengineering*. 74:492–497.

Guan, B., Chen, F., Lei, J., Li, Y., Duan, Z., Zhu, R., Chen, Y., Li, H., Jin, J., 2013. "Constitutive expression of a rhIL-2-HSA fusion protein in *Pichia pastoris* using glucose as carbon source." *Applied Biochemistry and Biotechnology* 171:1792-1804.

Güneş, H., Boy, E., Ata, O., Zerbe, G.H., Calik, P., Ozdamar, T.H., 2015. "Methanol feeding strategy design enhances recombinant human growth hormone production by

*Pichia pastoris*”. *Journal of Chemical Technology and Biotechnology* doi: 10.1002/jctb.4619.

Güneş, H., Çalık, P., *submitted* “Fine tuning the oxygen transfer conditions for recombinant protein production by *Pichia pastoris* under glyceraldehyde-3-phosphate dehydrogenase promoter” *Biochemical Engineering Journal*.

Hlima, H.B., Aghajari, N., Ali, M.B., Haser, R., Bejar, S., 2012. “Engineered glucose isomerase from *Streptomyces* sp. SK is resistant to  $\text{Ca}^{2+}$  inhibition and  $\text{Co}^{2+}$  independent.” *Journal of Industrial Microbiology and Biotechnology* 39:537-546.

Hohenblum, H., Gasser, B., Maurer, M., Borth, N., Mattanovich, D., 2003. ”Effects of gene dosage, promoters, and substrates on unfolded protein stress of recombinant *Pichia pastoris*.” *Biotechnology and Bioengineering* 85(4):368-375.

Hu, X., Chu, J., Zhang, Z., Zhang, S., Zhuang, Y., Wang, Y., Guo, M., Chen, H., Yuan, Z., 2008. “Effects of different glycerol feeding strategies on *S*-adenosyl-L-methionine biosynthesis by  $\text{P}_{\text{GAP}}$ -driven *Pichia pastoris* overexpressing methionine adenosyltransferase.” *Journal of Biotechnology* 137:44-49.

Idiris, A., Tohda, H., Kumagi, H., Takegawa, K., 2010. “Engineering of protein secretion in yeast: Strategies and impact on protein production.” *Applied Microbiology and Biotechnology* 86:403-407.

Invitrogen. 2002. “*Pichia* Fermentation Process Guidelines.”

Jahic, M., Veide, A., Charoenrat, T., Teeri, T., Enfors, S., 2006. “Process technology for production and recovery of heterologous proteins with *Pichia pastoris*.” *Biotechnological Progress* 22:1465-1473.

Jokela, J., Pastinen, O., Leisola, M., 2002. “Isomerization of pentose and hexose sugars by an enzyme reactor packed with cross-linked xylose isomerase crystals”. *Enzyme and Microbial Technology* 31:67-76.



- Karimi, A., Golbabaie, F., Mehrnia, M.R., Neghab, M., Mohammad, K., Nikpey, A., Pourmad, M.R., 2013. "Oxygen mass transfer in a stirred tank bioreactor using different impeller configurations for environmental purposes." *Iranian Journal of Environmental Health Sciences and Engineering* 10:6.
- Keskin, A., 2014. "Feeding strategy development for recombinant human growth hormone production in *Pichia pastoris* under *glyceraldehyde-3-phosphate dehydrogenase* promoter." M.Sc. Thesis. Middle East Technical University, Turkey.
- Khasa, Y.P., Khushoo, A., Srivastava, L., Mukherjee, K.J., 2007. "Kinetic studies of constitutive human granulocyte-macrophage colony stimulating factor (hGM-CSF) expression in continuous culture of *Pichia pastoris*." *Biotechnology Letters* 29:1903-1908.
- Kirk, R.E., Othmer, D.F., 1994. *Encyclopedia of Chemical Technology*. 4th ed. The Interscience Encyclopedia.
- Kurtzman C, 2009. "Biotechnological strains of *Komagataella (Pichia) pastoris* are *Komagataella phaffii*s determined from multigene sequence analysis." *Journal of Industrial Microbiology and Biotechnology* 36:1435–1438.
- Kuyper, M., Hartog, M.M.P., Toirkens, M.J., Almering, M.J.H., Winkler, A.A., van Dijken, J.P., Pronk, J.T., 2005. "Metabolic engineering of a xylose-isomerase-expressing *Saccharomyces cerevisiae* strain for rapid anaerobic xylose fermentation." *FEMS Yeast Research* 5:399-409.
- Laemmli, U.K., 1970. "Cleavage of structural proteins during the assembly of the head of bacteriophage T4." *Nature* 227(5259):680-685
- Lambeir, A., Lauwereys, M., Stanssens, P., Mrabet, N.T., Snauwaert, J., van Tilbeurgh, H., Matthyssens, G., Lasters, I., De Maeyer, M., Wodak, S.J., Jenkins, J., Chiadmi M., Janin, J., 1992."Protein engineering of xylose (glucose) isomerase from *Actinoplanes missouriensis*. 2. Site-directed mutagenesis of the xylose binding site." *Biochemistry* 31:5459-5466.

Lee, C., Bhatnagar, L., Saha B.C., Lee, Y., Takagi, M., Imanaka, T., Bagdasarian, M., Zeikus, J.G., 1990. "Cloning and expression of the *Clostridium thermosulfurogenes* glucose isomerase gene in *Escherichia coli* and *Bacillus subtilis*." *Applied and Environmental Microbiology* 56(9):2638-2643.

Liu, Z., Tyo, K.E.J., Martinez, J.L., Petranovic, D., Nielsen, J., 2012. "Different expression systems for production of recombinant proteins in *Saccharomyces cerevisiae*." *Biotechnology and Bioengineering* 109(5):1259-1268.

Lu, W., Wu, H., Ju, M., 1997. "Effects of baffle design on the liquid mixing in an aerated stirred tank with standard Rushton turbine impellers." *Chemical Engineering Science* 52(21:22):3843-3851.

Macauley-Patricki S., Fazenda, M.L., McNeil, B., Harvey, L.M., 2005. "Heterologous protein production using the *Pichia pastoris* expression system." *Yeast* 22:249-270.

MarketsandMarkets, <http://www.marketsandmarkets.com/Market-Reports/industrial-enzymes-market-237327836.html>, last visited on June 2015.

Marshall, R. O., E. R. Kooi., 1957. Enzymatic conversion of D-glucose to D-fructose. *Science* 125:648–649.

Menéndez, C., Hernández, L., Banguela, A., Pais, J., 2004. "Functional production and secretion of the *Glucanacetobacter diazotrophicus* fructose-releasing exo-levanase (LsdB) in *Pichia pastoris*." *Enzyme and Microbial Technology* 34:446-452.

Menendez, J., Valdes, I., Cabrera, N., 2003. "The *ICL1* gene of *Pichia pastoris*, transcriptional regulation and use of its promoter." *Yeast* 20:1097-1108.

Mishra, A., Debnath, M., 2002. "Effect of pH on simultaneous saccharification and isomerization by glucoamylase and glucose isomerase." *Applied Biochemistry and Biotechnology* 102-103(1-6):193-199.

Moes, C.J., Pretorius, I.S., van Zyl, W.H., 1996. "Cloning and expression of the *Clostridium thermosulfulogenes* D-xylose isomerase (xyk4) in *Saccharomyces cerevisiae*." *Biotechnology Letters* 18:269-274.

Moon, S. H., Parulekar, S. J., 1991. "A parametric study of protease production in batch and semi-batch cultures of *Bacillus firmus*." *Biotechnology and Bioengineering* 37:467-483.

National Center for Biotechnology Information, <http://www.ncbi.nlm.nih.gov/nucleotide/D90256>, last visited on June 2015.

Nielsen, J., Villadsen, J., Bioreaction engineering principles. 1<sup>st</sup> ed., Plenum Press, New York. 1994.

Orman, M.A., 2007. "Extracellular recombinant human growth hormone production by *Pichia pastoris*." M.Sc. Thesis, Middle East Technical University, Turkey.

Öztürk, S., 2014. "Semi-defined medium based feeding strategy development for human growth hormone production by recombinant *Bacillus subtilis*." M.Sc. Thesis, Middle East Technical University, Turkey.

Pal, Y., Khushoo, A., Mukherjee, K.J., 2006. "Process optimization of constitutive human granulocyte-macrophage colony-stimulating factor (hGM-CSF) expression in *Pichia pastoris* fed-batch culture." *Applied Microbiology and Biotechnology* 69:650-657.

Palmer T., Bonner P., Enzymes: Biochemistry, biotechnology, clinical chemistry. 2nd ed. Woodhead Publishing, 2007.

Park, B.C., Koh, S., Chang, C., Suh, S.W., Lee, D., Byun, S.M. 1997. "Cloning and expression of the gene for xylose isomerase from *Thermus flavus* AT62 in *Escherichia coli*." *Applied Biochemistry and Biotechnology* 62(1):15-27.

- Pepeliaev, S., Krahulec, J., Cerny, Z., Jilkova, J., Tlusta, M., Dostalova, J., 2011. "High level expression of human enteropeptidase light chain in *Pichia pastoris*." *Journal of Biotechnology* 156:67-75.
- Prielhofer, R., Maurer, M., Klein, J., Wenger, J., Kizial, C., Gasser, B., Mattanovich D., 2013. "Induction without methanol: Novel regulated promoters enable high-level expression in *Pichia pastoris*." *Microbial Cell Factories* 12:5.
- Rainer, B.W., 1990. "Determination methods of the volumetric oxygen transfer coefficient  $k_{La}$  in bioreactors." *Chemical and Biochemical Engineering Quarterly*, 4(4):185-186.
- Raven, P.H., Johnson, G.B., Mason, K., Losos, J., Singer, S., Biology. 10th Ed. McGraw Hill, 2013.
- RCSB Protein Data Bank, <http://www.rcsb.org/pdb/explore/explore.do?structureId=1BXB>, last visited on June 2015.
- Sanchez, S., Demain, A., 2012. "Special issue on the production of recombinant proteins." *Biotechnology Advances* 30(5):1100-1111.
- Schaepe, S., Kuprijanov, A., Sieblist, C., Jenzsch, M., Simutis, R., Lübbert, A., 2013. " $k_{La}$  of stirred tank bioreactors revisited." *Journal of Biotechnology* 168:576-583.
- Schlieker, C., Bukau, B., Mogk, A., 2002. "Prevention and reversion of protein aggregation by molecular chaperones in the *E. coli* cytosol: implications for their applicability in biotechnology." *Journal of Biotechnology* 96(1):13-21.
- Schmidt, F., 2004. "Recombinant expression systems in the pharmaceutical industry". *Applied Microbiology and Biotechnology* 65(4):363–372.
- Sears, I.B., O'Connor, J., Rossanese, O.W., Glick, B.S., A versatile set of vectors for constitutive and regulated gene expression in *Pichia pastoris*." *Yeast* 14:783-790.

Shen, S., Sulter G., Jeffries, T.W., Cregg, J.M., 1998. "A strong nitrogen source-regulated promoter for controlled expression of foreign genes in the yeast *Pichia pastoris*." *Gene* 216:93-102

Sieblist, C., Hagelholz, O., Aehle, M., Jenzsch, M., Pohlscheidt, M., Lübbert, A., 2011. "Insights into large-scale cell-culture reactors: II. Gas-phase mixing and CO<sub>2</sub> stripping." *Biotechnology Journal* 6(12):1547-1556.

Sjöblom, M., Lindberg, L., Holgersson, J., Rova, U., 2012. "Secretion and expression dynamics of a GFP-tagged mucin-type fusion protein in high cell density *Pichia pastoris* bioreactor cultivations." *Advances in Bioscience and Biotechnology* 3:238-248.

Tan, H.R., He, S., Zhuang, Z.H., Xue, Y.G., Zhang, Q.J., 1990. "Cloning and expression of *E. Coli* glucose isomerase gene in *Streptomyces lividans*." *Journal of Genetics and Genomics* 17(5):390-397.

Thomson, C.A., 2010. "FDA approves kallikrein inhibitor to treat hereditary angioedema." *American Journal of Health-System Pharmacy* 67(2):93.

UCTEA Chamber of Food Engineers, <http://www.gidamo.org.tr/resimler/ekler/938b20f9f210570ek.pdf?dergi=45>, last visited on June 2015.

Tschopp J.F., Brust P.F., Cregg, J.M., Stillman, C.A., Gingeras, T.R., 1987. "Expression of the *lacZ* gene from two methanol-regulated promoters in *Pichia pastoris*." *Nucleic Acids Research* 15:3859-3876.

Vassileva, A., Chugh, D.A., Swamnathan, S., Khanna, N., 2001. "Expression of hepatitis B surface antigen in the methylotrophic yeast *Pichia pastoris* using the *GAP* promoter." *Journal of Biotechnology* 88:21-35.

Voet, D., Voet, D.G., Pratt, C.W. *Biochemistry: Life at molecular level*. 4th ed., John Wiley & Sons Inc., New Jersey, 2013.

- Vongsuvanlert, V., and Tani, Y., 1988. "Purification and characterization of xylose isomerase of a methanol yeast, *Candida boidinii*, which is involved in sorbitol production from glucose." *Agricultural and Biological Chemistry* 52:1817–1824.
- Walfridsson, M., Bao, X., Anderlund, M., Lilius, G., Bülow, L., Hahn-Hagerdal, B. 1996. "Ethanol fermentation of xylose with *Saccharomyces cerevisiae* harboring the *Thermus thermophilus xylA* gene, which expresses an active xylose (glucose) isomerase." *Applied and Environmental Microbiology* 62(12):4648-4651.
- Wang, J., Jin, C., Fu, R., Shen, D., 2011. Isolated DNA encoding recombinant glucose isomerase. US Patent 8,067,561 B2
- Wang, P.Y., Johnson, B.F., Schneider, H., 1980. "Fermentation of D-xylose by yeasts using glucose isomerase in the medium to convert D-xylose to D-xylulose." *Biotechnology Letters* 2:273–278.
- Wang, X., Sun, Y., Ke, F., Zhao, H., Liu, T., Xu, L., Yan, Y., 2012. "Constitutive expression of *Yarrowia lipolytica* Lipase LIP2 in *Pichia pastoris* using GAP as a promoter." *Applied Biochemistry and Biotechnology* 166:1355-1367.
- Waterham, H.R., Digan, M.E., Koutz, P.J., Lair, S.V., Cregg, J.M., 1997. "Isolation of *Pichia pastoris* glyceraldehyde-3-phosphate dehydrogenase gene and regulation and use of its promoter" *Gene* 186:37-44.
- Whitman, W.G., 1923. "Preliminary experimental confirmation of the two-film theory of gas absorption." *Chemical and Metallurgical Engineering* 29:146-149.
- Zaman, S., Lippman, S.I., Zhao, X., Broach, J.R., 2008. "How *Saccharomyces* respond to nutrients." *Annual Review of Genetics* 42:27-81.
- Zhang, A., Luo, J., Zhang, T., Pan, Y., Tan, Y., Fu, C., Tu, F., 2009. "Recent advances on the GAP promoter derived expression system of *Pichia pastoris*." *Molecular Biology Reports* 36:1611-1619.

Zheng, H., Wang, X., Chen, J., Zhu, K., Zhao, Y., Yang, Y., Yang, S., Jiang, W., 2006. "Expression, purification, and immobilization of His-tagged D-amino acid oxidase of *Trigonopsis variabilis* in *Pichia pastoris*." *Applied Microbiology and Biotechnology* 70:683-689.





## APPENDIX A

### BUFFERS AND STOCK SOLUTIONS

#### Fermentation Media

<b>1 M Potassium phosphate buffer, pH= 6.0</b>	56.48 g $\text{KH}_2\text{PO}_4$ and 14.8 g $\text{K}_2\text{HPO}_4$ were dissolved in $\text{dH}_2\text{O}$ and the volume is completed to 500 ml. The solution is sterilized by autoclave and stored at room temperature.
<b>Antifoam solution</b>	100 ml, 10% antifoam solution is prepared with $\text{dH}_2\text{O}$ and sterilized by autoclave.
<b>Base</b>	25% $\text{NH}_3\text{OH}$ . No need to sterilize.

#### SDS-PAGE Solutions

<b>Resolving gel</b>	6 ml BioRad FastCast <sup>®</sup> resolving gel solution, 50 $\mu\text{l}$ ammonium persulfate and 5 $\mu\text{l}$ $\text{N,N,N',N'}$ -tetramethylethylenediamine are mixed and poured into
<b>Stacking gel</b>	3 ml BioRad FastCast <sup>®</sup> stacking gel solution, 25 $\mu\text{l}$ ammonium persulfate and 5 $\mu\text{l}$ $\text{N,N,N',N'}$ -tetramethylethylenediamine.
<b>4X SDS-PAGE Sample loading buffer</b>	200 mM Tris-HCl, pH 6.8; 40% glycerol; 6% SDS; 0.013% Bromophenol blue; 10% 2-mercaptoethanol. Store at $-20^\circ\text{C}$ .

**5X SDS-PAGE Running buffer**      15 g Tris Base, 72 g glycine, 5 g SDS, dH<sub>2</sub>O to 1 liter. Store at +4°C.

### **Silver Staining Solutions**

**Fixer**      Mix 100 ml methanol, 24 ml acetic acid, 100 µl 37% formaldehyde and complete to 200 mL with dH<sub>2</sub>O. Store at room temperature up to 1 month.

**Pretreatment**      Dissolve 0.05 g Na<sub>2</sub>S<sub>2</sub>O<sub>3</sub>·5H<sub>2</sub>O in 250 ml distilled water by mixing with a glass rod. Take 2 ml and set aside for further use in developing solution preparation.

**Silver nitrate**      Dissolve 0.2 g silver nitrate in 100 ml dH<sub>2</sub>O and add 75 µl 37% formaldehyde.

**Developing**      Dissolve 2.25 g potassium carbonate in 100 mL dH<sub>2</sub>O. Add 2 ml from pretreatment solution and 75 µl 37% formaldehyde.

**Stop**      Mix 50 ml ethanol, 12 ml acetic acid and dilute to 100 ml with dH<sub>2</sub>O.

### **Protease Assay Solutions**

**0.05 M Sodium acetate buffer**      Mix 0.713 ml acetic acid in 25 ml dH<sub>2</sub>O. Dissolve 2.052 g sodium acetate in 50 ml dH<sub>2</sub>O. Titrate sodium acetate solution with acetic acid solution until pH = 5.0 and dilute to 500 ml. Autoclave and store at +4°C.

## APPENDIX B

### CALIBRATION CURVE FOR GLUCOSE CONCENTRATION

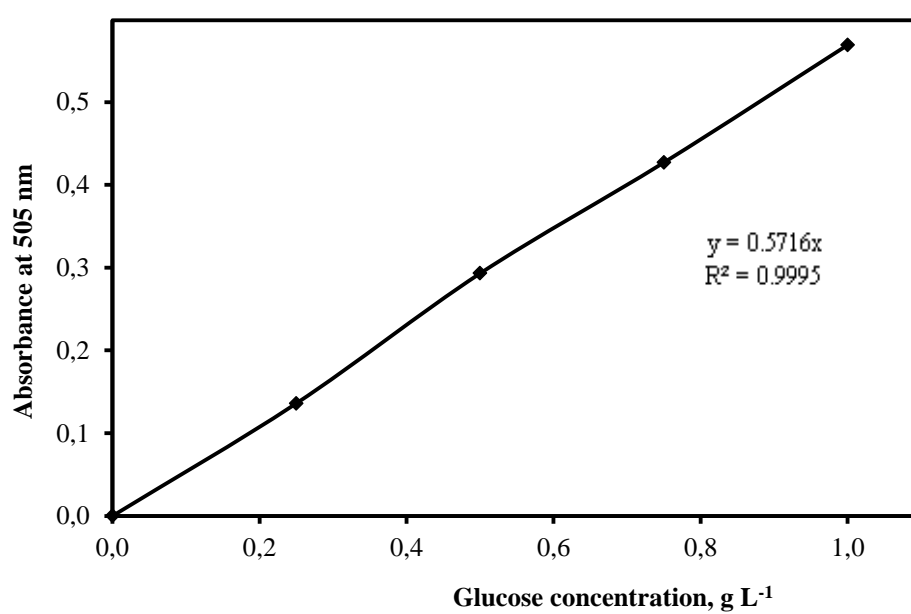


**Figure 43.** Calibration curve for glucose concentration



## APPENDIX C

### SILVER STAINING PROCEDURE

Step	Time of Treatment	Comments
Fixing	> 1 h	Overnight treatment is acceptable.
Washing	3 x 20 min	Solution must be freshly prepared.
Pretreatment	1 min	Solution must be freshly prepared.
Rinsing	3 x 20 s	Timing must be exact.
Impregnation	20 min	Solution must be freshly prepared.
Rinsing	3 x 20 s	Timing must be exact.
Developing	As long as the desired bands can be seen. (~5 min). Time should be determined by observation of the staining.	dH <sub>2</sub> O can be added after few minutes to slow down the reaction.
Stop	>10 min	Gels can be stored in this solution.



## APPENDIX D

### CALIBRATION CURVES FOR ORGANIC ACIDS

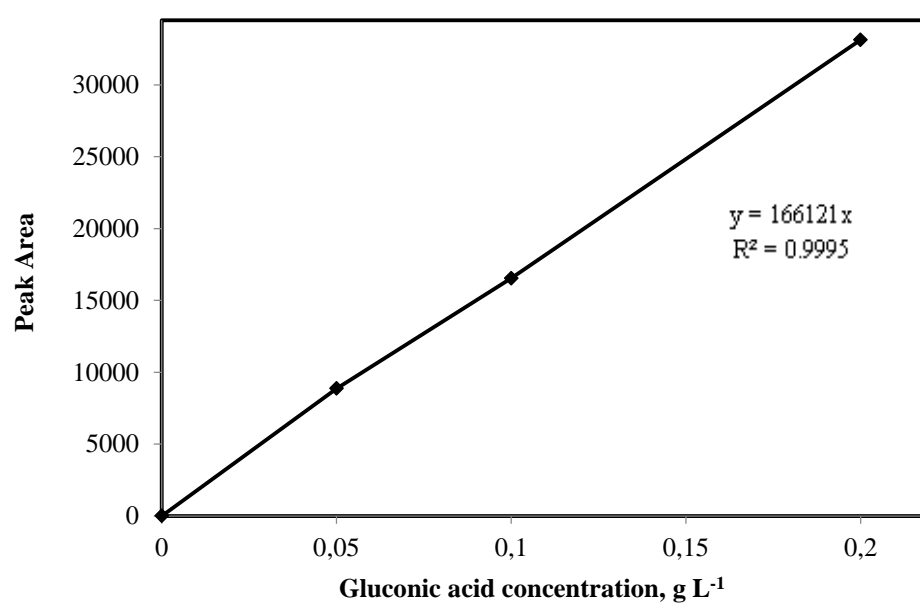


**Figure 44.** Calibration curve for gluconic acid concentration determination by HPLC.

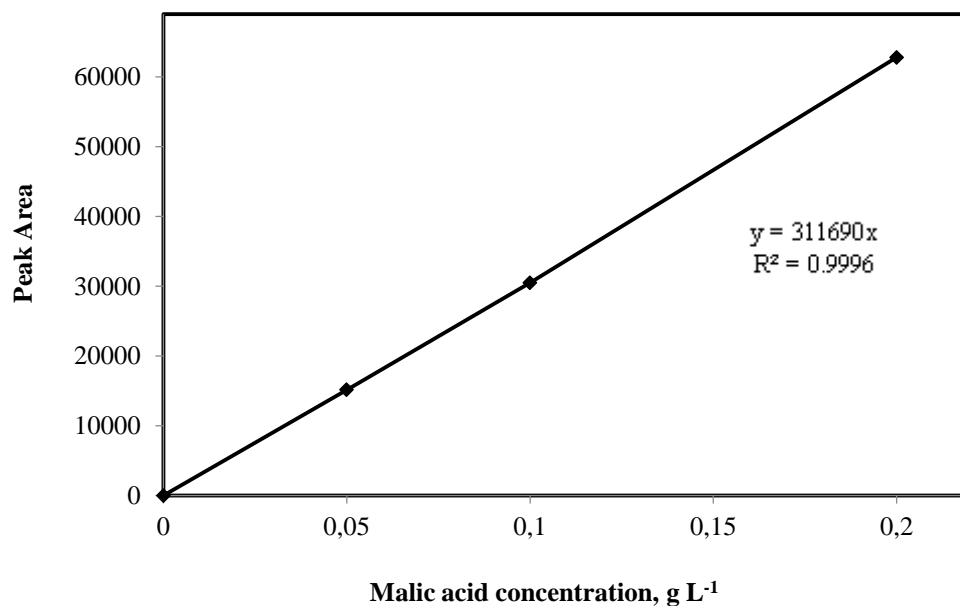


**Figure 45.** Calibration curve for malic acid concentration determination by HPLC.

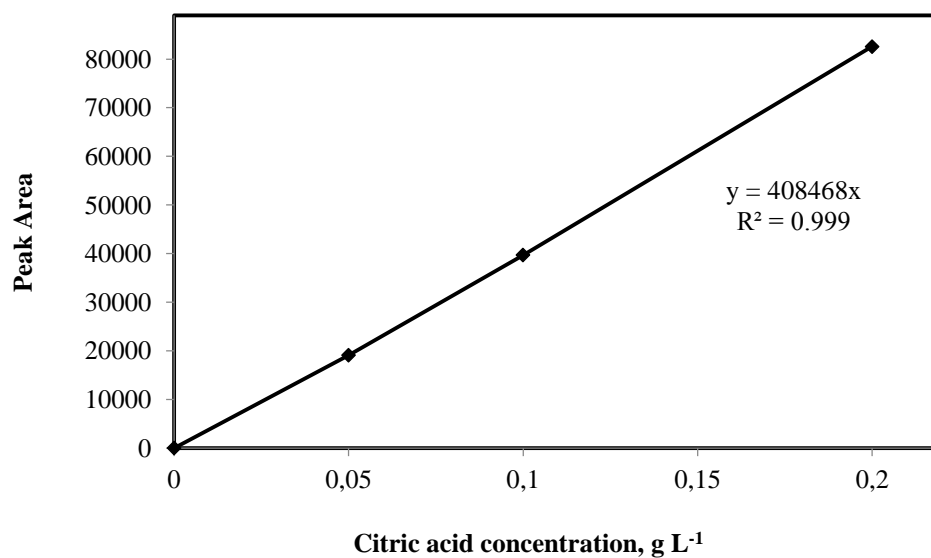


**Figure 46.** Calibration curve for citric acid concentration determination by HPLC.



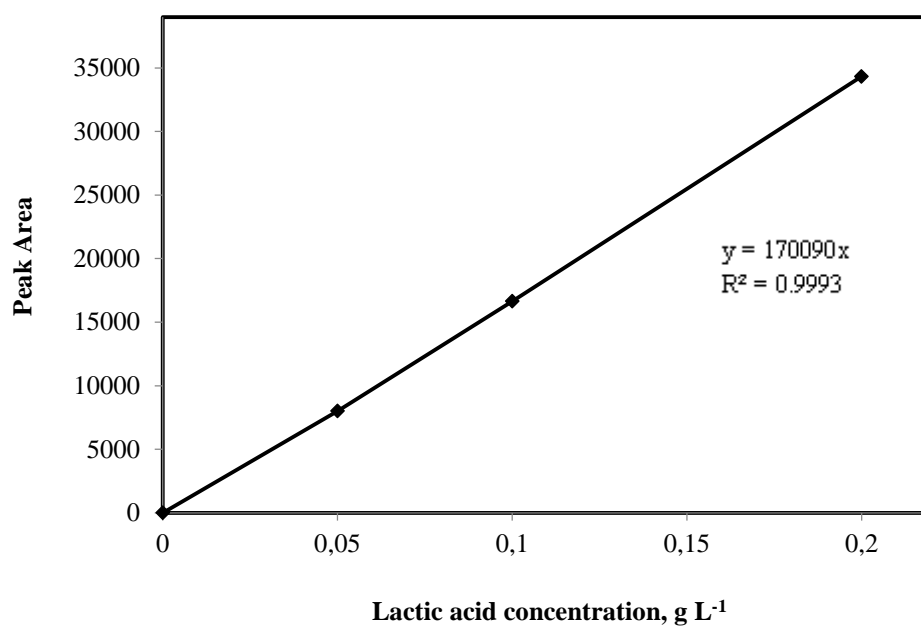


**Figure 47.** Calibration curve for lactic acid concentration determination by HPLC.

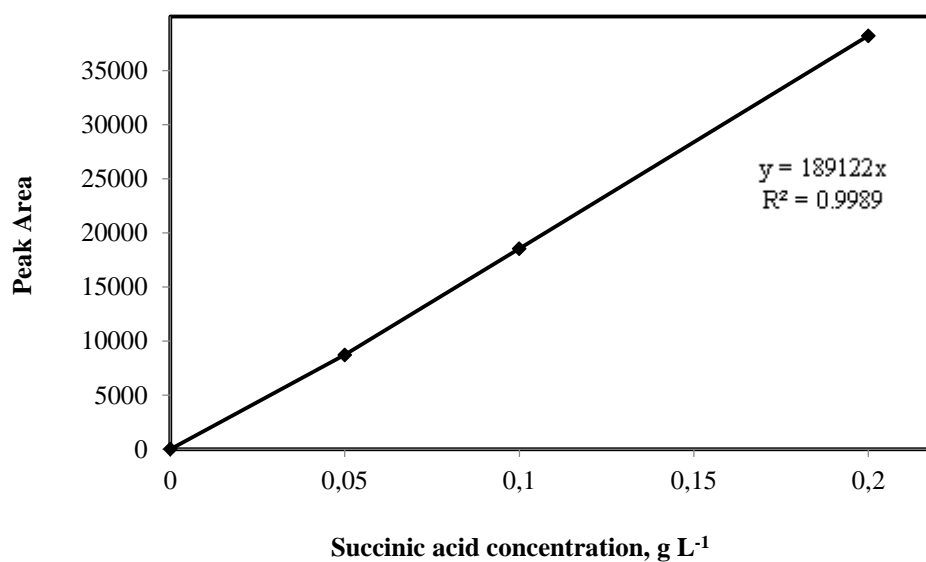


**Figure 48.** Calibration curve for succinic acid concentration determination by HPLC.

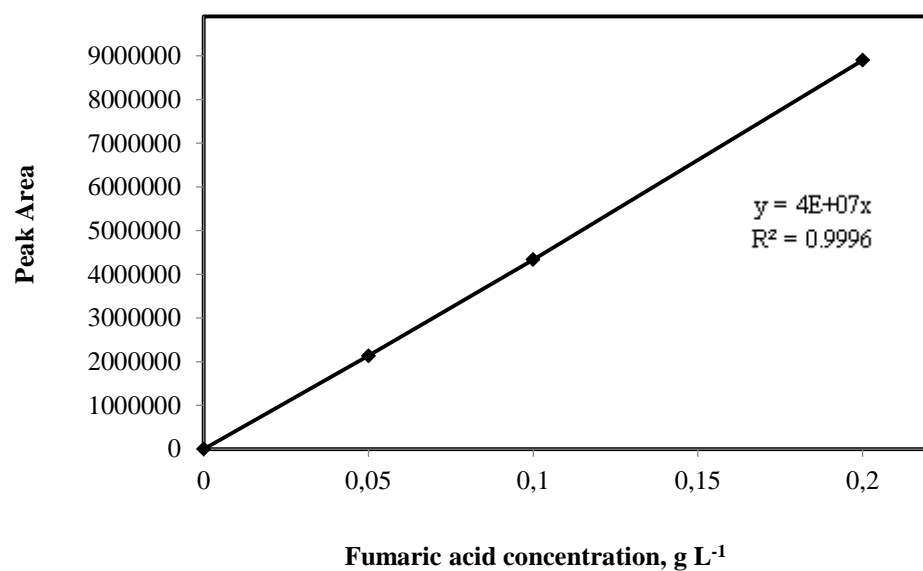


**Figure 49.** Calibration curve for fumaric acid concentration determination by HPLC.

## APPENDIX E

### ORGANIC ACID CONCENTRATIONS

**Table 13.** Organic acid accumulation in the bioreaction medium with cultivation time.

		Organic Acid Concentration, g L <sup>-1</sup>				
		3 h	6 h	9 h	12 h	15 h
OTC <sub>1</sub>	Gluconic Acid	0.99	1.27	1.52	1.93	2.11
	Malic Acid	-	-	-	-	-
	Citric Acid	-	0.02	0.02	0.03	0.03
	Pyruvic Acid	0.06	-	-	-	-
	Lactic Acid	-	0.38	0.72	0.79	0.69
	Acetic Acid	0.29	0.26	0.38	0.31	1.46
	Succinic Acid	-	-	0.52	0.61	0.70
	Fumaric Acid	-	-	0.01	0.03	0.04
OTC <sub>2</sub>	Gluconic Acid	-	1.90	2.55	4.56	3.61
	Malic Acid	0.36	1.65	-	-	-
	Citric Acid	-	0.01	0.01	0.02	0.02
	Pyruvic Acid	-	-	-	-	-
	Lactic Acid	-	0.19	0.35	0.69	0.69
	Acetic Acid	-	1.18	1.57	2.30	3.11
	Succinic Acid	-	-	0.68	0.71	0.77
	Fumaric Acid	-	-	-	0.02	0.03

**Table 13.** Continued.

		<b>Organic Acid Concentration, g L<sup>-1</sup></b>				
		<b>3 h</b>	<b>6 h</b>	<b>9 h</b>	<b>12 h</b>	<b>15 h</b>
<b>OTC<sub>3</sub></b>	<b>Gluconic Acid</b>	-	-	-	-	-
	<b>Malic Acid</b>	0.14	0.18	-	-	-
	<b>Citric Acid</b>	-	-	0.01	0.01	0.02
	<b>Pyruvic Acid</b>	-	-	-	-	-
	<b>Lactic Acid</b>	-	-	0.07	0.13	0.18
	<b>Acetic Acid</b>	0.12	0.13	0.45	0.55	0.64
	<b>Succinic Acid</b>	0.13	0.16	0.91	0.80	0.67
	<b>Fumaric Acid</b>	-	-	-	-	-
<b>CDO<sub>1</sub></b>	<b>Gluconic Acid</b>	0.33	0.49	1.25	2.05	1.50
	<b>Malic Acid</b>	-	-	-	-	-
	<b>Citric Acid</b>	-	0.01	0.01	0.02	0.03
	<b>Pyruvic Acid</b>	-	-	-	-	-
	<b>Lactic Acid</b>	0.01	0.17	0.50	0.56	0.91
	<b>Acetic Acid</b>	0.04	0.09	0.24	0.63	0.45
	<b>Succinic Acid</b>	-	-	-	0.71	0.82
	<b>Fumaric Acid</b>	-	-	0.02	0.06	0.03

**Table 13.** Continued.

		Organic Acid Concentration, g L <sup>-1</sup>				
		3 h	6 h	9 h	12 h	15 h
<b>CDO<sub>2</sub></b>	<b>Gluconic Acid</b>	-	-	-	-	-
	<b>Malic Acid</b>	-	-	-	-	-
	<b>Citric Acid</b>	-	0.01	0.01	0.01	0.02
	<b>Pyruvic Acid</b>	0.01	0.03	-	-	-
	<b>Lactic Acid</b>	0.06	0.11	0.44	0.63	0.62
	<b>Acetic Acid</b>	-	0.11	0.31	0.45	0.66
	<b>Succinic Acid</b>	-	0.21	0.68	0.76	0.70
	<b>Fumaric Acid</b>	-	-	0.01	0.03	0.03
<b>CDO<sub>3</sub></b>	<b>Gluconic Acid</b>	-	-	-	-	-
	<b>Malic Acid</b>	-	0.01	0.01	-	-
	<b>Citric Acid</b>	-	-	-	-	0.01
	<b>Pyruvic Acid</b>	-	-	-	-	-
	<b>Lactic Acid</b>	0.02	0.04	0.16	0.39	0.58
	<b>Acetic Acid</b>	-	-	0.01	0.05	0.13
	<b>Succinic Acid</b>	-	-	-	-	0.11
	<b>Fumaric Acid</b>	-	-	-	0.01	0.02

**Table 13.** Continued.

		Organic Acid Concentration, g L <sup>-1</sup>				
		3 h	6 h	9 h	12 h	15 h
<b>CDO<sub>4</sub></b>	<b>Gluconic Acid</b>	-	-	-	-	-
	<b>Malic Acid</b>	-	-	-	-	-
	<b>Citric Acid</b>	-	-	-	-	-
	<b>Pyruvic Acid</b>	-	0.02	-	-	-
	<b>Lactic Acid</b>	-	-	-	-	-
	<b>Acetic Acid</b>	0.07	0.05	0.18	0.53	0.74
	<b>Succinic Acid</b>	-	-	-	-	0.34
	<b>Fumaric Acid</b>	-	-	-	0.01	0.02
<b>CDO<sub>5</sub></b>	<b>Gluconic Acid</b>	-	-	-	-	-
	<b>Malic Acid</b>	-	-	-	-	-
	<b>Citric Acid</b>	-	-	-	-	-
	<b>Pyruvic Acid</b>	-	0.01	0.07	-	-
	<b>Lactic Acid</b>	-	-	-	-	-
	<b>Acetic Acid</b>	0.11	0.13	0.47	0.61	0.83
	<b>Succinic Acid</b>	-	-	-	-	0.81
	<b>Fumaric Acid</b>	-	-	-	-	-